A PROTEOMIC APPROACH TO THE COMPARISON OF TWO PINE SPECIES: PROTEOMES OF *PINUS BRUTIA* AND *PINUS SYLVESTRIS* UNDER ENVIRONMENTAL STRESS

A THESIS SUBMITTED TO
THE GRADUATE SCHOOL OF NATURAL AND APPLIED SCIENCES
OF
MIDDLE EAST TECHNICAL UNIVERSITY

BY

CAN YILMAZ

IN PARTIAL FULFILLMENT OF THE REQUIREMENTS
FOR
THE DEGREE OF DOCTOR OF PHILOSOPHY
IN
BIOCHEMISTRY

OCTOBER 2013

Approval of the thesis:

A PROTEOMIC APPROACH TO THE COMPARISON OF TWO PINE SPECIES: PROTEOMES OF *PINUS BRUTIA* AND *PINUS SYLVESTRIS* UNDER ENVIRONMENTAL STRESS

Submitted by **Can YILMAZ** in partial fulfillment of the requirements for the degree of **Doctor of Philosophy in Biochemistry Department, Middle East Technical University** by,

Prof. Dr. Canan ÖZGEN _____
Dean, Graduate School of **Natural and Applied Sciences**

Prof. Dr. Orhan ADALI _____
Head of Department, **Biochemistry**

Prof. Dr. Mesude İŞCAN _____
Supervisor, **Dept. of Biological Sciences, METU**

Prof. Dr. Tülin GÜRAY _____
Co-supervisor, **Dept. of Biological Sciences, METU**

Examining Committee Members:

Prof. Dr. Nazmi ÖZER _____
Faculty of Medicine, NEU

Prof. Dr. Meral YÜCEL _____
Dept. of Biological Sciences, METU

Prof. Dr. Orhan ADALI _____
Dept. of Biological Sciences, METU

Associate Prof. Dr. Sertaç ÖNDE _____
Dept. of Biological Sciences, METU

Associate Prof. Dr. Çağdaş D. SON _____
Dept. of Biological Sciences, METU

Date: 11.10.2013

I hereby declare that all information in this document has been obtained and presented in accordance with academic rules and ethical conduct. I also declare that, as required by these rules and conduct, I have fully cited and referenced all material and results that are not original to this work.

Name, Last name: **Can YILMAZ**

Signature:

ABSTRACT

A PROTEOMIC APPROACH TO THE COMPARISON OF TWO PINE SPECIES: PROTEOMES OF *PINUS BRUTIA* AND *PINUS SYLVESTRIS* UNDER ENVIRONMENTAL STRESS

YILMAZ, Can
Ph.D., Department of Biochemistry

Supervisor: Prof. Dr. Mesude İŞCAN
Co-supervisor: Prof. Dr. Tülin GÜRAY

October 2013, 122 pages

Drought and cold are environmental factors that affect the development and dispersion of plant species. In this study, two pine species adapted to different environmental conditions: *Pinus brutia* Ten. (Turkish red pine) and *Pinus sylvestris* L. (Scots pine) were subjected to a proteome research under those stresses. 20 trees from each species, located in the same region and elevation at Yalıncak area in METU Campus, were marked and sampled for their needles, three times in a year: at the end of dry and hot summer, cold winter and, mild and rainy spring. The changes in the photosynthetic pigments, biochemical stress markers such as proline, Malodialdehyde (MDA), Glutathione (GSH) contents and Glutathione S-transferase (GST) enzyme activities were recorded to provide supportive data for the presence and magnitude of stress for both conifer species. The changes in air temperature, humidity and total rainfall provided by Turkish State Meteorological Service were also used to strengthen the hypothesis. A new and relatively more efficient protein extraction method was introduced and by using this method two dimensional SDS-polyacrylamide gel electrophoresis (2D-SDS-PAGE) images of samples were analysed and compared with each other. The analysis of LC-MS/MS data were performed by two different search machines (OMMSA and X!Tandem) having different algorithms and the results of these applications and supportive data provided by western blotting experiments revealed the proteomic changes in *P. brutia* and *P. sylvestris* needles with respect to season.

As stated in many studies, proline content of both pine species were relatively higher in winter season to protect osmotic balance against increased water stress created by sub-freezing temperatures. The fate of this molecule in summer season might be shaped by some other metabolic necessities. MDA levels didn't exhibited expected changes, however the changes in the GSH pool were purposeful with respect to the specific activity values of the total GST in both species: when the enzymatic activity rose, the pool was waned because of increased demand. Moreover, this relationship strengthens the proposition of higher oxidative stress in summer for *P. sylvestris* and in winter for *P. brutia*.

P. sylvestris decreased photosynthetic machinery, exalted chlorophyll-(a+b)/carotenoid ratio and significantly increased HSPs and chaperonin levels as a part of cold-hardening. On the other hand, as expected, *P. brutia* trees were not as successful as scots pine in management of sub-freezing temperatures. The meteorological data showed the presence of frost days in spring season and, an early increase in the photosynthetic machinery in the *P. brutia* needles in this period might be a reason for elevated stress levels. Under cold stress conditions both

of the species tend to increase the rate or the dimension of energy harvesting mechanism to meet the ATP need. Up-regulated respiratory system enzymes such as UDP-Glucose Pyrophosphate, Phosphoglycerate kinase, ATP-citrate synthase beta chain protein 1-like, citrate synthase, citrate synthase 3, NAD-dependent malic enzyme 1 pointed an increased ATP production. Moreover, the increase in the amount of Alcohol Dehydrogenase, which protects the sustainable proceeding of glycolysis, might be an indicator of this exalted need for energy because it seemed that it forced needle cells to gather energy even from anaerobic respiration.

Key words: *Pinus brutia*, *Pinus sylvestris*, environmental stress, proteome, 2D-PAGE, mass spectrometry

ÖZ

İKİ ÇAM TÜRÜNÜN KARŞILAŞTIRILMASINA PROTEOMİK BİR YAKLAŞIM: *PINUS BRUTIA* VE *PINUS SYLVESTRIS*'IN ÇEVRESEL BASKI ALTINDA PROTEOMLARI

YILMAZ, Can
Doktora, Biyokimya Bölümü

Tez Yöneticisi: Prof. Dr. Mesude İŞCAN
Ortak Tez Yöneticisi: Prof. Dr. Tülin GÜRAY

Ekim 2013, 122 sayfa

Kuraklık ve soğuk bitki türlerinin gelişimini ve dağılımını etkileyen çevresel faktörlerdir. Bu çalışmada, farklı çevresel koşullara adapte olmuş iki çam türü: *Pinus brutia* Ten (kızıl çam) ve *Pinus sylvestris* L. (sarı çam) bu baskı koşulları altında, bir proteom çalışmasına konu edilmişlerdir. Her bir türden olmak üzere, aynı bölge ve yükseklikten 20 sağlıklı ağaç işaretlenmiş ve iğne yaprakları yılda üç kez; kurak ve sıcak yaz mevsimi, soğuk kış mevsimi ve ılıman ve yağışlı bahar mevsimi sonunda örneklenmiştir. Fotosentetik pigmentlerdeki, prolin, malondialdehit (MDA), glutatyon (GSH) miktarlarındaki ve Glutatyon-S-transferaz (GST) enzim aktivitelerindeki değişimler her iki çam türü üzerindeki çevresel baskının varlığını ve büyüklüğünü göstermek üzere izlenmiştir. Devlet Meteoroloji Müdürlüğü tarafından sağlanan hava sıcaklığındaki, toplam nem ve yağış miktarlarındaki değişimler de hipotezin güçlendirilmesi için kullanılmıştır. Yeni ve nispeten daha etkili bir protein özütleme metodu tasarlanmış ve bu metodun kullanımıyla örneklere ait iki boyutlu-SDS-poliakrilamit jel elektroforezi (2D-SDS-PAGE) görüntüleri analiz edilip karşılaştırılabilmiştir. LC-MS/MS verilerinin analizleri farklı algoritmalar ile çalışan iki farklı arama motoru (OMMSA ve X!Tandem) ile gerçekleştirilmiştir ve bu analizlerin sonuçları ve western blotlama ile elde edilen destekleyici veriler kızıl çamın ve sarı çamın proteomlarının mevsimlere gore gösterdiği değişimleri açıklamıştır.

Her iki çam türüne ait prolin ölçümleri, pek çok çalışmada da ifade edildiği gibi, sıfırın altındaki sıcaklığın ortaya çıkardığı su baskısına karşı ozmotik dengeyi koruyacak şekilde artış göstermiştir. Bu molekülün yazın gösterdiği değişimler ise başka metabolik yolaklar tarafından şekillendirilmiş olabilir. MDA seviyeleri beklenen değişimleri sergilememiştir, ancak, GSH havuzundaki değişimler toplam GST aktivitesinde izlenen değişimler ile uyumludur: enzim aktivitesi arttığında, GSH havuzu artan ihtiyacın sonucu olarak küçülmüştür. Bu ilişki, yazın *P. sylvestris* ve kışın *P. brutia*'da oksidatif baskının arttığına yönelik önermeyi de kuvvetlendirmektedir.

P. sylvestris kışın soğuk aklimasyonu kapsamında fotosentetik mekanizmalarını azaltmakta, klorofil-(a+b)/karotenoid oranını düşürmekte, ve HSP ve chaperon seviyelerini önemli derecede artırmaktadır. Diğer yandan, tahmin edildiği şekilde, *P. brutia* dondurucu sıcaklık değerleriyle başa çıkmakta sarı çam kadar başarılı değildir. Meteorolojik veriler bahar döneminde de don olaylarının bulunduğunu göstermiştir ve aynı dönemde *P. brutia*'nın fotosentetik mekanizmasındaki erken artış yüksek baskı seviyesinin bir nedeni olabilir. Soğuk baskısı altında, her iki tür de artan ATP ihtiyacını karşılayacak şekilde enerji üretim

mekanizmalarının hızını ve oranını artırmışlardır. UDP-Glukoz pirofosforilaz, Fosfogliserat kinaz, ATP-sitrat sentez beta zinciri proteini benzeri-1, sitrat sentez, sitrat sentez 3, NAD-malik enzim 1 gibi solunum sistemi enzimlerindeki artış, artan ATP üretimini işaret etmektedir. Ayrıca glikolizin devamlılığının sağlanmasında önemli bir işlevi olan alkol dehidrogenaz miktarındaki artış yine artan enerji ihtiyacının göstergesi olabilir.

Anahtar kelimeler: *Pinus brutia*, *Pinus sylvestris*, çevresel baskı, proteom, 2D-PAGE, kütle spektrometresi.

To the memory of my professor and my teacher Prof DrMesude İŞCAN...

ACKNOWLEDGEMENTS

I dedicate this thesis to the memory of my lovely teacher Prof. Dr. Mesude İŞCAN. I will always be grateful for her spirit, encouragement and infinite support. At the first anniversary of the day I lost the person who'd thought me how to be an honest, hardworking and curious scientist, I took my daughter Öykü Ece in my arms for the first time; to whom I will teach how to be an honest, hardworking and curious person. And, I believe this coincidence beatifies the remembrance of my professor and I will commemorate her in every birthday of my daughter by imaging as she's smiling with my family.

Besides Prof Dr Mesude İŞCAN, I have some other people to thank:

I thank to Prof Dr Michael HIPPLER and his lab-team for their valuable supports and participation in my study; and, their great hospitality in my life in Muenster, Germay.

I thank to Prof Dr Nazmi ÖZER, Prof Dr Meral YÜCEL and Prof Dr Tülin GÜRAY for their support and guidance; and for their contribution in the evaluation and preparation of my thesis.

I thank to Prof Dr Orhan ADALI, Assoc. Prof Dr Sertaç ÖNDE and Assoc. Prof Dr Çağdaş D. SON for their valuable comments and contributions in my thesis.

I'm grateful to Assist. Prof Dr Metin KONUŞ, Dr. Pembegül UYAR, Dr.Nizamettin ÖZDOĞAN, Assist. Prof Dr Ebru SAATÇİ, Assist. Prof Dr Gökhan SADİ, Deniz İRTEM KARTAL, Elif AŞIK, Elif SAKALLI, Bade KAYA, Melih DAĞDEVİREN, Selis YILMAZ, Derya KANÇAĞI, Deniz HİSARLI, Neşe ÖRNEK, Şule ŞAHİN, Yeşim KÜMBET, Aslıgül AKSOY, Dr. Serap TOPSOY KOLUKISA, Associate Prof Belgin İŞGÖR, Associate Prof Dr Serpil OĞUZTÜZÜN, Associate Prof Dr Gülçin CELEP, Nermin ŞAHAN, Suna GÜL, Assist. Prof Dr Cengiz BALOĞLU, Dr. Tufan ÖZ, Assist. Prof Dr Şevki ASLAN, Volkan YILDIRIM, Dr. Burcu TEFON, Orhan ÖZCAN, Dr. Serdar KARAKURT, Dr. Kubilay YILDIRIM, Evrim YILDIRIM, Oya ERCAN AKÇA, Ceyhun KAYIHAN, Melih ONAY, Hamit BATTAL, Taner TUNCER, Associate Prof Dr Ferhat CELEP, Associate Prof Dr Evren CABİ, Dr. Babacan TAŞDEMİR, Central Laboratory team and all other friends for their helps and encouragement.

For their never-ending helps and support, thanks to my father Yusuf YILMAZ (and also, for his inestimable contribution in collecting needle samples in all seasons), my mother Haney YILMAZ and my brother Muharrem YILMAZ…

Thanks to my uncle Associate Prof Dr İbrahim ŞAHBAZ for his valuable support, comments and advices.

I commemorate my grandmother Tamiş ŞAHBAZ whose advices helped me in my all life, so far.

Thanks to OYP program that supported my research and provided the budget for my travel to Germany and thanks to TUBITAK that supported me with a fellowship during my PhD education.

And thanks to my lovely wife Sevgi YILMAZ for her endless patience, invaluable support and eternal love that strengthen my will to complete this thesis in the best way.

TABLE OF CONTENTS

LIST OF FIGURES

FIGURES

LIST OF TABLES

TABLES

ABBREVIATIONS

ABC	Ammonium bicarbonate
AET	Anion Exchange Tip
APS	Ammonium persulfate
APX	Ascorbate peroxidase
BRUB	Britton-Robinson Universal Buffer
BSA	Bovine serum albumin
CBB	Coomassie Brilliant Blue
CCB	Colloidal Coomassie Blue
CDNB	1-chloro-2,4-dinitrobenzene
CHAPS	3-[(3-cholamidopropyl) dimethylammonio]-1-propanesulfonate
CID	Collision-induced dissociation
DDT	Dithiothreitol
DIGE	Difference gel electrophoresis
DMSO	Dimethyl sulfoxide
DTNB	5`-dithiobis-(2-nitrobenzoic acid)
ECA	Europe and Central Asia
ECL	Enhanced Chemiluminescence
EDTA	Ethylenediaminetetraacetic acid
ESI	Electrospray Ionization
ETS	Electron transport system
FASP	Filter-aided sample preparation
Fd-GOGAT	Ferrodoxin-Glutamate synthase
FTICR	Fourier Transform-Ion Cyclotron Resonance
FtsH	Filamentation temperature-sensitive H
GAPDH	Glyceraldehyde 3-phosphate dehydrogenase
GR	Glutathione reductase
GS	Glutamine synthase
GSH	Reduced glutathione
GSSG	induced GSH
GST	Glutathione S-transferases
HSP	Heat stress proteins
IAA	Iodoacetamide
IAA	iodoacetamide
ICAT	Isotope coded abundance tag
IEF	Isoelectric Focusing
IPCC	Intergovernmental Panel on Climate Change
IPG	Immobilized pH gradient
IPI	International Protein Index
iTRAQ	Isobaric tags for relative and absolute quantitation
KCl	Potassium chloride
LC	Liquid Chromatography
LHCSR	Light Harvesting Complex Stress Related
LPO	Lipid Hydroperoxide
LTQ	Linear Trap Quadrupole
MALDI	Matrix-assisted laser desorption/ionization
MCAT	Mass-coded abundance tag
MDA	Malondialdehyde
MS	Mass Spectrometry
NADP-MDH	NADP-Malate dehydrogenase
OMSSA	Open mass spectrometry search algorithm

P5C	D1-pyrroline-5-carboxylate
PB	*Pinus brutia*
PGK	Phosphoglycerate kinase
pI	Isoelectric Point
PIR	Protein Information Resource
PMF	Peptide mass fingerprint
PMSF	Phenylmethylsulfonyl fluoride
PS	*Pinus sylvestris*
PS-II	Photosystem-II
PTFE	Polytetrafluoroethylene
PTM	Post-translational modification
PVPP	Polyvinylpolypyrrolidone
RCA	Rubisco activase
ROS	Reactive Oxygen Species
RP-HPLC	Reverse Phase-High Performance Liquid Chromatography
SDS	Sodium dodecyl sulfate
SIL	Stable Isotopic Labelling
SOD	Superoxide dismutase
SPP	Sucrose phosphatase
SPS	Sucrose phosphate synthase
SuSy	Sucrose synthase
TBA	2-thiobarbituric acid
TCA	Trichloroacetic acid
TEMED	N, N, N′, N′-Tetramethylethylenediamine
TK	transketolase
TOF	Time of flight
UDPGP	UDP-Glucose Pyrophosphate

CHAPTER 1

INTRODUCTION

1.1. Global climatic change and its consequences

Atmospheric circulations, the sun, activities of volcanoes and many other natural factors shape the climate of earth and generate changes in considerably long time intervals. However, especially in the last century, human activities have become the dominating force in climate change. The magnitude and the rate of this change are correlated with the amount of greenhouse gases and aerosol emissions, and also, the sensitivity of the climate itself. The IPCC (Intergovernmental Panel on Climate Change) reports claimed that the increase especially in the amount of greenhouse gases will continue till the end of 21st century.

Climate change can be divided into spatial and temporal changes in weather (e.g., precipitation and air temperature) and changes in atmospheric chemistry (e.g., CO, O_3, NO_X, and SO_X) (McNulty, 1996). Those changes directly affect the temperature, atmospheric gases (such as carbondioxide) and even sea levels besides some other variables like the frequencies and the numbers of floods, droughts and freeze incidents which are supposed as the secondary impacts. In Mediterranean region, those secondary impresses will probably take more important roles in shaping the habitats by changing precipitation pattern, moisture availability and the frequency and severity of extreme events. For the regions where annual precipitation decreases, droughts are likely to become more. For areas where opposite conditions are consistent, floods are common. Furthermore, warmer conditions over the Mediterranean region will probably generate an increase in the occurrence of extremely high temperatures.

1.1.1. Climatic Changes in Euro-Asia Region

Europe and Central Asia (ECA) region is assailable to the consequences of changing climate. The extremes such as heat waves, floods, droughts, windstorms, and forest fires together with changing hydrology and warmer temperatures throughout the year affect the countries in this area. Moreover, experts claim that even if we stop the world emitting CO_2 anymore, the concentration of greenhouse gases already in the atmosphere would still cause similar or greater changes.

Meteorological measurements have already stated 0.5^{o} C of increase in the average temperatures for south of Euro-Asia region and this increase is even higher in north as 1.6^{o}C pointing an overall 1.6- 2.6^{o}C of elevation by the middle of the century. Such an increase in the temperature will cause glaciers to be melted and a considerable decrese in the total snowfall in winter season. Many ECA countries experience floods in winter and droughts in summer seasons which might dispatch the region with severe water-shortage (The World Bank Report, 2009).

Baettig *et al* (Baettig, 2007) proposed an index describing the strength of future climate change with respect to natural variabilities of today and it points that Russia, Albania, *Turkey* and Armenia are the ECA countries that are most exposed to increased climate extremes.

1.1.2. Climatic Changes in Turkey

In recent years, statistical records in Turkey showed that climate has been clearly changing throughout the country. Synthesizing the observed changes yields the following conclusions regarding Turkey's current climate:

*a general upward trend in average air temperature especially in southern region,

*distinct and widely distributed warming trends seen in minimal air temperatures in spring and summer

*rapid urbanization in Turkey has a large effect on these warming effects at minimal temperatures

*general trend in maximal temperatures are in an upward trend in summer seasons

*significant precipitation decrease trends are seen in winter seasons

*significant precipitation decrease periods of North Atlantic Oscillation are corresponding to strong positive anomaly periods (The Ministery of Environment and Forestry, 2010).

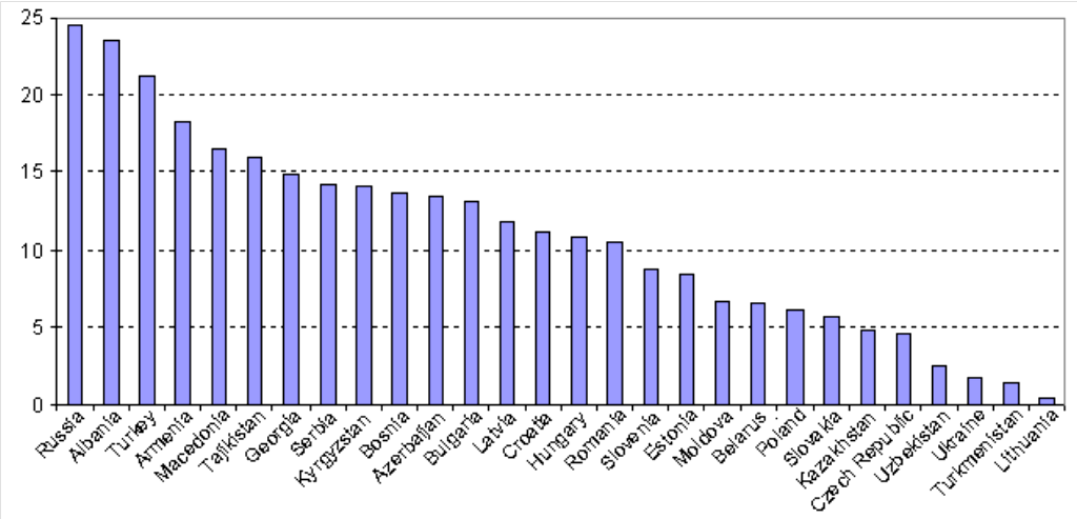

Figure 1.1 ECA countries which are judged to encounter extreme climatic events by the end of 21st centuary. The vertical axis demonstrates the number of climate extremes in the period of 2070-2100 apart from the ones that have already been faced by those countries (The World Bank Report, 2009)

IPCC, also, alert Turkey for future climate change and probable consequences in its Fourth Assessment Report because Turkey is located in the Eastern Mediterranean basin where countries are in the highest risk group. Ecological and meteorological models showed an overall reduction in summer moisture availability in response to rising concentrations of greenhouse gases (IPCC, 1996).

Because of the fact that it is surrounded by seas (Mediterranean, Black, Aegean, and Marmara) Turkey is highly vulnerable against climate change (Figure 1.1 and Table 1.1)). Karaca (Karaca, 2008) states that a 1m of rise in the sea level would affect almost 30% of all the Turkish people who populates coastline.

Table 1.1 Reported increased incedence of weather-induced disasters in Europe and Central Asia (The World Bank Report, 2009)

Country	Hazard
Bulgaria	Cold wave, floods
Croatia	Floods
Czech Republic	Cold wave, floods
Estonia	Cold wave
Hungary	Wind storms, floods
Latvia	Snow fall, extreme cold, power shortage
Lithuania	Snow fall, extreme cold, power shortage
Moldova	Snow fall, extreme cold, power shortage
Montenegro	Floods
Poland	Cold wave, floods
Romania	Cold wave, floods
Russia	Cold wave
Serbia	Floods
Slovakia	Floods
Turkey	Cold wave, floods

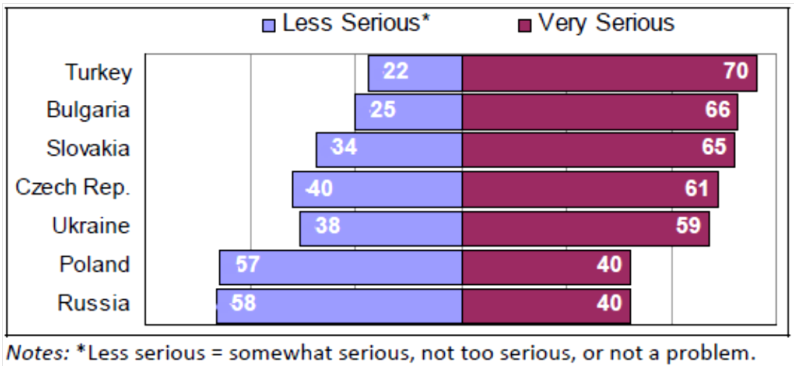

Figure 1.2 "In which degree people aware of the climate change?" Some of the results of a survey on the full sample of 48 countries (The World Bank Report, 2009)

Agriculture needs to be paid attention because scientific reports on the climate change and its possible effects in near future states that it would be the most vulnerable sector in Turkey. European Environment Agency (European Environment Agency, 2010) pointed the thread of changing climate on the water sources that is highly critical for rural areas where the agriculture is the main meal ticket of local people. Although the majority of Turkish people are aware of the consequences of the situation (Figure 1.2), there are still important precautions for the Turkish government, especially for sustainable agriculture and forestry.

In the report of World Bank (The World Bank Report, 2009) scientists claimed that Turkey will suffer of the various effects of climate change in different ways. The overall decrease in the annual precipitation and increased number of storms and floods will cause more soil erosion and salinization, increased evapotranspiration and increased irrigation demand which in turn would create a higher stress on water supplies. This will especially influence the south part of Anatolian Peninsula where large forests recline towards Tauros Mountains. The higher average temperatures, heat waves and drought in summer seasons will lead shorter development periods for almost all plant species and tree species will become very vulnerable to storms and increased pest thread.

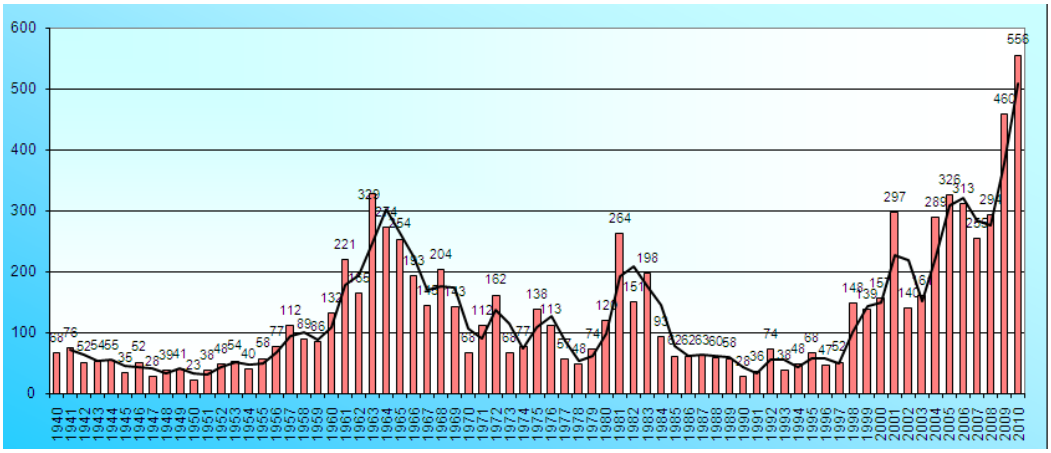

Figure 1.3 The number of the extreme cases that caused harm in Turkey, from 1940 to 2010, increased in between the years 1960-1970, 1981-1983 and 2001-2010. In 2010, totally 556 extreme weather cases had been detected (TC Çevre ve Orman Bakanlığı, 2010).

In summary, natural life in Turkey is under the thread of rapid and devastating changes in the climate (Figure 1.3), and this situation forces the government to develop new strategies in conservative politics for environmental (ecological and biological) issues. This trend would make the people search for effective solutions in all fields including forestry. Developing/breeding new lines of forest trees resistant to those climatic extremes will be a part of all programmes suggested in near future.

1.2. Two pine species: *Pinus brutia* and *Pinus sylvestris*

1.2.1. Classification of species

Pinus brutia Ten (Turkish red pine) is a member of Division Gymnospermae, Class Coniferae, and Family Pinaceae, Genus *Pinus* L. Turkish red pine is a coastal tree and it is one of the most resistant pine species of Mediterannean basin for water scarsity.

"The Turkish pine is a tree to 27-35 m, with a usually open crown of irregular branches. The bark on the lower trunk is thick, scaly, fissured, and patterned red-brown and buff, and thin, flaky and orange-red higher in the crown. The shoots are slender, 3-7 mm thick, grey-buff, and rough with persistent small decurrent scale-leaf bases. The winter buds are ovoid-acute, with red-brown scales with long free tips revolute and fringed with white hairs. The adult leaves are retained for 1.5-2.5 years, with a persistent 1-1.5 cm sheath; on most trees they are in fascicles of two, and 10-18 cm long. They are bright green to yellow-green, slender, about 1mm thick, with serrulate margins, fine lines of stomata on both faces, and several marginal resin canals. The juvenile leaves are glaucous, 1.5-4 cm long, and continue to be grown for 2-4 years, mixed with the first adult foliage produced from 9 months from seed. The cones are erect to forward pointing on short stout stalks, symmetrical, broad conic, (4-) 6-10 (-12) cm long, 4-5 cm broad when closed, green, ripening shiny red-brown in April two years after pollination. They open the same summer or 1-2 years later, to 5-8 cm broad, though the seeds are often not shed till winter rain softens the scales. The scales are short, broad, thick, woody, and very stiff; the apophysis is 10-15 x 15-20 mm, smoothly rounded, with a slight to moderate transverse ridge; the umbo is dorsal, flat to slightly raised, 5-7 mm wide, and grey-buff. The seeds are grey-brown, 7-8 x 5 mm with a broad, auricled 15-20 x 10 mm wing, yellow-buff streaked darker brown" (Tenore, 1811).

"*Pinus sylvestris* is a tree to 25-40 m tall and 0.5-1.2 m dbh. Stem straight (contorted only if lead shoot damaged when young, often by pine shoot moth *Evetria turionana*). The crown is variable, with a variety of shapes common in wild populations from level branches to near-fastigiate; open ovoid-conic when young and usually eventually becoming dense, broadly domed or even flat-topped. Bark on lower stem thick, scaly-plated, grey-brown; on upper stem and branches, thin, flaking, orange-red. Branching uninodal. Shoots green at first, becoming grey-buff by the end of the first summer. Buds ovoid-conic, orange-brown, thinly to occasionally thickly covered in white resin. Leaves in fascicles of two, (2.5-) 4-6 (-9) cm long, 1.5-2 mm wide, always moderately to often strongly glaucous (the only two-leaved hard pine with blue-green or grey-green leaves - an easy pine to identify), longest on vigorous young trees (5-9 cm), short on old trees (2.5-5 cm), commonly slightly twisted, margins finely serrulate; persistent for 2-6 (-9) years; leaf sheath grey, 5-8 mm, slowly eroding to 3-4 mm by leaf senescence. Male cones 8-12 mm, yellow or pink. Cones (2.5-) 3-

6 (-7.5) cm long, conic, symmetrical or nearly so, green ripening matt grey-buff to grey-green; mature in November-December, 20 months after pollination, opening from February to April and falling soon after seed shed; scales rhombic, flat to protuberant and (rarely) hooked (with a full range of variation inbetween), with a minutely mucronate dorsal umbo. Seeds black, 4-5 mm, with a 12-20 mm wing" (Linnaei, 1753).

1.2.2. Distribution of species

Turkish red pine is a coastal tree and when compared with other timber species found in the same region, it withstands more aridity and poor soils. *Pinus brutia* is the dominant tree of forests located in the Mediterranean, the Aegean and the Marmara regions. They range from the sea level up to 1500 m in the Mediterranean region, 700-800 m in the Aegean and 300-400 m altitude in the Marmara region (Kaya, 2001). Although it requires mild winters, it has some populations at drier and cooler climates (Gezer, 1986).

Pinus brutia shows a relatively restricted distribution, especially in the Mediterannean region (Figure 1.4). It is distributed to Italy, Greece, Cyprus, Syria, Lebanon, Jordan, Palestine, and the many islands of Aegean and Mediterannean, northern Iraq and over the north coast of Crimea (Gezer, 1986). However, this conifer species is found largely in the Eastern Mediterranean region and primarily (85% of all natural populations in the world) in Turkey (Boydak, 2003) where this species grows in southern and western Anatolia and is also found in the Marmara region. It is rarely found on the coastal areas of interior Black Sea region at the bottom of the drier and warmer valleys, too.

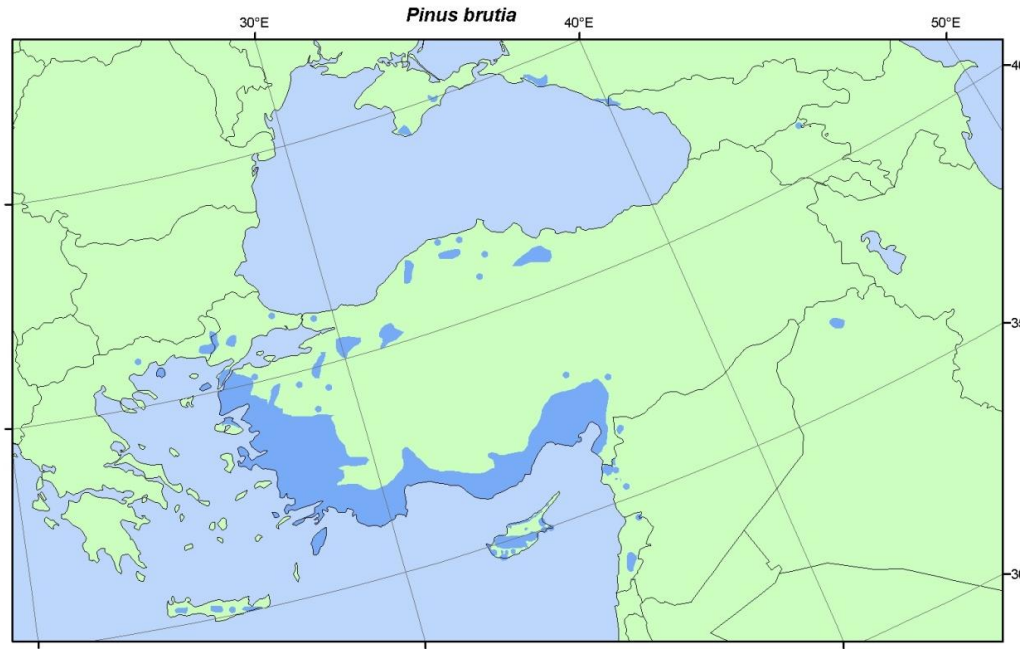

Figure 1.4 Distribution of Turkish Red Pine (*Pinus brutia*) (EUFORGEN, 2008)

The climatic conditions in the growing range of *P. brutia* are mild during whole year and the annual precipitation is adequate, but it is poorly distributed throughout the year. In its natural habitat, frost is rare but very high temperature values and water stress for long periods are observed in its growing season. Because of the fact that the moisture is adequate, it can resist the temperature stress. *P. brutia* is found in localities which have precipitation as low as 412.8 mm annual average and only 128.4 mm average in its growing-season. In Muğla and Antalya regions where are primary commercial areas, the average annual precipitation is about 1200 mm, and 250-350 mm of this amount falls during the growing season (Gezer, 1986). For this species, the average annual temperature range is 12.5- 22.9^{o}C and the minimum and maximum annual averages are 1.4-8.1 ^{o}C and 18.1- 22.7 ^{o}C, respectively.

Prof Işık and his colleague (Kurt *et al*, 2011) reported that *P. brutia* is a complex species with regional adaptations including the elevation. The relatively higher intraspecific variations like many other conifer species make these plants hard to study in a genetic research and to suggest common generalizations. There is not enough evidence to establish a clear association between discovered genes and phenotypic measurements. One important reason of such a situation for pine species is basicly their enormous genome size. Pine species have genome sizes of 18000-40000 Mbp with 2n=24 chromosomes and it is clear that conifer genome complexity is enormous compared to typical diploid angiosperms (Morse *et al*, 2009). Grotkopp *et al* (Grotkopp *et al*, 2004) stated that genome size is one of the major actors shaping the life-history traits of many plant species. Correlated evolution of these traits and their molecular bases are still beyond a complete understanding. For Mediterranean pines, the lack of a consistent phylogeny has prevented revealing the evolutionary relevance of phenotypic traits (Grivet *et al*, 2013).

At this point, we should consider the effect of climate change on the distribution of this species in Anatolian Peninsula; Kandemir *et al* (Kandemir *et al*, 2010) informed that the 2-3 degrees of temperature increase and a 20% decrease in precipitation would lead an expand in the range of natural populations. Such a situation makes it more difficult to prepare conservation programmes for sustainable management of this species in near future.

Pinus brutia Ten. is an economically important forest tree species for Turkey (Figure 1.5); its wood is an important export good as travers. In addition, Turkish red pine is used in local needs like in packing industry and in resin gum production (Aslan, 1994). The timber of *Pinus brutia* is used in a very wide range from fencing posts through telephone and transmission poles to pit wood, railway sleepers and saw logs for box-making, general construction and joinery industries, its wood is also suitable for pulp and board manufacture (Gezer, 1986).

P. brutia is a commercially important forest tree species in Turkey because red pine forests cover an area of larger than 4 million ha and its relatively short rotation and high growth rate make this conifer species a very valuable source in forestry. In reforestration issues of fire damaged sites, clear-cutting with direct seeding is used; so, the seed germination and survival of different populations have great importance for natural or artificial regeneration (Boydak, 2003). This means that the future of this species (like many others) depends on genetic diversity among populations and even individuals.

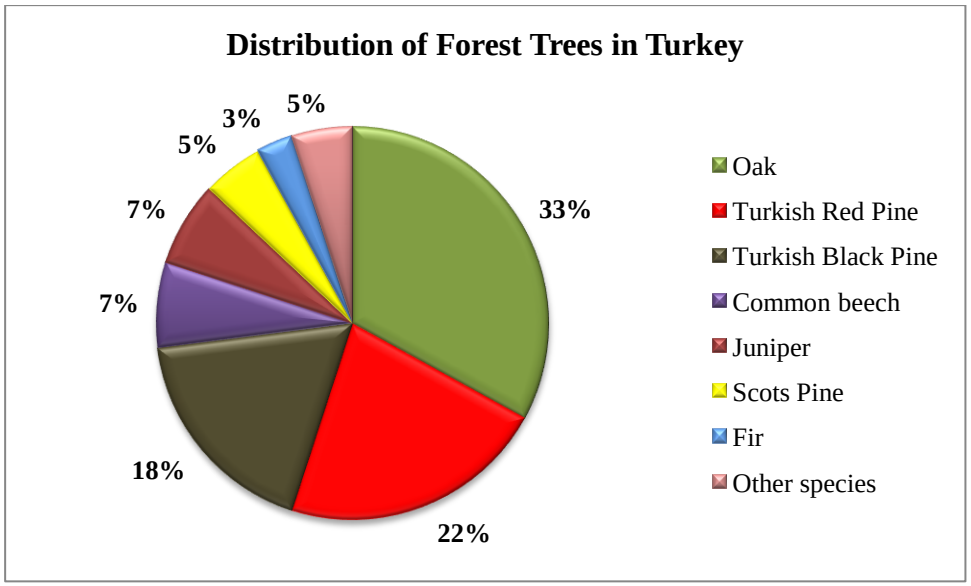

Figure 1.5 Distribution of forest trees in Turkey; *Pinus brutia* (Turkish red pine) covers 4,167,524 ha of total area (approximately 22% of all forests of Turkey) (Türkiye Çevre Atlası, 2004)

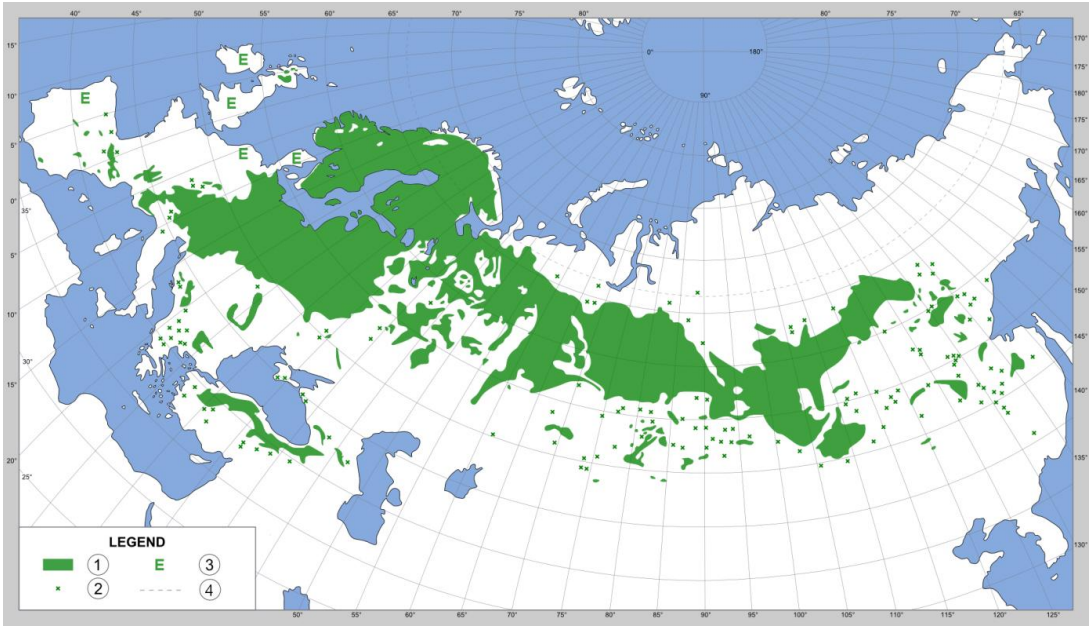

Figure 1.6 Distribution of Scots Pine (*Pinus sylvestris*) (EUFORGEN, 2009)

With a natural range from the Arctic Circle in Scandinavia to southern Spain and from western Scotland to the Okhotsk Sea in eastern Siberia, *P. sylvestris* is the most widely distributed conifer in the world (Figure 1.6). It grows from sea level to elevation reaching 2500 m (Labra, 2006). *P.* sylvestris var. hamata is native to the Balkan Peninsula, *North Turkey* and South-West Transcaucasia, at altitudes of 500-2600 m. (derived from www.conifers.org)

1.3. Proteomics

1.3.1. General concepts and definitions

Marc Wilkins coined the term ‘‘proteomics’’, during the 1994 Siena Meeting, to simply refer to the ‘‘PROTein complement of a genOME’’ (Wilkins & Appel, 2007).

Although all the cells of an organism have essentially the same genome, under specific conditions and at some time intervals, the set of all expressed proteins in some of them may vary. Because of this fact, the term *proteome* may have the meanings either the all the proteins encoded by the genome of a species and/or the set of proteins expressed in a particular cell (or tissue or organ) at a particular time and under specific conditions. So, *Proteomics*, as a term, can be defined as the study of the subsets of proteins located at different parts of the cell or organism, and all the scientific techniques reveals how those proteins are changed with time and different conditions.

Proteomics have two approaches: *top-down proteomics* and *bottom-up proteomics*. In the top-down paradigm, intact proteins are directly used for the analysis. The other one needs those macromolecules to be digested into relatively smaller parts. After that, identification, characterization, and quantification issues could be completed according to the main peptide properties. *Peptide mass fingerprinting* (PMF) is the process of comparing experimental masses of those peptides to theoretical masses (Eidhammer *et al*, 2007).

1.3.2. General techniques and computational methods

The experimental design of most proteomics studies includes three steps: sample preparation, separation by electrophoresis or chromatography and at last, the MS analysis of the isolated proteins.

1.3.2.1. Sample preparation

Sample preparation is not the only step, but it is one of the most critical steps in proteome research. The quality of protein samples is critical to generate accurate and informative data. There are two sets of aspects for sample preparation in proteomics:

Technically dependent aspects includes all technical hardware and software in the research center, experimental setting, handling of data flow, usage of various chemicals/reagents for their possible negative effects on further analysis, the number of samples and finally the total cost.

Sample-dependent aspects consider the origin of the sample, the localization of the protein(s) of interest, evaluation of the amount/abundance of the targets, recovery, stahndardizaton and the storage of the proteins after isolation procedure, determination or the accommodation of the internal standard(s) especially for quantitative affairs, innovation of a universial procedure for protein isolation from different tissue types (Andrecht & von Hagen, 2008).

Because of those aspects, it is almost imposible to assert a standard method for the preparation of protein samples for further analysis by MS. At this point, workflows that incorporate subcellular fractionation, optimized cellular lysis, removal of highly abundant proteins or enrichment of selected proteins, and mass tagging tools enable us to perform quantitation of proteins in complex samples.

In MS analysis, the proteins of interest are found in a complex mixture with other proteins, and this generates two important problems: First, the ionization techniques work better when the mixture contains roughly equal amounts of constituents. However, in nature, the dynamic range of protein concentrations in biological samples may exceed 10 orders of magnitude. When those mixtures are ionized without preliminary processes, the more abundant species may suppress the signals of less-abundant ones. Secondly, because of the number of components, the mass spectrum of a complex mixture is very difficult to fully analyze. In short, the success MS and/or MS/MS depends on clean samples with limited complexity and prevention of MS undersampling of eluting peptides. At this point, a relatively new and promising method can help researchers: *Filter-aided sample preparation (FASP)* includes the complete solubilization of the protein extract in SDS, which was then exchanged by urea on a standard filtration device. Pure peptides are eluted after digestion (Wiśniewski *et al*, 2009).

1.3.2.2. Isoelectrical Focusing (IEF) and 2D-PAGE

Separation on isoelectric point is performed by *isoelectric focusing (IEF)*, where a *pH gradient* is used for the separation. The proteins are moved into the gradient by absorption from a buffer with the sample (preferably by the help of electric current). In the next step, an electric field movesall the proteins towards the opposite charge. When the protein reaches the point in the pH gradient equal to its pI, the net charge becomes zero, and the migration ends. IEF is completed with SDS-PAGE for better separating power in a so-called 2D SDS-PAGE method. Despite its relatively higher resolution, there are some foibles, too. The very small or very large proteins might be lost during gel electrophoresis and the ones with low-abundancy might remain unstained and escape detection. The hydrophobic proteins might form complexes and precipitate before they could be loaded, while the proteins possessing pI values that were out of the range usually fall off the edges of the pH strip (Eidhammer *et al*, 2007).

Sample preparation for two-dimensional electrophoresis is the most crucial part of proteomics techniques. Plants and especially green plant tissues originate considerable challenges here, because of low protein concentration and the presence of deleterious compounds in the cell. Remarkably stable plant proteases may increase the challenge because of their being persistently active in various conditions such as low/high pH, low temperature, high amounts of urea and/or guanidine hydrochloride (Flengsrud, 2008).

Another handicap about 2D-PAGE electrophoresis is created by the fact that any spot containing more than one protein might be considered as a single protein type and this would lead a false-positive result in quantitative studies. Moreover, even if the spot is known to hold more than one protein, it is not possible to trace back which protein contributed which amount of staining to the spot. Moreover, if there are modifications on the protein (or, a

percentage of it have modifications or truncation), then, more than one spot located at different parts of the gel should be considered together for a correct total quantification. Any missed spot which might be, also, a result of the usable interval of staining procedures causes an underestimation of the quantification (Eidhammer *et al*, 2007).

1.3.2.3. Mass Spectrometry: MS and Tandem MS (MS/MS)

When mass spectrometer was first introduced, it was preferred for mass determination and structural investigations of volatile molecules and molecule fragments because those first systems were not proper for the analysis of such big and complicated molecules like proteins and peptides. Furthermore, under the high-energetic electron bombardment they would disintegrate into countless components (Rehm, 2006). However, by the introduction of various ionization techniques suitable for peptides and protein molecules, a new era has begun in biological and biomedical sciences (Kinter & Sherman, 2000). The speed of mass spectrometric experiments and the amount of information they generate, which could be derived from multiple proteins at a time, make MS applications much more popular.

Mass analysis is essentially a separation of ions according to their *m/z ratio.* The term "tandem mass spectrometry" defines two stages of mass analysis: using first separation as a preparative tool to collect an ion with a specific *m/z* and perform further analysis by fragmenting it and determining the *m/z* of the fragment ions to declare the structure (Kinter & Sherman, 2000). One mass spectrometry analysis is sufficient for measuring the masses, using an MS instrument (Figure 1.7) but for the analysis of the sequence, two mass analyses are used in the MS/MS-capable instruments (Figure 1.8).

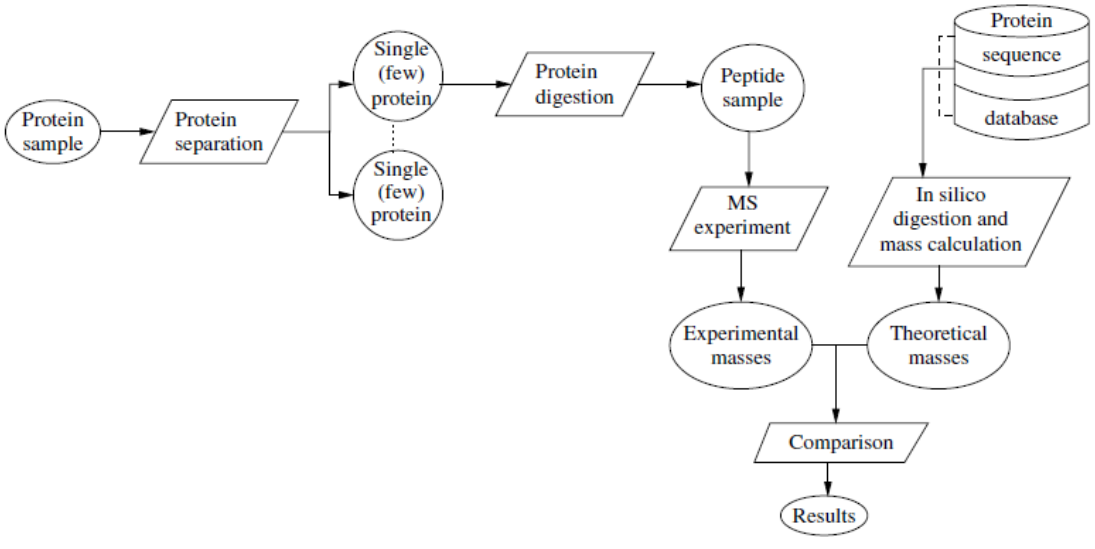

Figure 1.7 MS protein analysis approach (for proteins) (Eidhammer et al, 2007).

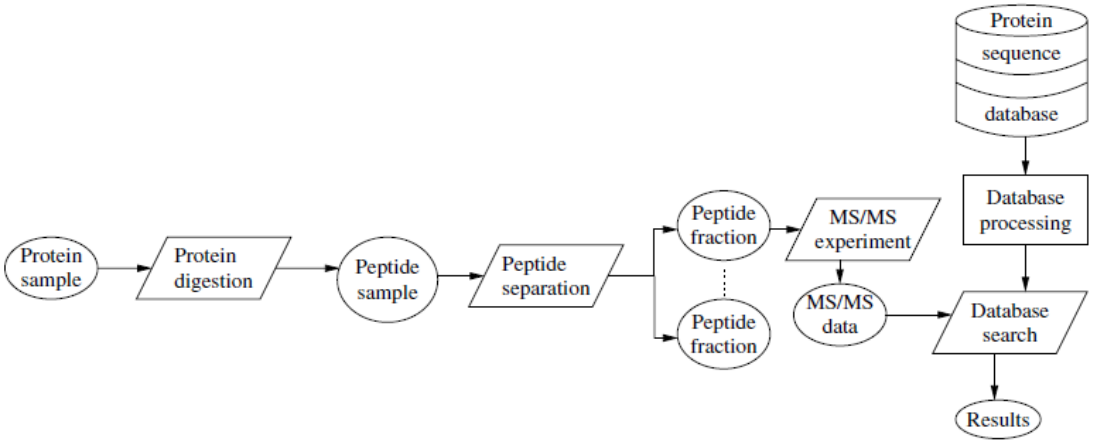

Figure 1.8 MS/MS protein analysis approach (for peptide residues) (Eidhammer et al, 2007).

1.3.2.3.1. Instruments used in research

High Performance Liquid Chromatography (HPLC), which is a chromatographic technique that is used to separate the components of a mixture for identification and quantification purposes, is a fixed component of a group of MS systems routinely used in the research laboratories. The two most common HPLC methods in proteomics are *reverse phase chromatography* (RP-HPLC) and *strong cation exchange chromatography*. The eluate of the RP-HPLC may be loaded directly into a mass spectrometer by electrospray ionization. In this type of chromatography system, there are two solvent systems denoted by A (mostly water with a small amount of organic acid-often 0.1 % formic acid) and B (an organic solvent such as acetonitrile); and after the sample proteins that are dissolved in solution A are bound to the column, solution B is gradually pumped into the system to collect the fractions with respect to this gradient solvent system. When the gradient reaches 60 % organic solvent, all peptides are normally eluted from the stationary phase. The criteria of separation is rooted by the fact that the speed of a component's migration through the column depends on the properties of the peptides, the dimension of the column, the temperature, the chemistry of the stationary and mobile phase and the speed of the mobile phase. The time between sample application and the detection of the maximum peak is called *Total retention time*, t_R, and, *the dead time*, t_0, is the time it takes for a non-interacting component to elute through the column from the point of injection (Eidhammer *et al*, 2007).

In HPLC analysis, if all the conditions are kept constant, subsequent applications of the same analyte give the same retention time pattern. "Therefore, with a theoretical model for calculating the retention time from a peptide sequence, a measured retention time can be compared to calculated retention times for possible theoretical peptides" (Agrawal & Randeep, 2008). The main factor which shapes the retention time for RP-HPLC is the hydrophobicity of the sample peptide molecule, so, by assigning a *retention coefficient* for each amino acid based on this property, one could calculate a rough value for the whole peptide molecule by the sum of the retention coefficients of all the residues, plus coefficients for the end groups, plus dead time.

In a classical MS based quantification study, the *retention time alignment* should be performed by using all identified peptides in more than one sample set. In all samples, the retention time of the first identification is recorded for each peptide residue. Then, the average retention time for a specific peptide measured for every sample is subtracted from the one of a certain sample, resulting per peptide retention time alignments for every sample. The median of the peptide retention time differences of a sample is used to demonstrate the shift in this parameter for a whole sample set. This is used for the correction of the retention times of the raw quantification results (Terashima & Hippler, 2010).

Very schematically, a mass spectrometer consists of three main parts: the *ionization source*, the *mass analyzer*, and the *detector* (Figure 1.9). All mass spectrometers use electric or electromagnetic fields to move the sample. Therefore, the ionization of the components before entering these electric fields is obligatory and this crucial step is performed by ionization source. In the next stop, the mass analyzer separates ions according to the mass-to-charge ratio (m/z). In the last part, a detector unit creates a *mass spectrum* that is a graph of which horizontal axis shows m/z ratio while vertical one demonstrates the intensity of the signal for each component (Agrawal & Randeep, 2008).

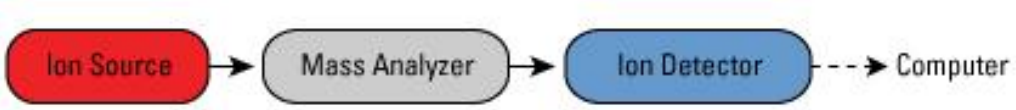

Figure 1.9 Basic components of a mass spectrometer (derived from the official website of Piercenet, ThermoScientific)

Matrix-Assisted Laser Desorption Ionization (MALDI) and *Electrospray Ionization (ESI)* are two popular soft ionization sources which generate only a limited number of fragments. MALDI is generally used in MS applications (and occasionally in MS/MS issues) because the resulting peptide ions generally have the charge +1. ESI, on the other hand, is mostly used with MS/MS systems because most of the ionized peptides carry two or more protons which enable the system to create charged fragments in the analyzer unit. In this system, the peptides are brought into the ionization source by a liquid flow mostly fed by a HPLC unit (Agrawal & Randeep, 2008).

There are different mass analyzers with different principles:

In the MALDI *time-of-flight (TOF)* mass analyzer, due to the short laser pulses, ions are sent to the analyzer in short pulses and accelerated by an electric field to force them enter a field-free drift tube. The mass to charge ratio of the ions is the factor that determine their velocity, and this velacity is used to calculate the m/z ratio by measuring the time spent by the ions in the drift tube (Agrawal & Randeep, 2008). A *quadrupole* analyzer has four parallel rods of which each of two forms an electrically connected pair, and by the application of a radio-frequency voltage those pairs generates an oscillating field. This system filters the ion mixture in a way that the ions with a specific *m*/*z* value are stabilized in this field at a specific voltage, and the rest crashes to the rods. For MS/MS issues, this system is constructed as a triple quadrupoles and commonly in combination with a TOF mass analyzer. The *ion trap* mass analyzer consists of one ring electrode and two end-cap electrodes allowing the 3D trap of the ions. The analyte is pumped into the system by pulsing

of the ion gate, unlike the quadrupole where there is a continuous ion entrance into the chamber. Another difference of this relatively cheaper, faster and high throughput system with respect to quadrupole analyzers, all steps of mass analysis could be completed in the same part of the system although there might be a loss in mass accuracy because of space-charge effect. *Collision-induced dissociation (CID)* is the process by which the collision of the helium molecules with precursor ion results in fragmentation which could be recorded in the form of MS/MS spectra. Ions are trapped in a 3D space in *Fourier Transform-Ion Cyclotron Resonance (FTICR)* (Alan & Marshall, 1998) like ion trap analyzers, however, in FTICR; a static magnetic field is used to keep ions in an orbit till the one group in this mixture was excited to be separated by an oscillation in electrical field. The detector plates measure the change in the radius of the circular motion and at the end there exists an image current. The mass spectrum is handled after the Fourier-transformation. Although FTICR is an expensive and highly complicated option for researchers, the ions are measured more than once that increase the accuracy dramatically and they are not harmed by moving in an orbit without crashing any surface which affect the quality of the procedure positively.

The *Orbitrap* is the last mass analyzer system derived from the FTICR by the usage of ion trap technology which is based on the electrostatic quadro-logarithmic field created by a set of barrel shaped electrodes.When the trapped ions around the central spindle are oscillated, there exists a current image of which the frequency change points the m/z ratio of the molecule after Fourier-transformation (Hu, 2005) (Hardman & Makarov, 2003). Besides being relatively cheaper to work with, Orbitraps have high sensitivity, resolution and mass accuracy like FTICR.

The *noise* is an important problem in mass spectrometry issues. It is grouped in two types as *chemical noise* which may be generated by either the chemical contaminants such as detergents, polymers, salts etc. or proteins or peptides that have been unintentionally introduced during sample handling such as human keratins. *Electronic noise* is the result of electronic disturbances, and occurs with random fluctuations between the chemical noise (Agrawal & Randeep, 2008).

1.3.2.3.2. Software for data analysis: Identification and Quantification

Mass spectrometry is used for three general purposes:

(i) qualitative analysis
(ii) quantitative analysis
(iii) sequence analysis

A qualitative measurement aims to detect the number of different peptides in a sample by claiming resolved peaks with respect to some important performance criteria. Mass spectrometry can be used for quantitative issues; after some alignment and normalization procedures, the comparison of peak heights or peak integrals may give valuable information on mass differences of the particles under consideration. Finally, mass spectrometers can unravel the amino acid sequence and possible post translational modifications (PTMs) of the peptides in a sample.

1.3.2.3.2.1. Identification

Protein identification can, basicly, be performed by comparing the experimental outcomes to the calculated properties of the proteins. The general procedure has three main steps:

(i) Determination of the appropriate protein database.
(ii) Comparison of the detected properties to the documented ones to chose the one which fits best.
(iii) Running a probability test to check whether the protein nominee is the same with our unknown one.

The most common protein sequence databases are Universal Protein Resource (UniProt), the The National Center for Biotechnology Information (NCBI) database and The International Protein Index (IPI). *UniProt KnowledgeBase* has three main bases: The *Swiss-Prot*, *TrEMBL* (Translated EMBL), and *PIR* (Protein Information Resource) databases. In order to establish which annotations are clearly supported by trustworthy evidence, various information sources are delibrated and cross-verified during manual curation process. *NCBI database* cluster sequence data from a variety of sources such as TrEMBL, Swiss-Prot and RefSeq which is composed of two types of entries: NP that has various evidences for its validity and XP which is a predicted one (Eidhammer *et al*, 2007).

The identification of proteins with MS is done in a database-dependent or -independent manner. *Peptide mass fingerprint (PMF)* is one of the fastest methods to identify proteins, and it does not require MS/MS. *Peptide fragmentation identification* and *de novo sequencing* both need MS/MS data, while the latter one does not use a database as a reference (Figure 1.10).

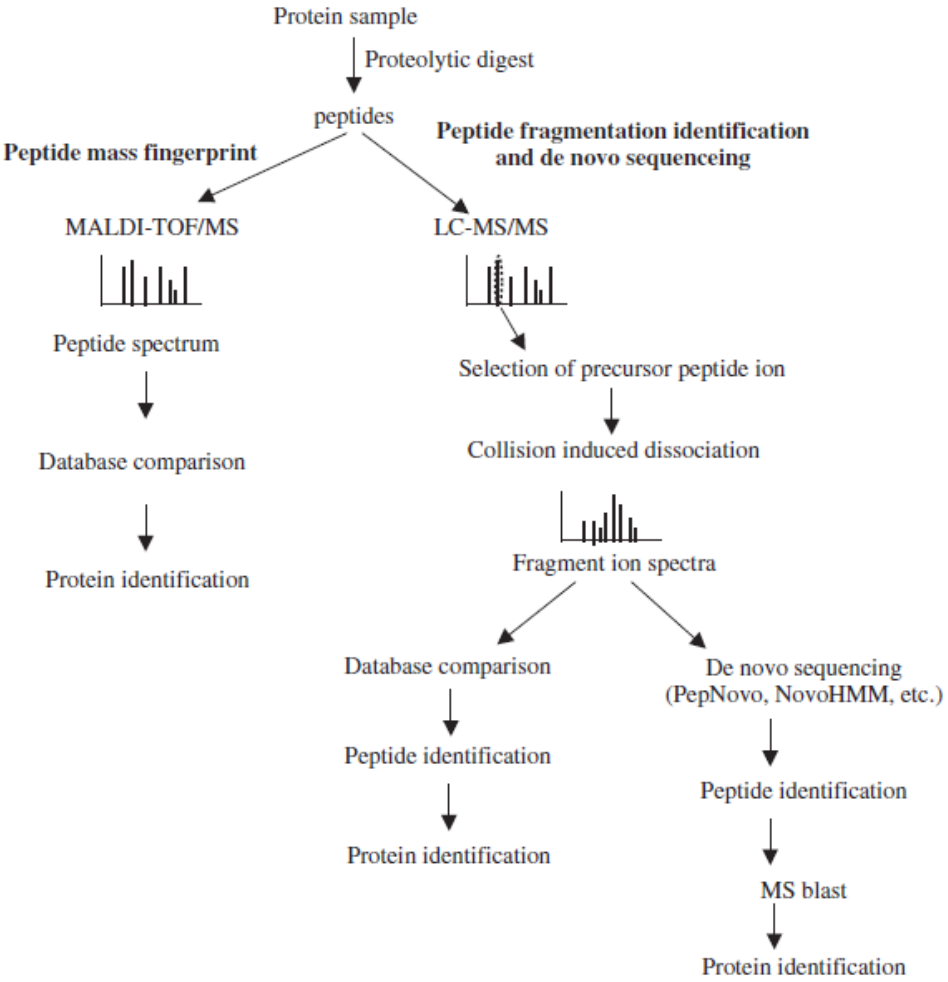

Figure 1.10 Differences between PMF, peptide fragmentation identification, and de novo sequencing (Agrawal & Randeep, 2008)

A general approach for PMF starts with the separation of the proteins by 2-DE. When the spots are visualized and cut-off for digestion, peptide particles are produced by enzyme applications like trypsin. Then, MALDI-TOF analysis and the MS spectrum reveal the experimental results of peptide sequences which are compared with the genomic data *in silico*. The products of theoretical digestion of the protein sequences provided by the database are compared to the protein of interest. Statistical softwares present a respective score to be used in evaluation of the matching. Although this approach is straight-forward and effective, the presence of post translational modifications and the fact that one spot on the 2-DE gel might contain more than one protein species, it is still complicated to use it.

Peptide fragmentation identification starts with the fragmentation of peptides in specialized chambers of MS/MS systems. Computer softwares compare the results of fragmented ion patterns with the ones produced from the database provided peptide sequences. By this way, both the peptide mass and amino acid sequence information is obtained. The correct peptide interpretation is based on MS/MS search algorithms that are provided by search engines such as Mascot™ (Perkins, 1999), SEQUEST™ (Eng *et al*, 1994), OMSSA (Geer, 2004) and X!Tandem (Craig & Beavis, 2004).

Two mass analyzers and a collision cell are used to handle the MS/MS spectra of an analyte. One of the analyzers detects the mass of the precursor ion and the other one enrols the fragment ions whose types and percentages among the others mainly determined by the amino acid content. Fragmentation propagates different ions of which the most plenteous ion types are *b-ions* (if the N-terminus is included) and *y-ions* (if the C-terminus is included). The sequence of the peptide is simply guessed by considering the mass disparity between those ion series. Besides these ions, other internal fragment ions are also obtained.

1.3.2.3.2.2. Quantification

Quantitative presentation of protein species is essential for informative modeling. 2D-based proteomics allow quantification by staining of protein spots. Fluorescent probes, CBB or silver staining give acceptable evaluation of a relative expression of proteins. Staining allows generally well, though variable linearity and sensitivity of protein detection and quantification. Modified labeling of proteins with fluorescence dyes in DIGE allows evaluation of relative levels of proteins in samples that are mixed after labeling with different fluorescent dyes, and they are run in one gel. Staining is an efficient way to visualize proteins, but it provides assessment of a relative, and not an absolute, protein concentration.

There are two main approaches in MS-based quantification studies:

Stable Isotopic Labelling (SIL) is generally used to compare the expression of particular cellular proteins which are the outcomes of gene regulation and differential signal transduction between different sets of samples. In SIL-MS method, by bringing in a mass tag to the protein synthesis pathway, either control or test group is examined for any mass shift so that the tagged peptides could be considered separately in the bulk of cellular proteins and compared with the non-tagged peptides for its quantification if the two type were mixed in equal concentrations (Agrawal & Randeep, 2008).

Plant cellular proteins can also be mass-tagged through cellular metabolism in the process of protein translation either by ^{15}N universal labeling or SILAC. Because individual peptides may contain different number of nitrogen atoms related with their amino acid contents, ^{15}N-labelling may generate difficulties in assessing the peptide. Plants are autotrophs and they can use amino acid, which they absorb from the medium, to synthesize some other macromolecules. This makes it difficult to use SILAC strategy that tags a particular type of amino acid residue.

SIL is not a cost-effective method and it requires labouring sample preparation steps. The second approach in MS-based quantification contains a *label-free strategy*.

In the LC-MS spectrum, all peptide ions are individually extracted to retrieve total *signal spectral counts* using the same principle as for the labeling approach. The quantification of the relative difference of proteins in comparison between samples is performed by those spectral counts. Label-free strategy has the advantage of quantifying all the peptides unlike the labeling methods with which only the the tagged ones could be taken into consideration.

For the label-free quantitative approach, of most concern is

(i) the variability generated by experimental steps and chemicals in sample preparation and injection stages
(ii) substantiality and accuracy of LC-MS

One of the options to overcome these variables is to use the spectral count values of autocleavege products of the trypsin for normalization of the data if the total amount of this enzyme added to the analytes were the same. Moreover, the samples containing a huge number of proteins, a small percentage of them would show significant changes while the others might still to be used as in the same way defined before by the help of large-scale multiplex mathematical calculations done by automated softwares (Agrawal & Randeep, 2008).

1.3.2.3.2.3. *De novo* sequencing

Scientist commonly obtain high quality tandem mass spectral data of peptides for which no exact database match can be made, and the question remains whether these non-matching spectra are due to novel sequences, or are the result of less interesting possibilities such as interspecies variation, database sequence errors, or unexpected proteolytic cleavages (Johnson & Taylor, 1998).

In some cases, researchers need to derive the sequence of a peptide without any information provided by the database. This is referred to as *de novo* peptide sequencing. There is a wide variety of useful tools for this task such as PepNovo, PEAKS, Lutefisk, NovoHMM, InsPecT, and EigenMS, but almost all of them suffer because of inaccurate measurements, missing peaks (gaps), and noise (Agrawal & Randeep, 2008).

1.4. Scope of the Study

Pinus brutia is a native pine species to Turkey having great importance both economically and ecologically. Climate change affects Turkey more than most other countries in the same geography and this fact forces us to develop strategies to protect our forests against extreme weather conditions. Breeding new *P.brutia* lines which are relatively resistant to those environmental conditions such as low humidity, drought and harms of unexpected freezing temperatures needs an understanding of the biochemical responses of these trees to those effects. There are very limited genomic and proteomic data for *Pinus brutia* and this makes it very difficult to study on this species. For this reason, choosing of another pine species which is (relatively) well-studied was preferred to provide reference and validation for the results. *Pinus sylvestris* is one of the most common pine species on the world and unlike *Pinus brutia*, there are considerable proteomic and genomic data for it; so, by using it as the second sample in all analysis, changes in the proteome of both were aimed to be analyzed. Moreover, scots pine was adapted to survive under moderate cold stress that makes it useful to be compared with Turkish red pine which is, oppositely, adapted to live in mild even warm and relatively arid climates. Two species were targeted to be compared for three different sampling times with different stress conditions created by the seasons: hot and dry summer season, cold winter season and mild and rainy spring season which was used as a reference for other two sampling periods. Ankara, because of its climatic properties, provided all three climatic conditions so, two local populations located at the same region and almost the same elevations, in METU Campus were chosen. By this way, we had the advantage of removing the effects of different climate, soil type and elevation.

CHAPTER II

MATERIALS and METHODS

2.1. Materials

2.1.1. Chemicals and Reagents

Folin-Ciaceltau Phenol Reagent (Sigma), potassium dihydrogen phosphate (Fluka, min. 99%), dipotassium hydrogen phosphate (Merck, extra pure), reduced glutathione (GSH) (Sigma, min 99%), PVP-K30 (Fluka), hydroxymethyl aminomethane (Tris) (Sigma, min 99.9%), hydrochloric acid (Merck, 37%), Nonidet P-40 (Sigma), Bovine serum albumin (BSA) (Sigma), ethanol absolute (Riedel-de Haën, %99.8), 1-chloro-2.4-dinitrobenzene (CDNB) (Sigma, min 98%), copper sulfate (CuSO4.5H2O) (Riedel-de Haën, extra pure), sodium-potassium tartrate (Fluka, min. 99%), sodium hydroxide (Merck), sodium carbonate (Riedel-de Haën, extra pure), 2-mercaptoethanol (Merck, min. 98%), Pepstatin (Fluka), PVPP (Sigma), sucrose (Sigma, for molecular biology, ≥99.5%) , Sodium dodecyl sulfate (Sigma, BioXtra, ≥98.5%), trichloroacetic acid TCA (Sigma, for molecular biology, ≥99%), Methanol (Merck, pure), ammonium acetate (Fluka, ≥99.9%), phenol (Sigma, equilibrated with 10 mM Tris HCl, pH 8.0, 1 mM EDTA, BioReagent, for molecular biology), urea (Fluka, pure), 3-[(3-Cholamidopropyl)dimethylammonio]-1-propanesulfonate hydrate CHAPS (Sigma, suitable for electrophoresis, ≥98%), dithiothreitol DTT (BioChemica, ≥99.5%), Bio-Lyte Ampholytes pH range 3-10 (BIO-RAD), ReadyStrip™ IPG Strip (BIORAD), cOmplete Protease Inhibitor Cocktail Tablets (Roche Applied Science), Bromophenol Blue (Sigma, ACS grade), phenylmethanesulfonyl fluoride PMSF (Sigma, ≥99.9%), dimethylsulfoxide (BioChemica, cell culture grade), glycerol (Sigma, , ≥99%), Trizma Base (Sigma, , ≥99.9%), iodoacetamide (Sigma, BioUltra), acrylamide (Sigma, for electrophoresis, ≥99%), N,N,N′,N′-Tetramethylethylenediamine TEMED (Sigma, ≥99%), N,N′-Methylenebis-acrylamide (Sigma, ≥99.5%), ammonium persulfate APS (Sigma, ≥98%), acetic acid (glacial) (Merck), Coomassie Brilliant Blue CBB G-250, orthophosphoric acid (Merck, 85%), ammonium sulfate (Sigma, ≥99%), thiourea (BioChemica), (4-(2-hydroxyethyl)-1-piperazineethanesulfonic acid) HEPES (Merck, pure), ammonium hydrogen carbonate (Merck, pure), trypsin (sequencing grade, modified, from Porcine, PROMEGA), pH 11 Britton-Robinson Universal Buffer BRUB, acetonitrile (Sigma, LC-MS CHROMASOLV®), formic acid (Sigma, LC-MS Ultra), 2-thiobarbituric acid TBA (Sigma, ≥98%), 5-Sulfosalicylic acid hydrate (Sigma, 95%), 2,2-Dihydroxy-1,3-dioxohydrindene

Ninhydrin (Merck, ACS grade), toluene (Merck, LiChrosolv®), Ponceau Red, sodium chloride NaCl (Sigma, ≥98%), potassium chloride KCl (Sigma, ≥99%), non-fat dry milk, developer solution (Tetenal, SuperFix Plus), fixation solution (Tetenal, Ultrafin Liquid, B/W Negative Developer), 5-Amino-2,3-dihydro-1,4-phthalazinedione Luminol, p-coumaric acid (Sigma, ≥98%).

All chemicals were analytical grade and were obtained from commercial sources at the highest purity available.

2.1.2. Pine Species and Samples

Pine needles were harvested from healthy pine trees of each of two species (*Pinus brutia* and *Pinus sylvestris*) located at Yalıncak, METU Campus (approximately, at the same region and elevation). For this purpose, 20 individuals of *Pinus brutia* and 20 individuals of *Pinus sylvestris* were marked and a basic map was prepared (Figure 2.1).

Figure 2.1 Sampling areas of both species: (A) shows the GPS location of *P.brutia* trees and (B) demonstrates the GPS values of *P.sylvestris* trees.

Needles were collected from the tip parts of the branches having almost the same height with respect to ground and located all around the stem. Needle samples were wiped with wet paper towel to remove contaminants, and they were placed into special containers resistant to liquid nitrogen. Those samples were transported to the laboratory in liquid nitrogen tank and placed into -80°C ultra freezer as soon as possible.

Two pine populations were sampled in this way, three times: at the end of cold winter period, at the end of mild and rainy spring period and at the end of hot and dry summer season.

6 pools (3 sampling times of 2 different species) were prepared for the pine needles: all the needles from 20 trees were crushed and all the powder was mixed well in the mortar to get a homogeneous pool for further analysis. Then, this powder is stored in -80^{o}C ultra freezer until usage. For each experiment, this powder was weighted by keeping the stock in liquid nitrogen during the process.

2.2. Methods

2.2.1. Chlorophyll and Carotenoid Content Determination

Pulvarized pine needles are weighed and 25mg powder from a set of 6 different samples (winter, summer and spring picks of *Pinus sylvestris* and *Pinus brutia*) are taken into 2 ml eppendorf tubes. The spectrophotometric detection of chlorophylls and derivatives are achieved by dissolving those samples in 4 different solvent systems: 95% Ethanol, 100% Methanol, 100% and 80% Acetone. For each solvent, a set of 6 samples are prepared and 2 ml of that solvent is added into every ependorf tube. After they are vortexed well, overnight incubation is applied at 4^{o}C. Tubes are centrifuged at 1500g for 5 min, and absorbance values are measured at different wavelengths (Appendix A). This procedure was repeated three times at different days.

2.2.2. Malondialdehyde (MDA) Assay

Powdered needle samples are weighted in 2 ml eppendorf tubes as 0.3 g and 1.5 ml of ice-cold 5% TCA are added to each tube, in ice. After they are vortexed, centrifugation at 15000g, at 4^{0}C, is applied for 15 min. Supernatant are transfered into new eppendorf tubes and the same centrifugation step is repeated once more. 400µl aliquotes of the supernatant are taken and 400µl of 0.5%TBA-20%TCA mixture are added. All the eppendorf tubes are incubated at 96^{o}C for 25 min and they are centrifuged at 12000g for 5 min. Supernatants are transfered into new tubes and the absorbance values are measure at wavelengths 532 nm and 600nm by using 1:1 (v/v) 5% TCA / 0.5%TBA-20%TCA mixture as blank which was also incubated at 96^{o}C. This procedure was repeated three times at different days.

2.2.3. Determination of Proline Content

Powdered needle samples are weighted in 2 ml eppendorf tubes as 0.4 g and 1.5 ml of 3% sulphosalicyclic acid are added to each tube, in ice. Tubes are vortexed and centrifuged at 15000g for 5 min (at +4^{o}C). Supernatants are transferred into new eppendorf tubes and the

same step repeated once more. Then reaction mixtures are prepared by adding 200µl of acid ninhydrin (from 0.15M stock), 200µl of 96% acetic acid, 100µl of 3% sulphosalicyclic acid and 100µl of sample or standard (0,1 to 500 µM proline solutions prepared in 3% sulphosalicyclic acid). Tubes are vortexed and incubated at 96^{o}C for 1 hour. After cooling to room temperature, 1 ml of toluene is added into each and vortexed well. Eppendorf tubes are centrifuged at 15000g, at +4^{o}C, for 5 min, and the upper toluene layers are transfered into glass tubes to be measured for their absorbance values at 520nm. This procedure was repeated three times at different days.

2.2.4. Preparation of Needle Cytosolic Homogenates

As it was defined by Schröder and Berkau (Schröder & Berkau, 1993), pine needles are powdered in liquid nitrogen and 0.2 g of each sample is weighted into plastic tubes. Then, 2 ml (10 vol (w/v)) of ice-cold homogenization buffer (0.1 M Tris HCl buffer, pH 7.8, containing 0.07% (v/v) 2-Mercaptoethanol, 5% (w/v) PVP-K 30, 2 mM of EDTA, 0.5% Nonidet P40, 3µg/ml of Pepstatin A) is added and vortexed well. Homogenization was applied by using Ultra-Turrax T-25 at 13500rpm, for 15 sec intervals of totally 4 times, in ice. Homogenates are transferred into ependorf tubes and centrifuged at 12000g, at 4^{o}C, for 30 min. The supernatant are aliquoted and stored in -80^{o}C ultra freezer.

2.2.5. Determination of Total Thiol Groups

Cytosolic total thiol amount of each sample was determined by the method defined by (Sedlak & Lindsay, 1968). This method is based on the reduction of 5`-dithiobis-(2-nitrobenzoic acid) (DTNB) by sulfhydryl groups, to produce a characteristic yellow color which gives its maximum absorbance at 412 nm. Each free –SH group reduces the DTNB into 1 molecule of 2-nitro-5-mercaptobenzoic acid that creates the yellow color.

By an adaptation to the ELISA microplate reader, 10 µl of cytosol was added into 30 µl of 200 mM Tris Buffer, pH 8.2 containing 20 mM of EDTA. Then 20 µl of DTNB (2 mM) and 140 µl of MeOH were added into each well. After a 30 min of incubation period at room temperature, absorbance values were measured in ELISA microplate reader system at 405 nm and by the slope of the standard curve, concentration values were calculated by the Software KC Junior provided by the instrument.

2.2.6. GST Enzyme Activity Assay

GST enzyme activity was determined spectrophotometrically by monitoring the thio-ether formation at 340 nm using CDNB as substrate basicly according to the method of Habig *et al.* (Habig *et al*, 1974) as modified for ELISA plate reader system in our laboratory, previously. Each reaction mixture contained 100 mM potassium phosphate buffer, pH:7.8,

1.0 mM GSH, 1.0 mM CDNB and 3.5-6 mg/ml ctosolic homogenate in a final volume of 250 µl in 96 well plate.

The reactions are started by the addition of enzyme into each well. After the plate is being vortexed by the system, reading is started automatically at every 20 seconds for 10 minutes. The blank wells contained all the constituents except cytosolic homogenates. Slopes of the best lines drown for each well separately by the software of the instrument were used as the rate of reaction (dA/dt) and the further calculations were completed according to the formula:

$$\frac{dA/dt}{\varepsilon\,(9.6\,mM^{-1}cm^{-1})} \text{ x } \frac{1000\,\mu l}{250\,\mu l} \text{ x DF x } \frac{250\,\mu l}{25\,\mu l} \text{ x } \frac{1}{mg\ protein/ml}$$

2.2.7. Determination of Protein Concentration

For the detection of total protein concentration in various samples, Lowry Protein Assay is used. Lowry Method (Lowry *et al*, 1951) is adjusted for the measurement by ELISA Plate Reader (Bio-Tek ELx808) with crystalline bovine serum albumin (BSA) as the standard. Samples are diluted as 1:24 and 1:49, and added into the 96 well plates as triplicates as a final volume of 50 µl. Then, 200 µl of freshly prepared Lowry ACR (including 2% cupper sulfate ($CuSO_4.5H_2O$), 2% sodium-potassium tartarate, 2% (sodium hydroxide, sodium carbonate) in the ratio of 1:1:100) is added and mixed by pipetting. After 10 min of incubation at room temperature, Folin Cilcateu Phenol Solution (commercially available form was diluted 1:1) is added as 20 µl with immediate mixing. At the end of 45 min. incubation, plates are read at 650 nm. Protein concentration in each well is calculated by the software of the instrument (KC Junior) after providing necessary dilution factors. Standard curve was prepared by using BSA solutions diluted as 1, 2.5, 5, 10 µg/well.

2.2.8. Protein Extraction from Pine Needles

Two different methods (Ekramoddoullah, 1993), (Wang *et al*, 1996) proposed for protein extraction from plant tissues were combined and optimized for higher quality and for cleaning products off contamination of phenolic compounds, nucleic acids etc.

1 gram of needle powder with the addition of 0.1 g of PVPP is extracted with 10 mL of extraction buffer composed of 5% sucrose, 4% SDS and 5% 2-ME for 10 min at room temperature with gentle stirring. Centrifugation is applied at 12000 g for 30 min at 4^{o}C. Supernatant is divided into 1 ml aliquotes in 2-ml eppendorf tubes. Tubes are filled with 1 ml of chilling 20% TCA/Acetone and mixed well by vortexing. They are centrifuged at 16000 g for 3 min at 4^{o}C and supernatant are removed. Then, tubes are filled with chilling 80% methanol containing 0.1 M ammonium acetate and they are mixed well by vortexing. They are centrifuged at 16000 g for 3 min at 4^{o}C. After decanting the supernatant, tubes are filled with chilling 80% acetone to disperse the pellets, completely; then the same centrifuge step is applied at 16000 g, for 3 min, at 4^{o}C. Supernatant are discarded and the pellet are air-dried at 50^{o}C for 10 min. 1.6 ml of 1:1 phenol (buffered at pH: 8.0 by 10 mM Tris-HCl)/SDS

buffer mixture are added to each. Tubes are mixed thoroughly and incubated for 5 min at room temperature; then, they are centrifuged at 16000 g for 3 min at 4^{o}C. Upper phenol phase of each tube is transferred into a pool; then, 400 µl of aliquotes are taken into 2 ml eppendorf tubes. They are filled with chilling 80% methanol containing 0.1 M ammonium acetate. Tubes are incubated at -20^{o}C overnight and then centrifuged at 16000 g for 5 min at 4^{o}C. Supernatant are discarded carefully to handle the white precipitate at the bottom of tubes. Pellets are washed once with chilling 100% methanol and once with chilling 80% acetone by vortexing well, first; then applying centrifuge at 16000 g for 5 min at 4^{o}C after each washing step. Pellets are allowed to be air-dried.

2.2.9. Isoelectric Focusing and SDS-PAGE (2D-PAGE)

Protein samples are dissolved in rehydration buffer containing (8M urea, 2%CHAPS, 10mM dithithreitol and 0.5% Bio-Lyte Ampholytes pH range 3-10) by occasional vortex and by incubation at 45^{o}C. Then, they are centrifuged at 14000g for 5 min, and supernatant are collected in clean eppendorf tubes. Protein concentrations of the samples were determined by Micro Lowry procedure adopted from the method proposed in original paper (Lowry *et al*, 1951). Sample mixtures containing 400µg of protein are prepared for 17cm IPG Strips by mixing appropriate amount of sample with Roche Protease Inhibitor Cocktail (10%, from the stock prepared by dissolving 1 tablet in 1 ml of rehydration buffer), trace amount of Bromophenol Blue and PMSF (1%, from 10% stock prepared in DMSO). Final volumes are adjusted to 250µl by adding rehydration buffer and mixtures are spread into the channels of rehydration/equilibration tray. IPG strips are placed gel-surface down onto the sample in the tray and active rehydration protocol is applied over-night, at 50V and at 20^{o}C, on BIORAD Protean IEF Cell. After rehydration, IPG Strips are placed into clean channels as in the same position touching both ends to the wet paper-wicks located onto the electrodes. IEF Cell is adjusted to provide a gradual increase in the voltage over time and focusing is applied till the value of 40000Vh for each IPG Strip. Then, they are transported into the channels of disposable trays for 15 min of incubation, first, in equilibration buffer (6M Urea, 2% SDS, 20% Glycerol, 0.5M Tris-HCl pH: 6.8) containing 6% DTT and then 15 min more in 24% IAA containing one. After equilibration step, strips are placed onto 12% of SDS-polyacrylamide gel (Table 2.1) and run at 65V.

Table 2.1 Preparation of different concentrations of gels used in the study.

	Separating Gel (0.375 M Tris, pH:8.8)			**Stacking Gel (0.125 m Tris, pH:6,8)**
Monomer Concentration	**12%**	**10%**	**7.5%**	**4%**
Acrylamide/bis	12 ml	13.3 ml	10 ml	2.6 ml
dH_2O	11.1 ml	16.1 ml	19.4 ml	12.2 ml
1.5 m Tris-HCl, pH: 8.8	8.25 ml	10 ml	10 ml	-
0.5 M Tris-HCl, pH: 6.8	-	-	-	5 ml
10% (w/v) SDS	300 µl	400 µl	400 µl	200 µl
10% APS *(freshly prepared)*	150 µl	200 µl	200 µl	100 µl
TEMED	30 µl	30 µl	30 µl	30 µl
TOTAL	**30 ml**	**40 ml**	**40 ml**	**20 ml**

Gels are soaked into fixation solution composed of 40% ethanol and 10% acetic acid, for 2-3 hours. After washing them in distilled water, Colloidal Coomassie Blue Dye containing CBB G-250 (0.08%), ortophosphoric acid (0.96%), ammonium sulfate 0.08% and 20% methanol is poured onto the gels. They are incubated in the dye for 2-3 days at room temperature.

2.2.10. Analysis of Gel Images

Resulting gel images were analysed by the Ludesi REDFIN software system which is available online (Figure 2.2). Spot detection and image segmentation were performed in a composite image and the same spot positions and borders were then applied in all images, after compensation for geometric distortions. Although this protocol was simple to apply, there were still the disadvantages of assigning some spots with misshaped/misaligned borders which might lead to an incorrectly measured spot volume. Because of this problem, the results were later being quality controlled by inspection in the individual images and errors were manually corrected.

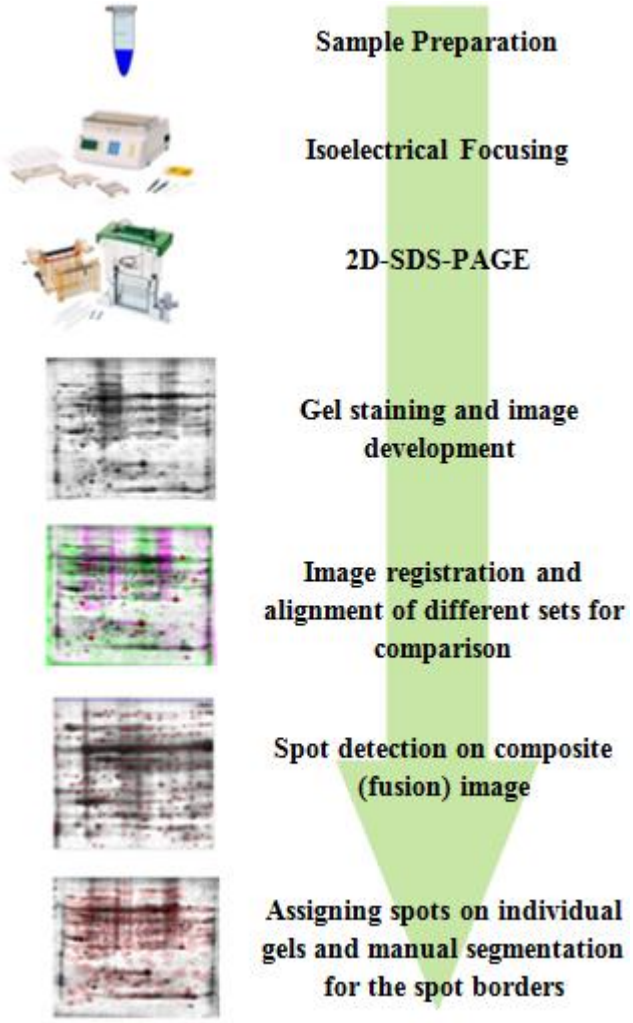

Figure 2.2 The flowchart demonstrating the 2D-PAGE and image analysis pathway. The gel images were uploaded to Ludesi REDFIN software and the algorithm finished the pre-analysis steps by determining the possible spots on the gels with their volumes/desities after manual evaluation of them and statistical filtering.

The first step was to register corresponding points in the gel images, based on features or patterns that could be seen in the image. Using this information, the images were aligned and geometrically transformed (warped) so that corresponding protein spots appeared at almost the same positions in the warped images. Ludesi Redfin Solo uses a semi-automatic approach, which means corresponding points were indicated in the images, which may then be improved by computer algorithms. One gel in each group of organisms was selected as the reference gel, and all other gels were aligned / warped to it. A composite image (fusion image) was created by merging all the gel images into a single representative image. This image contained all the spots from the individual gels. In order to avoid artifacts, such as cracks, large stain particles, dust, etc. from being included in the composite image, some regions or spots were excluded when creating the fusion image.

Spot detection involves using algorithms to detect all real protein spots in the images, while avoiding falsely detecting anything in the images that does not represent a true spot, in other words, all possible false-positive spots were eliminated. On the other hand, some false-negative regions were also marked. In the image segmentation step, it was determined what region in the images contains each protein spot. The region outline (spot border) should encompass all of the stained area belonging to the spot and nothing from nearby spots. In the

Redfin Solo protocol, spot borders are determined in the composite image and are then applied, after warping, to all the individual images. After this, verification and adjustment of spot positions and borders were done in each individual image.

Quantification is the process of measuring the cumulative staining intensity contained within a spot which in turn corresponds to the relative protein volume. This involves calculating the local background level around a spot, and subtracting this background level from the staining level contained within the spot as defined by the spot border. The result is a calculation of the total, background corrected, and staining level of the spot. Experimental differences in sample volume, staining and visualisation generate a need for the normalization of spot volumes to be compared with each other. The algorithm Ludesi uses forms a normalization factor for each of the gel images in this way:

- ✓ The top 50% of all spots (according to their volumes) matched between gel images are kept.
- ✓ Those volumes of the matched spots are divided to each other to find a ratio. The median of these ratios enables us to compute a pair-wise normalization factor between the gels.
- ✓ Each gel normalization factor is computed by optimizing an over-determined equation system, resulting from the pair-wise normalization factors.
- ✓ Finally, the spot volumes in each gel are multiplied with the corresponding gel normalization factor.

To help determine statistically significant differences between groups of samples two methods for statistical hypothesis testing were employed by the software: One-way ANOVA (Analysis Of Variance) and Mann-Whitney. For each spot ID, both an ANOVA and Mann-Whitney p-value is calculated using the quantified and normalized volumes for the matched spot in each of the images.

ANOVA is a parametric method that assumes independency and normal distribution of all values and is capable of comparing multiple groups. For comparisons between two groups only, the ANOVA becomes equivalent to the two-sided Student's t-test. The Mann-Whitney test is the non-parametric equivalent to the Student's t-test and only assumes that the distribution of the values in each group has the same shape. Mann-Whitney is only capable of comparing two groups to each other.

2.2.11. FASP (Filter Assisted Sample Preparation)

Samples are dissolved in freshly prepared UA buffer (8M Urea, 2M Thiourea, 10mM HEPES, at pH 6.5) and centrifuged at 14000 rpm (in Eppendorf minispin centrifuge). Supernatant are collected and transferred into Amicon 30K filter units (Millipore American Ultra Centrifugal Filters-0,5ml 30K Ultracell, 30K Membrane-Regenerated Cellulose 30.000 MWCO). After 20 min of centrifuge at 14000g at 20^{o}C, there remains approximately 30µl of sample at the bottom of filter units. Then, 200 µl of UA buffer are added into the units and centrifuge is applied at 14000g at 20^{o}C for 15min. This step is repeated once more and to each filter unit, 100 µl of IAA solution (50mM, prepared in UA buffer) is added. Tubes are mixed on a automatical mixer at 600rpm for 1 min. and incubated at room temperature for 20

min, at dark. After incubation, tubes are centrifuged at 14000 g for 15min and the filter units are washed with 100 µl of UA buffer twice to clean excess IAA off the samples by centrifugation at 14000g, again. To each filter unit, 100 µl of 50 mM ABC (Ammonium Bicarbonate) are added and centrifuged at 14000g and this step is repeated twice, too. Trypsin stock is prepared by dissolving lyophilized trypsin (sequencing grade modified trypsin from Porcine, PROMEGA V511A) in 40 µl of resuspension buffer provided with the trypsin vial and 24 µl of this stock is mixed with 216 µl of ABC solution to get the final trypsin solution enough for 6 samples. Filter units are placed into new eppendorf tubes and 40 µl of Trypsin solution is added into each. Tubes are mixed at 600rpm for 1 min, in Thermomixer and placed into incubator for overnight (16-18 hours) at 37^{o}C in a box containing a piece of wet filter paper at the bottom. After incubation, tubes are centrifuged at 14000g for 10 min and filter units are washed once by 50 µl of ABC and centrifuged at the same speed and time. The digested peptide solution collected at the bottom of eppendorf tubes are measured for their absorbance values at 280 nm (and 205 nm for empirical method, and at 260 nm for Christian Warburg Protein Impurity Tests) by using ABC solution as the blank.

2.2.12. Anion Exchange Chromatography

Small discs are cut apart from 3M Empore Anion Exchange material (3M Empore, 2252, Anion, 47mm; Formulation: 90% Sorbent Particles, 10% PTFE) and packed into the regular yellow colored 200 µl micropipette tips to form a column (Anion Exchange Tip-AET) of approximatelly 3 mm height. Those tips are placed into the 1.5 ml eppendorf tubes and conditioning procedure are applied: First, 100 µl of 100% Methanol is loaded and the AETs are centrifuged at 7000g for 5 min. This procedure is repeated for 100 µl of 1 M NaOH, and then, for pH 11 Britton-Robinson Universal Buffer (BRUB). 100 µl of pH 11 BRUB is loaded once more then the same centrifuge step is repeated last time. Samples are diluted according to the spectrophotometric values to provide equal amounts of peptides to be used in the next step: the most concentrated one is taken as 30 µl and 70 µl of pH 11 BRUB is added. Then, those samples are loaded into AETs and centrifuged at 7000g for 10 min to get the "First Eluent". 100 µl of pH 11 BRUB is loaded into each AET and centrifuge is applied at 7000g to get the "Second Eluent". The same procedure is repeated for 100 µl of pH 8, pH 6, pH 5, pH 4 and pH 3 BRUB for each column to get a complete set of those 6 different pH values (as 7 eluents) for each sample. All the eluents are placed into SpeedVac in AQ-aqua mode, and dried at 45^{o}C for approximately 90min.

2.2.13. Mass Spectrometry (MS) Analysis

Dried sample eluents are reconstituted in 6 µl of buffer A (5% acetonitrile / 0.1% formic acid) and sonicated for 2-5 min in bath sonicator. Then, they are centrifuged at maximum speed of MiniSpin for 5 min to remove any particulate matter. 5 µl of supernatant are transferred to auto-sampler vial for mass spectrometric analysis. 1 µl of each sample eluent are loaded into a pre-column of UltiMate Nano liquid chromatography system to clean any salt or detergent contamination off, then, it is transferred into the reverse-phase column.

Fragments, produced after this procedure, are sent to hybrid linear ion-trap mass spectrometer (LTQ-Orbitrap) by an Electron Sprey Ionization (ESI) ion source. MS and MS^n analyses are performed in this system and the data are stored as files with .RAW extension and then they are converted to .mzML files by the software Xcalibur™.

For all 6 samples (spring, summer and winter picks of both pine species), mass spectrometry application is repeated 3 times; in other words, study was completed with three independent sets of MS data.

2.2.14. Software Analysis of the MS Results

All mass spectrometry data are evaluated by using a free data processing pipeline developed by Prof Hippler's Lab (Specht *et al*, 2011). Open mass spectrometry search algorithm (OMSSA) and X!Tandem, which are tandem mass spectra search engines, are used to qualify and quantify the peptides in samples. RawMeat software is used to calculate the MS Count values of each and all measurements to check data quality. BioVenn application is used to compare sets of proteins for common and different members among the organisms and seasons.

2.2.15. Western Blotting

Protein samples extracted from pine needles were analysed for the presence of some photosynthesis and energy metabolism members as a proof for the results of mass spectrometry analysis. PerfectBlue™ Semi-Dry Electro Blotter Sedec™ system was used for western blotting analysis with Amersham Hybond ECL nitrocellulose membranes.

Blotting papers (Whatmann 3MM) and the nitrocellulose membrane are wet in Blotting Buffer (192 mM Glycine, 25 mM Tris and 20% methanol) about 10 min before the application. Then, 3 blotting papers are placed onto the anode, and then polyacrylamide gel is laid onto them. After removing air bubles, nitrocellulose membrane is placed onto gel and other 3 blotting papers spread. Lid is put and fixed well; then, 300 mA is applied for 2.5 hour. After transfer, nitrocellulose membrane is soaked into Ponceau Red solution (0,5% (w/v) Ponceau Red, 1% (v/v) acetic acid) to check whether the process was succesful or not. Then, membrane is rinsed 3 times (each for 10 min) within 2% non-fat dry milk solution prepared in phosphate buffered saline solution (PBS) at pH 7.4 containing 137mM NaCl, 2.7 mM KCl, 1,47 mM KH_2PO_4, 82 mM Na_2HPO_4.

Primary antibody is diluted in 2% non-fat dry milk PBS solution (pH 7.4) and poured onto the membrane. After over-night incubation at 4^oC, membrane is washed for 10 min. This step is repeated once more, then, secondary antibody solution, which is prepared in 2% non-fat dry milk PBS, is poured onto the membrane. After 1.5 hour of incubation at room temperature, membrane is rinsed with 2% non-fat dry milk PBS 2 times (each for 10 min), again.

2.2.16. Enhanced Chemiluminescence (ECL) Detection

Protein bands bounded by the specific antibodies that were used in this study were all detected by the usage of Enhanced Chemiluminescence (ECL) Detection technique. Two solutions of ECL method are prepared freshly as defined in the table below (Table 2.2) and mixed with each other just before usage:

Table 2.2 Preparation of the ECL Solutions

ECL solution I	ECL solution II
100 mM Tris-HCl pH 8.5	100 mM Tris-HCl pH 8.5
2.5 mM Luminol	0.000183 % H_2O_2
0.4 mM p-Coumaric acid	

Nitrocellulose membranes are incubated in the ECL solution mixture for 1 min and placed into the GE Healthcare Amersham Hypercassette Autoradiography Cassette System. Then, Amersham Hyperfilm™ ECL-High Performance Chemiluminescent film is fixed on it and casette is closed for the incubation. After incubation period, whose length was optimized for each primary antibody, film is soaked first into developer (Tetenal, SuperFix Plus) then, after rinsing in dH_2O for a while, left into fixation solution (Tetenal, Ultrafin Liquid, B/W Negative Developer).

2.2.17. Statistical Analysis

The results of chlorophyll and carotenoid content measurements, MDA and proline assays, determination of total thiol concentration and total cytosolic GST activity tests were evaluated statistically by the licensed software Minitab® 16. t-test of difference were applied for winter and summer samples against spring sample which was used as the reference group in all experiments. p values were calculated for the 95% confidence interval (CI) and any p value smaller than 0,05 pointed the statistically significant difference between the compared set of data.

Asterix (*) was used to show that the value was statistically different with respect to spring in the 95% CI ($p<0.05$) and the dagger (†) indicates a difference in the 99.5% CI ($p<0.005$).

CHAPTER III

RESULTS

Needle samples of 20 healthy trees from each species were collected at the end of three seasons and prepared for homogenization and extraction procedures. Those homogenates and protein extracts were used in enzyme assays, measurements of different biochemical markers and, electrophoresis and chromatography assays: GST enzyme activities, total thiol amounts, proline and MDA contents, chlorophyll and carotenoid quantities were all determined and protein samples were analyzed by 2D-SDS-PAGE, LC-MS/MS and western blotting techniques. All numerical values, gel/membrane images and MS/MS results were processed by softwares provided different computational techniques and different algorithms.

Under subsequent titles, the results of all those experiments and analysis are presented by segregating the major discussion and conclusion for the next chapter; i.e. Chapter III introduced only the solid data obtained in the study.

3.1. Protein Extraction

Sample preparation is the first yet the most important step in most biochemical procedures and for some specimens like plant tissues, this process becomes very problematic (Wang *et al*, 1996). The amount of secondary metabolites and their being difficult to eliminate from the extracts are knots in those issues to untie. Evergreen leaves like the ones of pinus species contain high levels of metabolites which interfere with most analysis including 2D-PAGE, resulting semearing, decreased number of spots/bands and streaking in vertical and horizontal directions (Saravanan & Rose, 2004).

In this study, two different protocols were compared for protein extraction and a third "combined" method was derived from them. The first protocol (called the Sucrose Method, here) (Ekramoddoullah, 1993) proposes the usage of a sucrose containing extraction buffer (5% sucrose, 4% SDS and 5% 2-ME) for the preparation of the mixture containing powdered sample, then the boiling of supernatant to precipitate them as pellet. By washing of the pellet with extraction buffer and 80% chilling acetone, proteins were cleared and became ready to use in the subsequent steps of 2D-PAGE procedure (Appendix B). Second procedure which

is proposed by Wang *et al* (Wang *et al*, 1996) is a phenol-based method and suitable for a wide range of recalcitrant plant samples (Appendix C).

Pine needles were pulvarized in liquid nitrogen and by using this sample source, those two methods were performed. Protein extracts were dissolved in SDS sample buffer (62.5 mM Tris-HCl, pH 6.8, 20% Glycerol, 2% SDS, 5% Mercaptoethanol) and used in SDS-PAGE procedure (4% stacking gel and 7.5% separating gel). The purpose of these trials was to check the quality (not the quantity) of the protein samples for their compatibility for Isoelectrical Focusing procedure. As it is seen in the gel image (Figure 3.1), the number of bands was almost the same for both, but the smearing for samples produced by Wang's Method were a little bit higher (Figure 3.2).

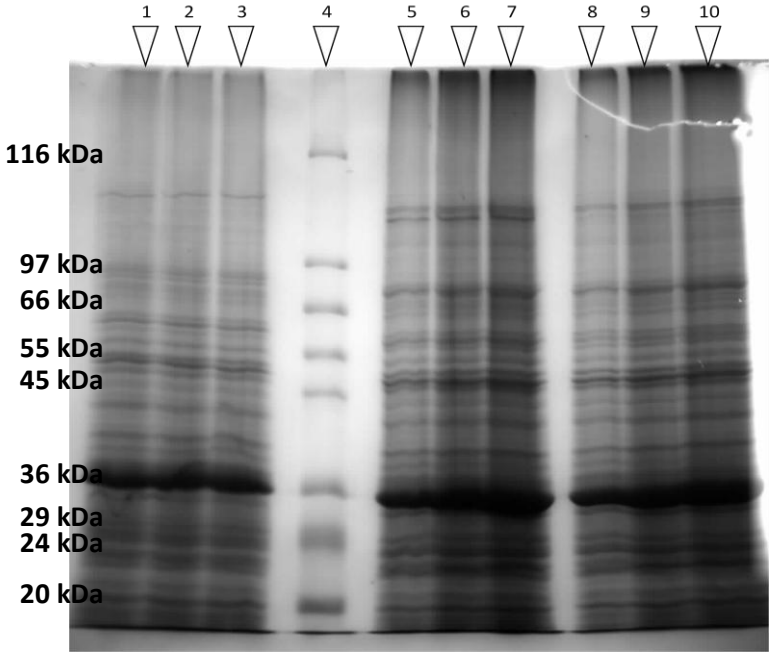

Well ID	Sample/Content	Protein Amount (µg/well)
1	Sucrose Method	209
2	Sucrose Method	418
3	Sucrose Method	627
4	Protein Marker	-
5	Wang's Method	85
6	Wang's Method	170
7	Wang's Method	255
8	Wang's Method	176
9	Wang's Method	352
10	Wang's Method	528

Figure 3.1 The SDS-PAGE gel image which was produced after the Colloidal Coomassie Blue Staining of the gel in which the protein samples that were yielded by sucrose using procedure and Wang's Method were run. (Photo was taken by the Vilber Lourmat Camera System)

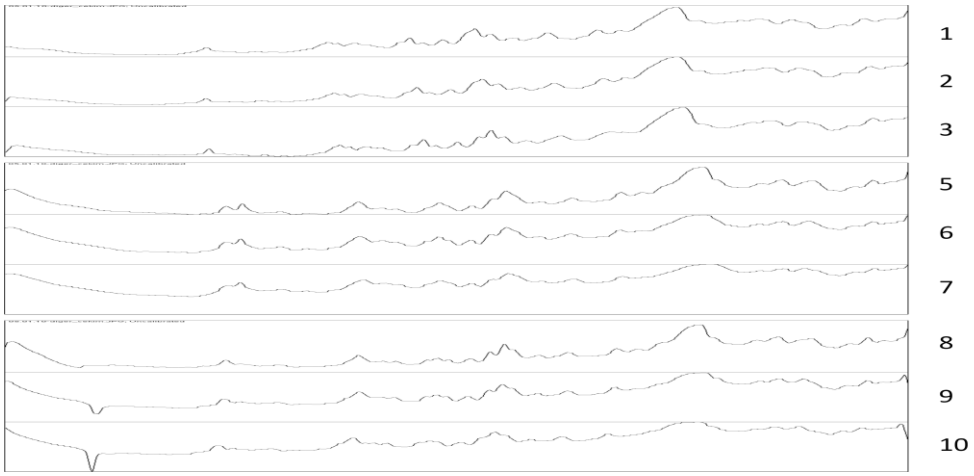

Figure 3.2 Lane Plot Analysis of the gel prepared by the ImageJ Software. Plot shows the presence of smearing lying down the wells till the 116 kD molecular weight marker.

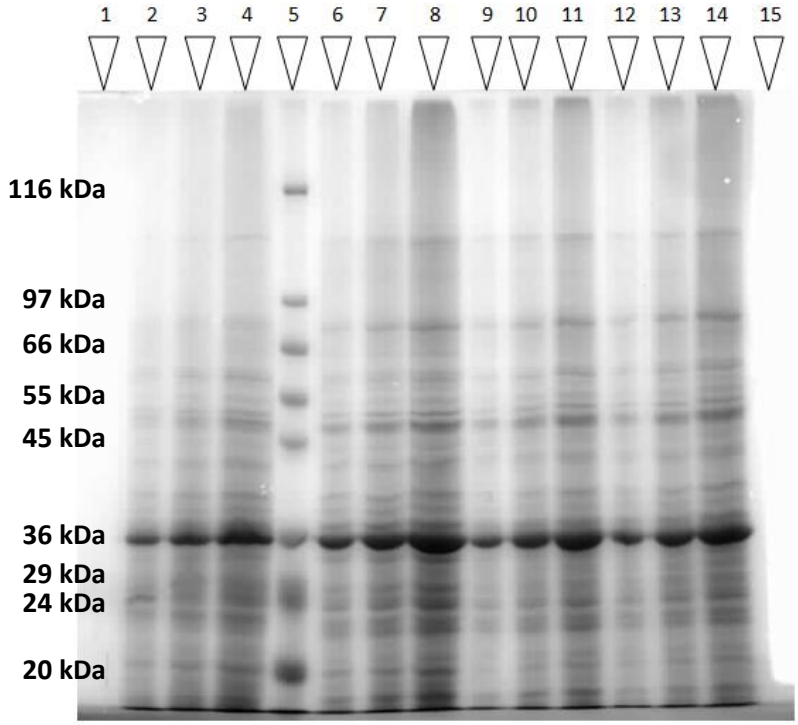

1	2	3	4	5	6	7	8	9	10	11	12	13	14	15
-	Sucrose Method			Marker	Wang's Method			Combined Method-500			Combined Method-750			-

Figure 3.3 The SDS-PAGE gel image which was produced after the Colloidal Coomassie Blue Staining of the gel in which the protein samples that were yielded by all methods were compared for band quality and number. For protein samples produced by using the combined method, 500 and 750 represents the volumes (in µl) of supernatant before the addition of chilling 10% TCA/Acetone. (Photo was taken by the Vilber Lourmat Camera System)

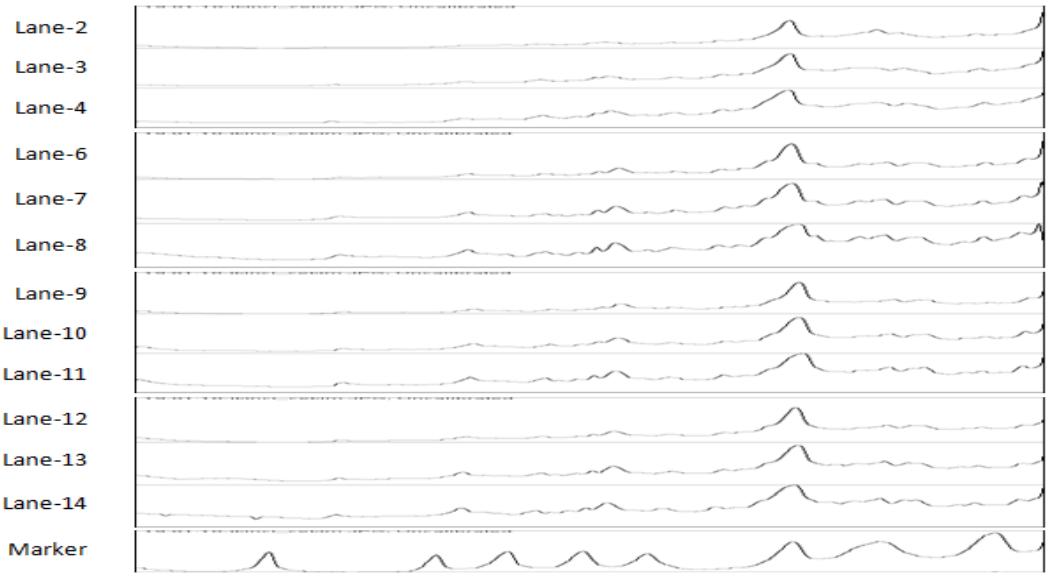

Figure 3.4 Lane Plot Analysis of the gel, prepared by the ImageJ Software.

When those samples were tried to be dissolved in rehydration buffer for IEF application, both had low solubility and impurities. Moreover, the yellowish color of protein precipitate in all samples was an indicator of a possible coprecipitation of phenolic compounds; i.e. a proof of the disabilities of the methods in eliminating such substances. A new procedure was proposed to handle this important problem by combining the sucrose-SDS extraction of the proteins and TCA-acetone precipitation followed by phenol extraction. Increasing the number of washing steps may cause the lost of some proteins, especially the infrequent ones; so, the samples produced by those three methods were compared by running them on SDS-PAGE (Figure 3.3). Lane analysis of the gel image showed similar patterns for all samples (Figure 3.4) which means the so-called combined method didn't affect the number of bands.

3.2. Isoelectric Focusing and SDS-PAGE (2D-PAGE)

Two dimensional polyacrylamide gel electrophoresis (2D-PAGE) comprehends two main parts: Isoelectric Focusing (IEF) (as the first dimension) and SDS-PAGE (as the second dimension). By the introduction of IPG strips by (Bjellqvist, et al., 1982), to provide a wide variety of reproducible pH gradients became possible. The main objective, here, should be the usage of the most appropriate pH range for the best resolution, because, IPG strips give the advantage of spreading proteins with pI values close to each other. For this purpose, the optimization issues were started with short (7cm) and wide range (pH 3-10) IPG strips to get an idea of the dispersion of proteins on the gel.

The short IPG strips with the widest pH gradient didn't provide enough resolution after trials (Figure 3.5), so, then, longer strips (17cm) were used for further optimization studies.

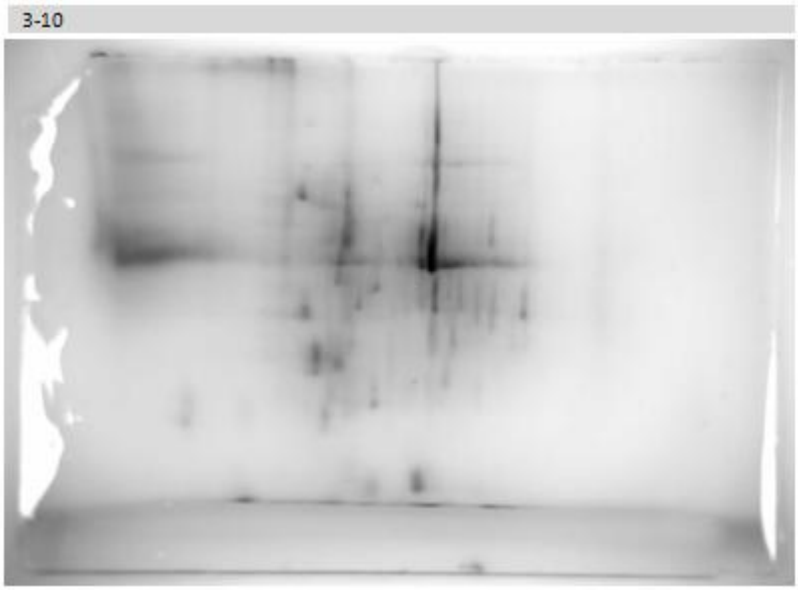

Figure 3.5 The 2D-PAGE gel image which was produced after the Colloidal Coomassie Blue Staining. 7 cm pH 3-10 IPG strip was used in the IEF step at which 404 µg of protein extracted from *P. brutia* needles was used and totally 11160 Volt-hours (Vh) was applied. pI range of the strip changes from left to right as from 3 to 10 (Photo was taken by the Vilber Lourmat Camera System)

Longer IPG strips provided better resolution for the same amount of sample applied; and, also, they revealed the necessity of using a narrow pH range to spread protein spots gathered at the middle of the gels (Figure 3.6). As a result, instead of pH gradient of 3-10, 17 cm IPG strips with pH gradient of 5-8 were prefered for the analysis (Valledor *et al*, 2008), (Costa, *et al*., 1999), (Gion, *et al*., 2005).

Colloidal Coomassie Blue Staining and silver staining procedures were also compared for their resolution in this case. Although silver staining yielded higher number of spots on the gels (Figure 3.7), because of its being difficult to be destained for further MS analysis and because of the difficulties in generating consistent images for the same experiment, CCB method was used for all gels.

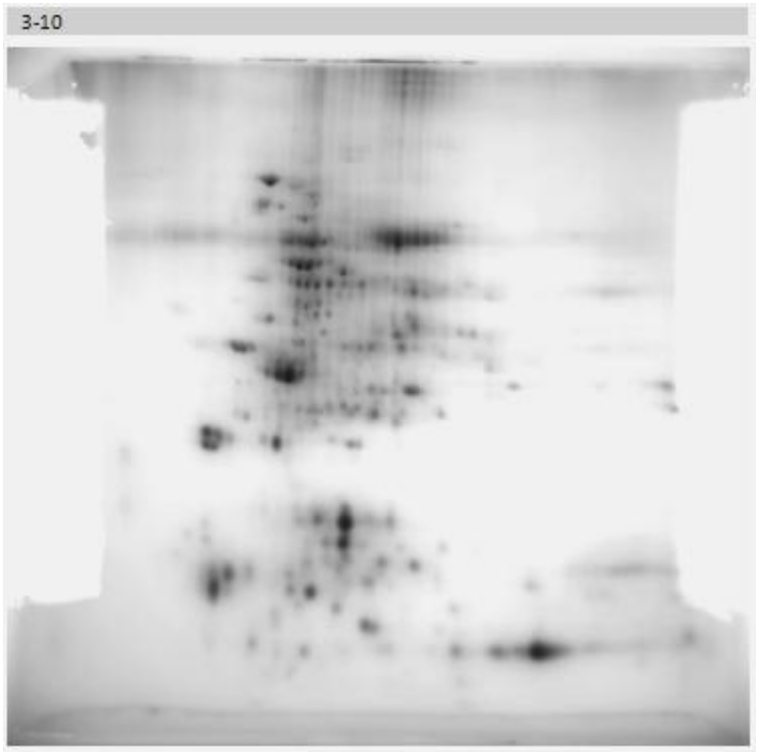

Figure 3.6 The 2D-PAGE gel image which was produced after the CCB Staining. 17 cm pH 3-10 IPG strip was used in the IEF step at which 417 µg of protein was used and totally 40000 Volt-hours (Vh) was applied as proposed in the BIO-RAD ReadyStrip™IPG Strip Instruction Manual. pI range of the strip changes from left to right as from 3 to 10 (Photo was taken by the Vilber Lourmat Camera System)

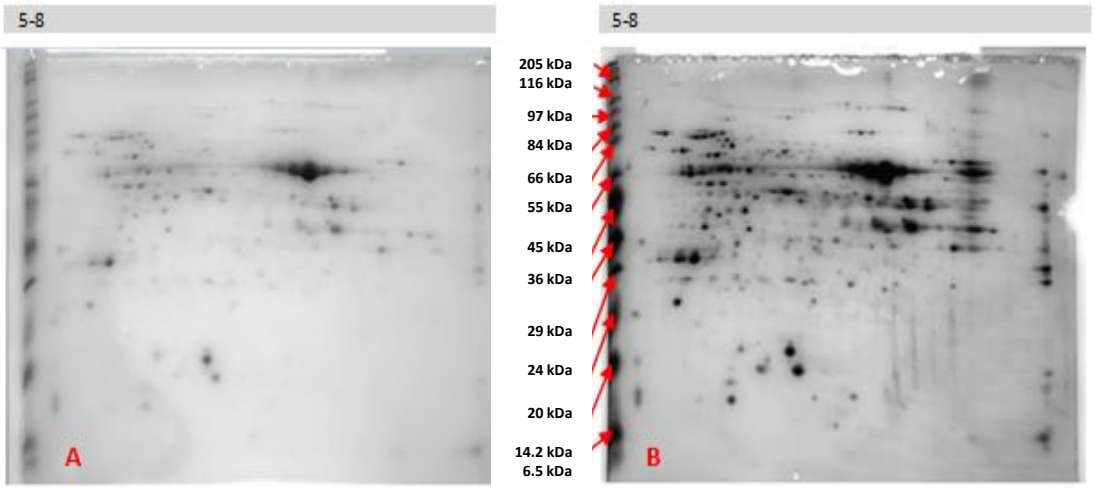

Figure 3.7 The comparison of the resolution of two staining methods applied for 2D-PAGE gels. The same sample was divided into two equal volumes for two IPG strips just before the IEF application and all the other steps were performed as the same. After second dimension, one of the gel was stained by following the CCB protocol (A) and the other (B) was stained with silver staining technique. pI range of the strips change from left to right as from 5 to 8 (Photos were taken by the Vilber Lourmat Camera System).

The 2D-PAGE gel images which were produced after the CCB Staining method (Figures 3.8-3.13) were analyzed by Ludesi REDFIN software Solo protocol as two different groups with respect to the organisms. The first group was formed by the gel images of *Pinus brutia* samples: A1: spring season (PB-spring), A2: summer season (PB-summer) and A3: winter season (PB-winter). The second group was formed by the gel images of *Pinus sylvestris* samples: B1: spring season (PS-spring), B2: summer season (PS-summer) and B3: winter season (PS-winter) (Figure 3.14).

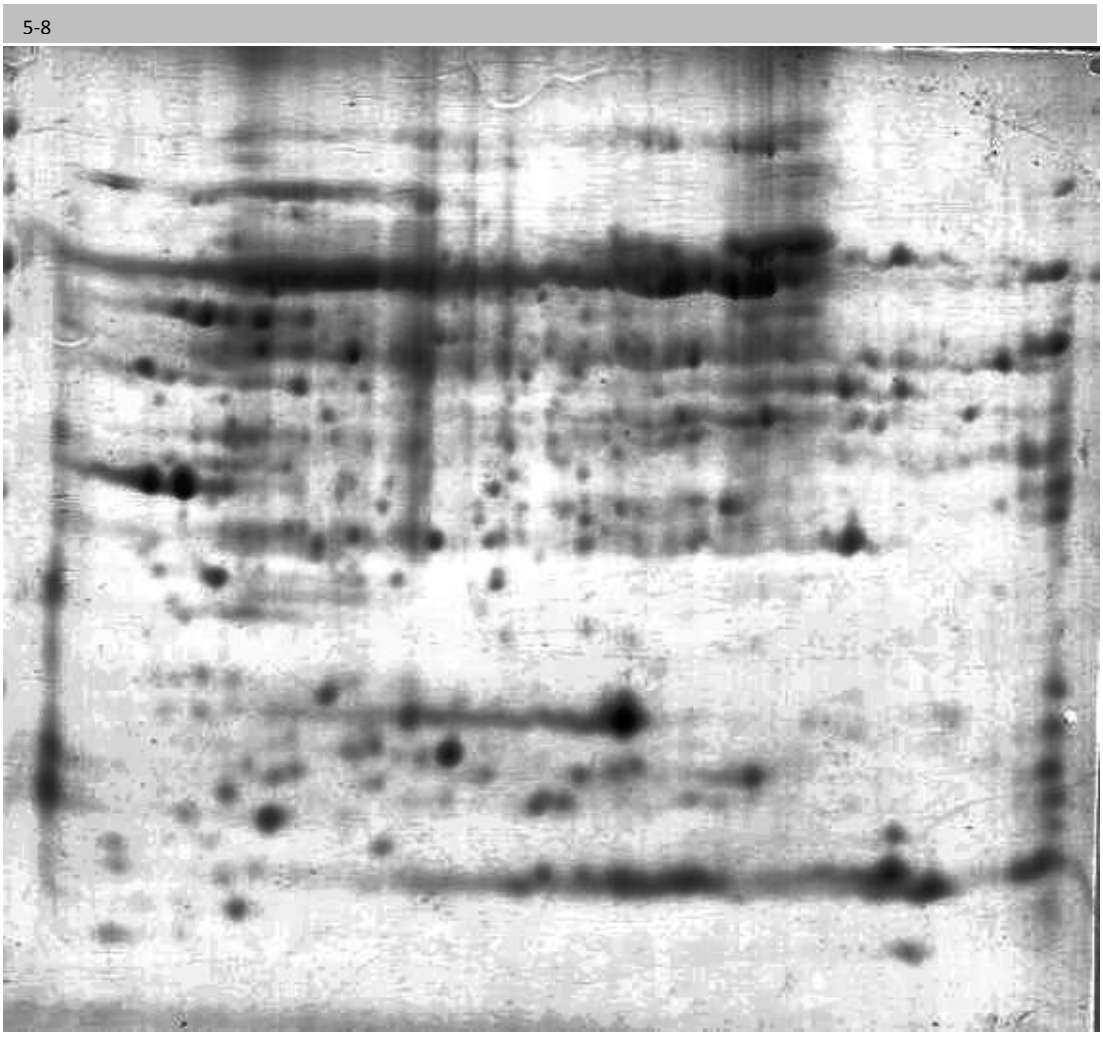

Figure 3.8 Enhanced gel image of *Pinus brutia* spring sample. pI range of the strip change from left to right as from 5 to 8 (Photos were taken by an ordinary office-type scanner).

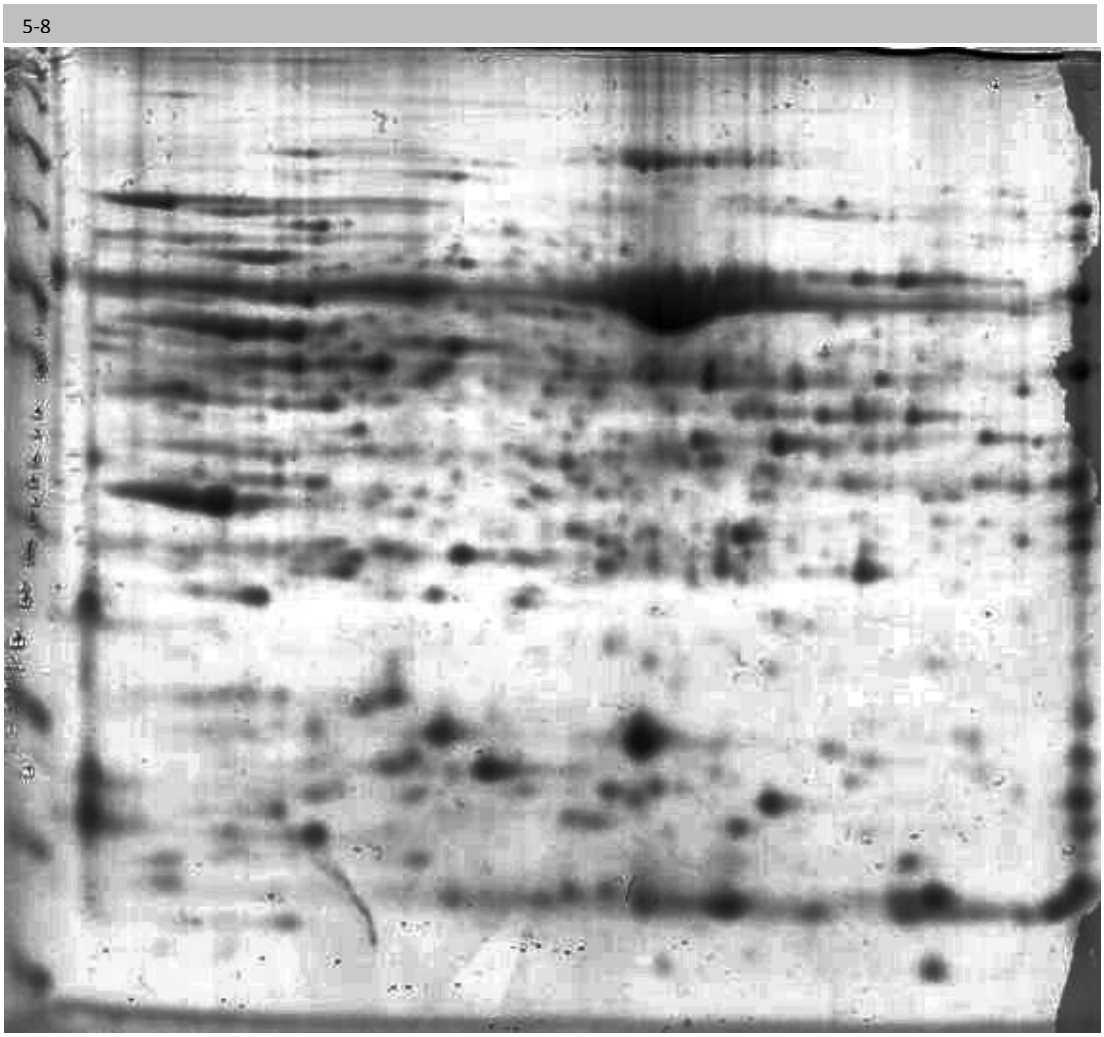

Figure 3.9 Enhanced gel image of *Pinus brutia* summer sample. pI range of the strip change from left to right as from 5 to 8 (Photos were taken by an ordinary office-type scanner).

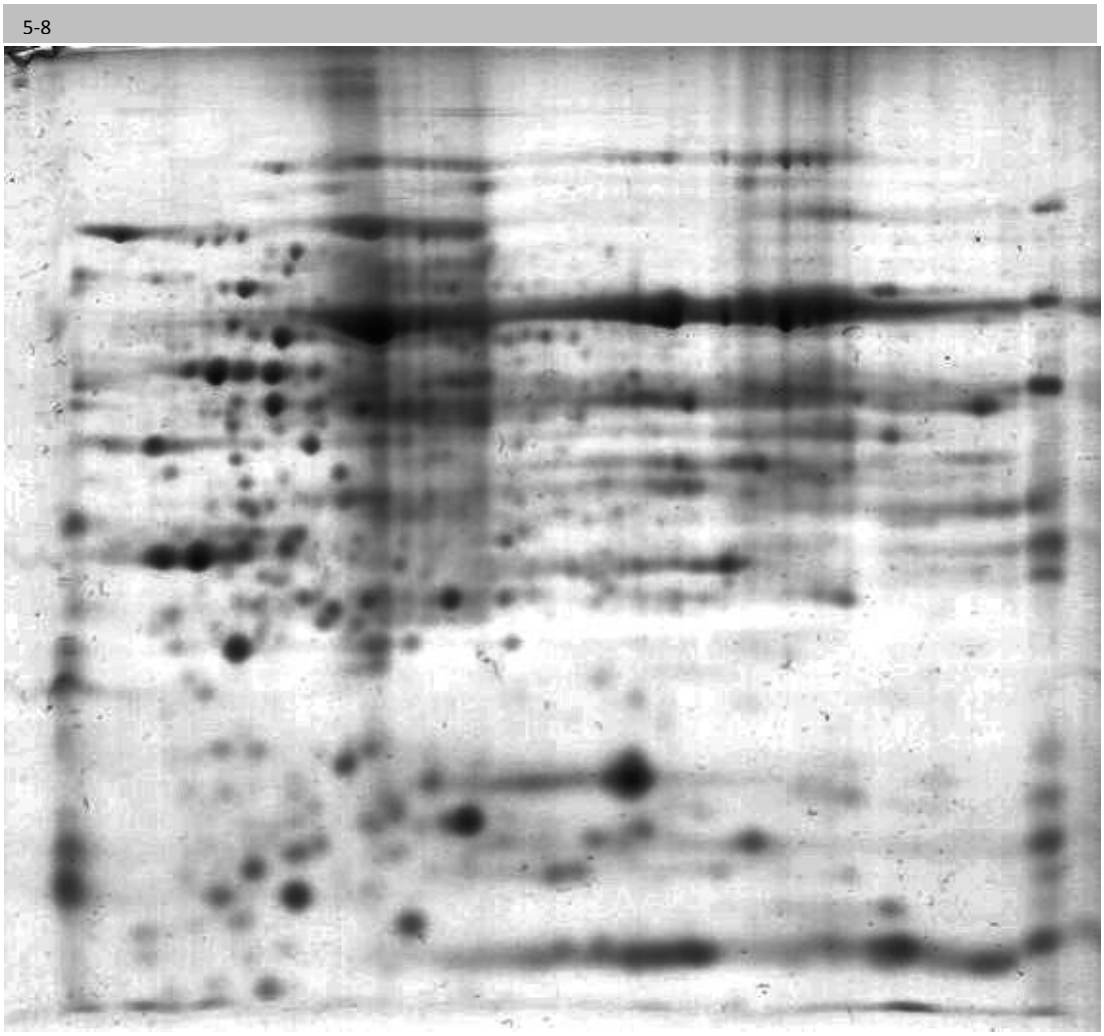

Figure 3.10 Enhanced gel image of *Pinus brutia* winter sample. pI range of the strip change from left to right as from 5 to 8 (Photos were taken by an ordinary office-type scanner).

Figure 3.11 Enhanced gel image of *Pinus sylvestris* spring sample. pI range of the strip change from left to right as from 5 to 8 (Photos were taken by an ordinary office-type scanner).

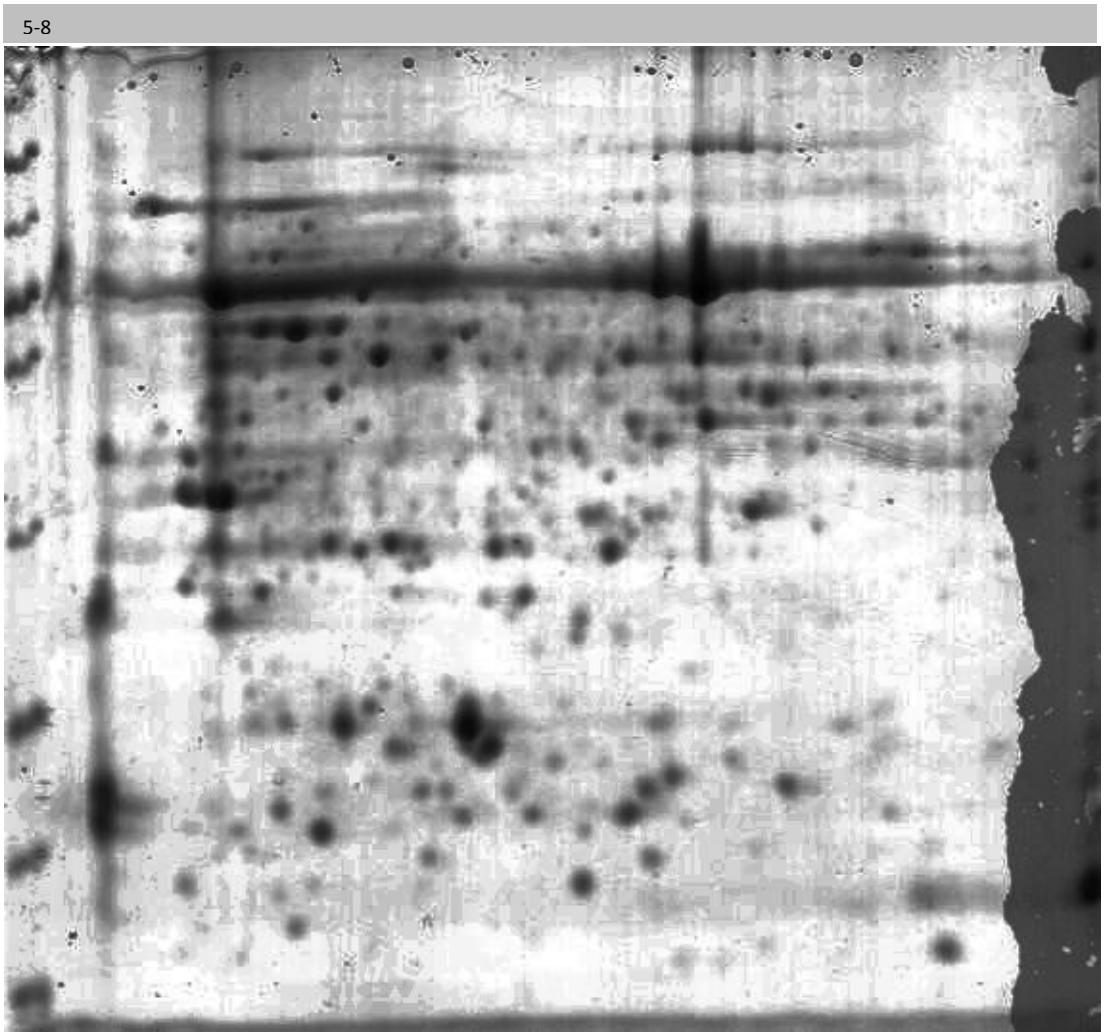

Figure 3.12 Enhanced gel image of *Pinus sylvestris* summer sample. pI range of the strip change from left to right as from 5 to 8 (Photos were taken by an ordinary office-type scanner).

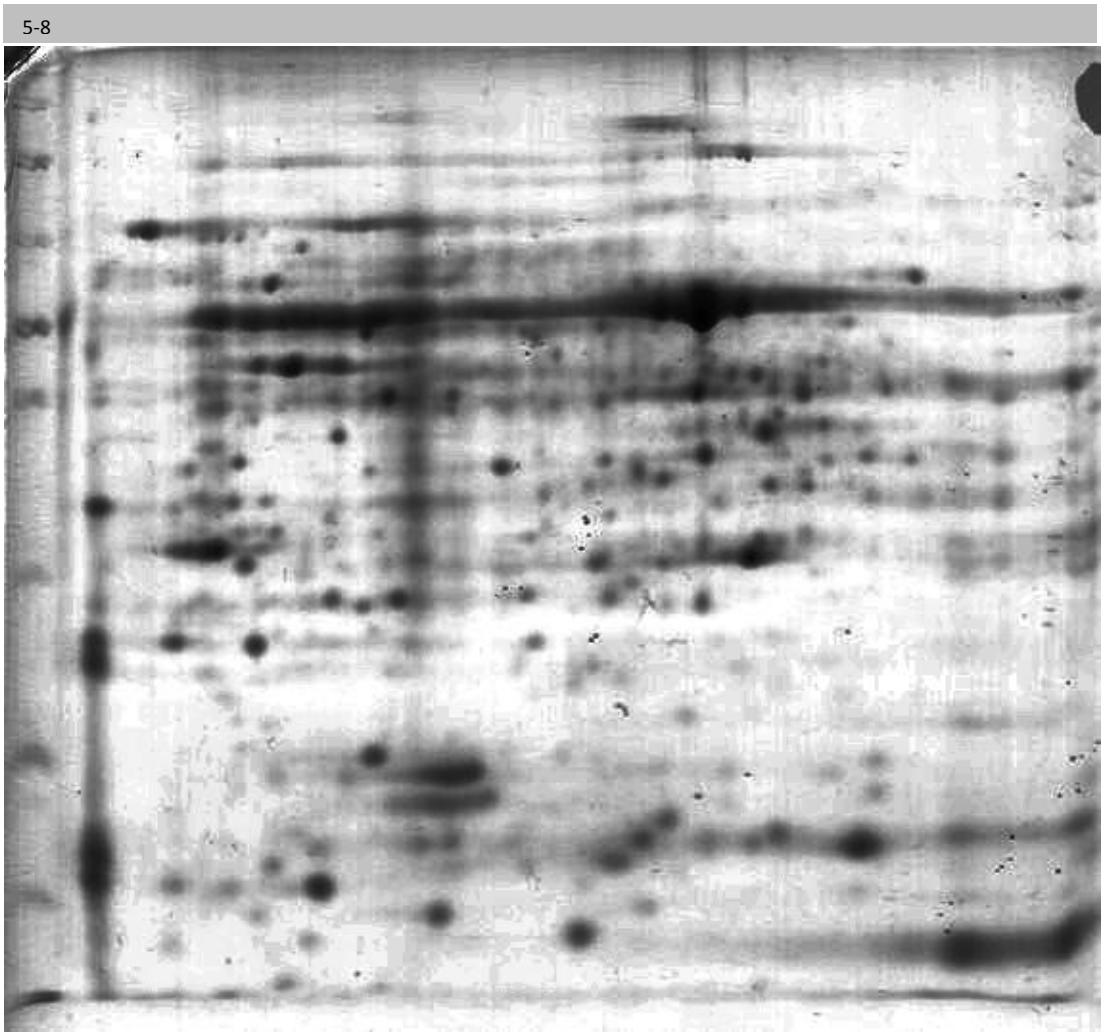

Figure 3.13 Enhanced gel image of *Pinus sylvestris* winter sample. pI range of the strip change from left to right as from 5 to 8 (Photos were taken by an ordinary office-type scanner).

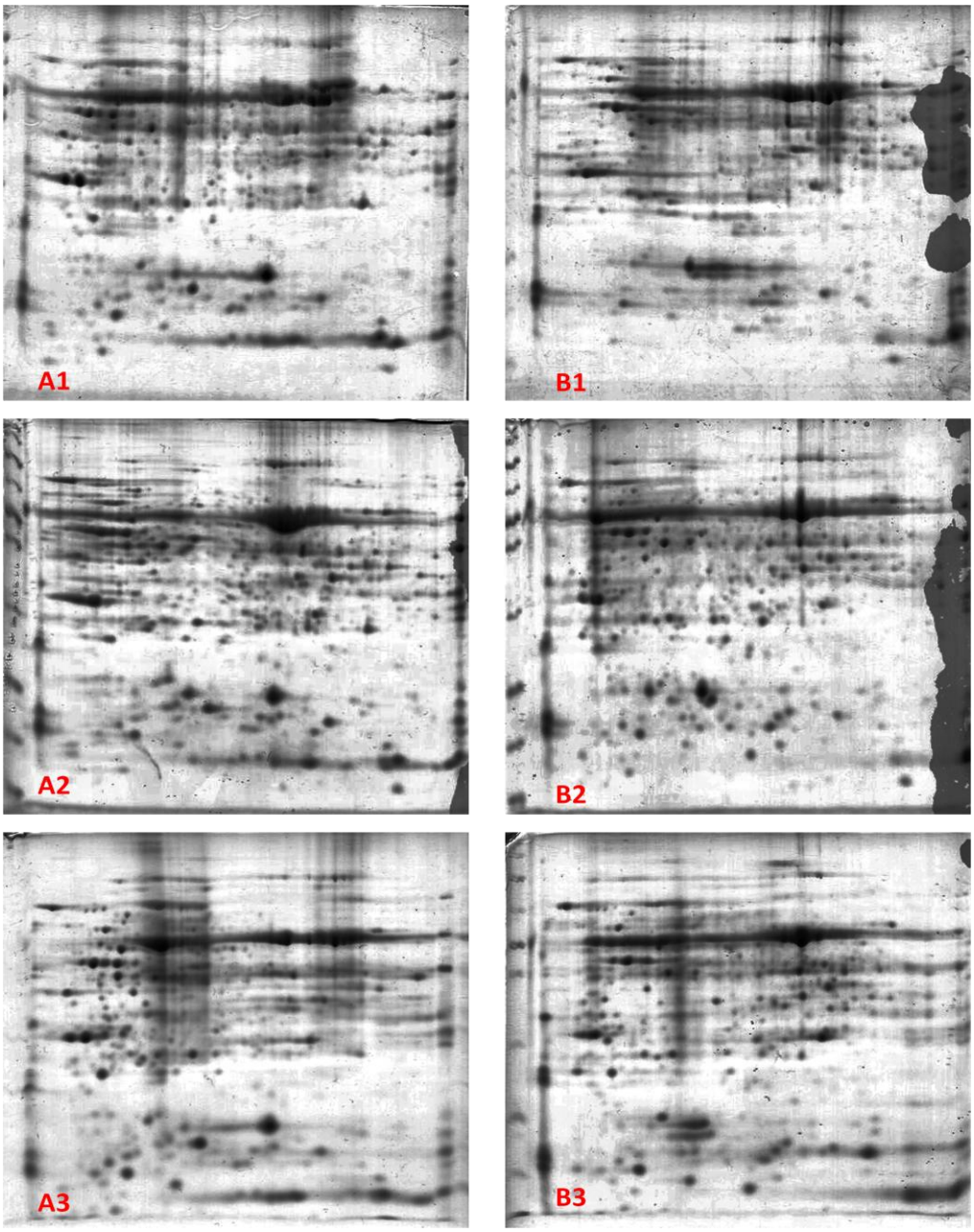

Figure 3.14 Enhanced gel images created by the Ludesi REDFIN software. PB-spring (A1), PB-summer (A2) and PB-winter (A3) were analyzed as a group to be compared with each other. The same procedure was performed for PS-spring (B1), PS-summer (B2) and PS-winter (B3). pI range of the strip change from left to right as from 5 to 8 (Photos were taken by an ordinary office-type scanner).

Those groups of gels were analyzed for the number of spots having changes in their volumes/densities in a way that the gel images of spring samples in each group were accepted as the reference because the samples collected at this season were accepted as the control group. The software calculates mean normalized volumes between groups and present fold-changes with a 2-fold filtering option which allow users to eliminate spot groups having less change.

Analysis were repeated for all degree of changes (by using no-filtering option) and for "2-fold" changes (by using 2-fold filtering option). As a result, the number of spots showing

twice or higher densities with respect to ones on the reference gel, and the number of spots with half or even less densities were all detected (Tables 3.1, 3.2, 3.3 and 3.4).

Table 3.1 Number of spots after "2-fold filtering" for the group of gels of *Pinus brutia*. Summer and winter samples were compared with spring one by one; i.e., the table shows the results of spring-winter and spring-summer analysis.

	Number of spots up-regulated 2 fold or more	**Number of spots down-regulated 2 fold or more**
Summer	34	79
Winter	63	58

Table 3.2 Number of spots after "2-fold filtering" for the group of gels of *Pinus sylvestris*. Summer and winter samples were compared with spring one by one; i.e., the table shows the results of spring-winter and spring-summer analysis.

	Number of spots up-regulated 2 fold or more	**Number of spots down-regulated 2 fold or more**
Summer	67	84
Winter	80	114

Table 3.3 The comparison of the number of spots after the analysis of all gels with 2-fold filtering option; i.e. table summarizes the result of spring-winter-summer analysis for *Pinus brutia*. (Green: spring, Red: summer, Blue: Winter)

	Increased spot volume/density in Winter sample	**Decreased spot volume/density in Winter sample**
Increased spot volume/density in Summer sample	**25** 	**52** 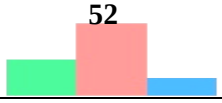
Decreased spot volume/density in Summer sample	**109** 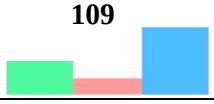	**25** 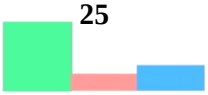

Table 3.4 The comparison of the number of spots after the analysis of all gels with 2-fold filtering option; i.e. table summarizes the result of spring-winter-summer analysis for *Pinus sylvestris*. (Green: spring, Red: summer, Blue: Winter)

	Increased spot volume/density in Winter sample	**Decreased spot volume/density in Winter sample**
Increased spot volume/density in Summer sample	**50** 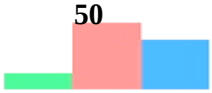	**74** 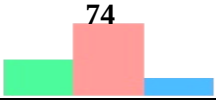
Decreased spot volume/density in Summer sample	**68** 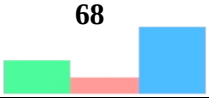	**79** 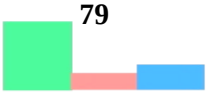

3.3. Chlorophyll and Carotenoid Content

Chlorophyll molecule is a central unit in the metabolism of plants and other photosynthetic organisms; so, it is also an indicator of growth, health and development (Mencarelli & Saltveit, 1988). Although it is not directly correlated with the rate of photosynthesis, still, the changes in the amount of chlorophyll content give supplementary data for the fate of total metabolism in the case of various stress conditions, too. In other words, the sensitivity of chlorophylls (Chl) and carotenoids (Car) to many stressors makes them good indicators of the physiological status of plants.

Spectrophotometric measurements of the extracts produced by using different solvent types demonstrated that the usage of those different solvent systems did not alter the general trend in the increase or the decrease of chlorophyll-a, chlorophyll-b and chlorophyll-(a+b)contents throughout the sampling seasons (Figures 3.15, 3.16 and 3.17). Moreover, the standard deviations between the values for different solvents were in 90% confidence interval (Table 3.5) which could be transfered into 95% confidence interval by the exclusion of 100% acetone data.

Table 3.5 Changes in the chlorophyll-a, chlorophyll-b and chlorophyll-(a+b) contents throughout the sampling seasons

		Raw Data (µgram/g of plant extract)				**Standard Deviation**
	Sample	**95% Ethanol**	**100% Methanol**	**100% Acetone**	**80% Acetone**	
Chlorophyll-a Content	PB-winter	638,17	624,48	601,21	532,83	±46,78
	PS-winter	487,45	524,74	444,65	460,09	±35,12
	PB-spring	904,74	974,12	883,28	892,16	±41,31
	PS-spring	623,64	675,50	616,15	570,92	±42,85
	PB-summer	530,39	592,58	583,61	527,87	±34,25
	PS-summer	773,24	827,66	689,96	671,77	±72,91
Chlorophyll-b Content	PB-winter	192,49	173,44	130,73	163,71	±25,84
	PS-winter	176,62	174,06	113,17	174,30	±30,94
	PB-spring	275,81	295,59	231,68	276,40	±27,07
	PS-spring	215,87	235,17	151,25	184,90	±36,76
	PB-summer	168,01	174,47	142,20	181,32	±17,09
	PS-summer	249,24	253,52	158,60	232,79	±44,20
Chlorophyll-(a+b) Content	PB-winter	830,64	797,92	731,94	696,54	±61,02
	PS-winter	664,08	698,80	557,82	634,39	±60,04
	PB-spring	1180,55	1269,71	1114,96	1168,56	±64,19
	PS-spring	839,52	910,67	767,40	755,81	±71,83
	PB-summer	698,39	767,05	725,81	709,19	±30,15
	PS-summer	1022,48	1081,18	848,56	904,55	±106,48

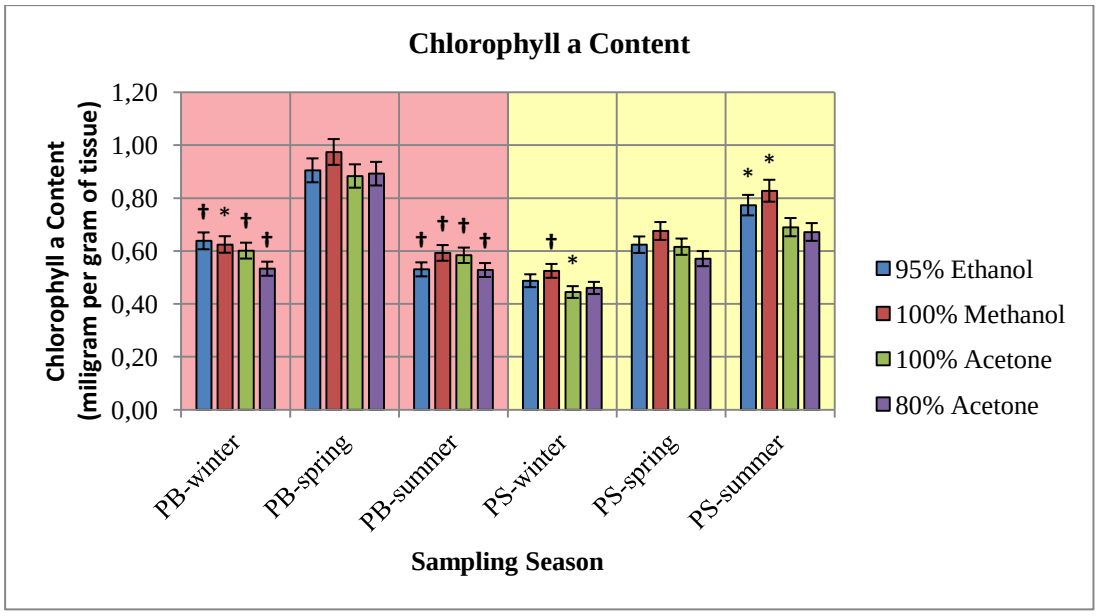

Figure 3.15 Chlorophyll-a contents measured for both species in all sampling seasons. Red area is for *P. brutia*, and yellow area is for *P. sylvestris*, and, standard deviation values are indicated as error bars. (*): $p<0.05$, (†): $p<0,005$

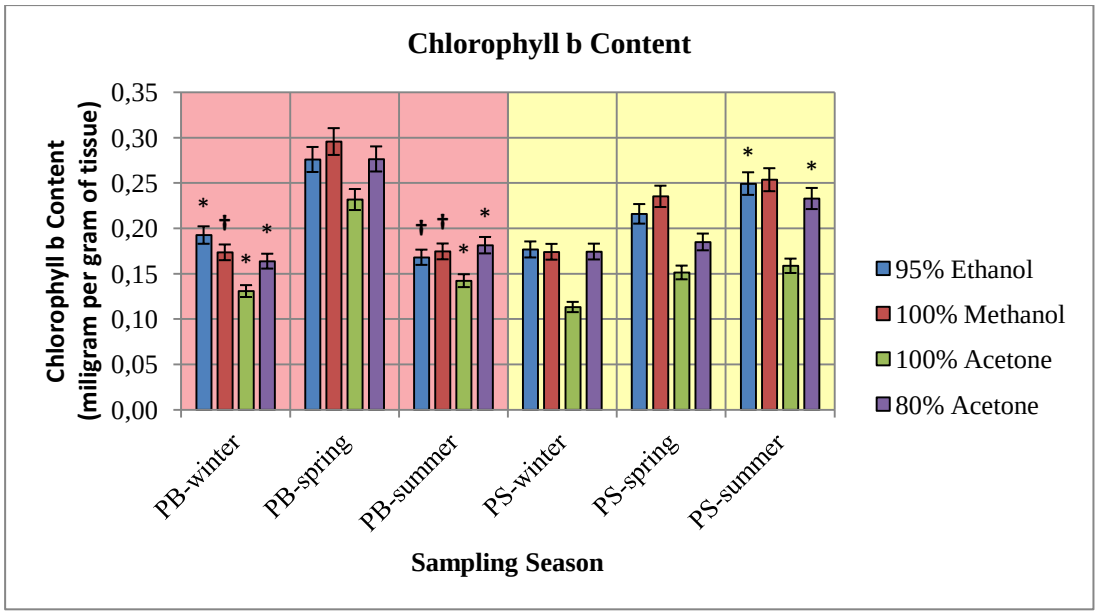

Figure 3.16 Chlorophyll-b contents measured for both species in all sampling seasons. Red area is for *P. brutia*, and yellow area is for *P. sylvestris*, and, standard deviation values are indicated as error bars. (*): $p<0.05$, (†): $p<0,005$

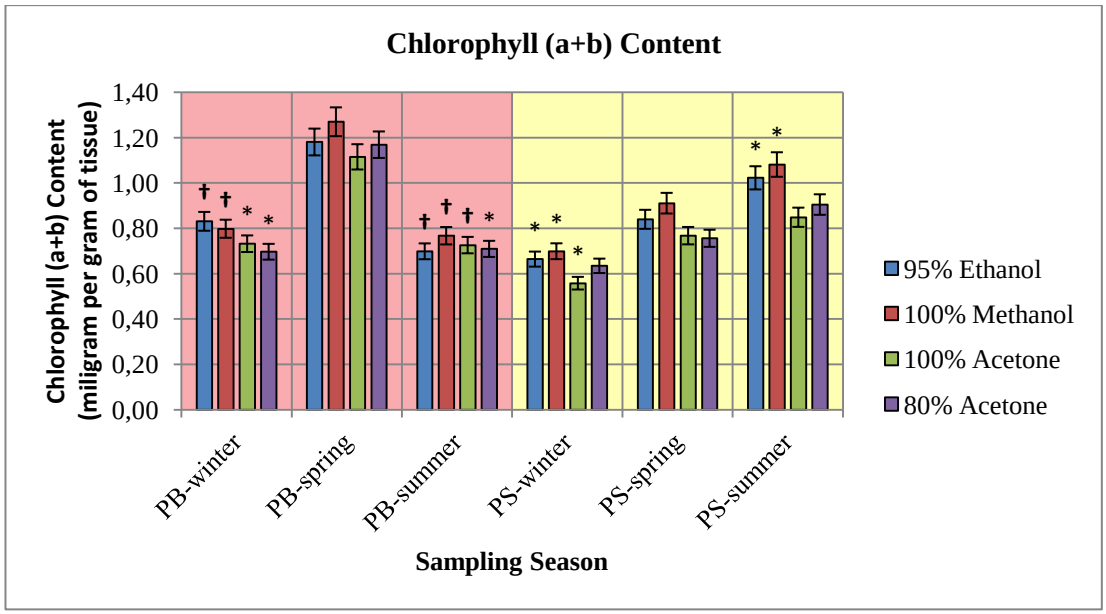

Figure 3.17 Chlorophyll-(a+b) contents measured for both species in all sampling seasons. Red area is for *P. brutia*, and yellow area is for *P. sylvestris*, and, standard deviation values are indicated as error bars. (*): p<0.05, (†): p<0,005

Carotenoids have well-established functions in harvesting light in the paths of photosynthesis and they, also, work as quenchers of triplet chlorophyll and singlet oxygen (Havaux, 1998). Carotenoid content and, chlorophyllide-a and chlorophyllide-b which are the precursors of chlorophyll production were all measured for the evaluation of photosynthetic rate and a possible stress regulation (Figure 3.18, 3.19 and 3.20) by using 80% acetone as the solvent system.

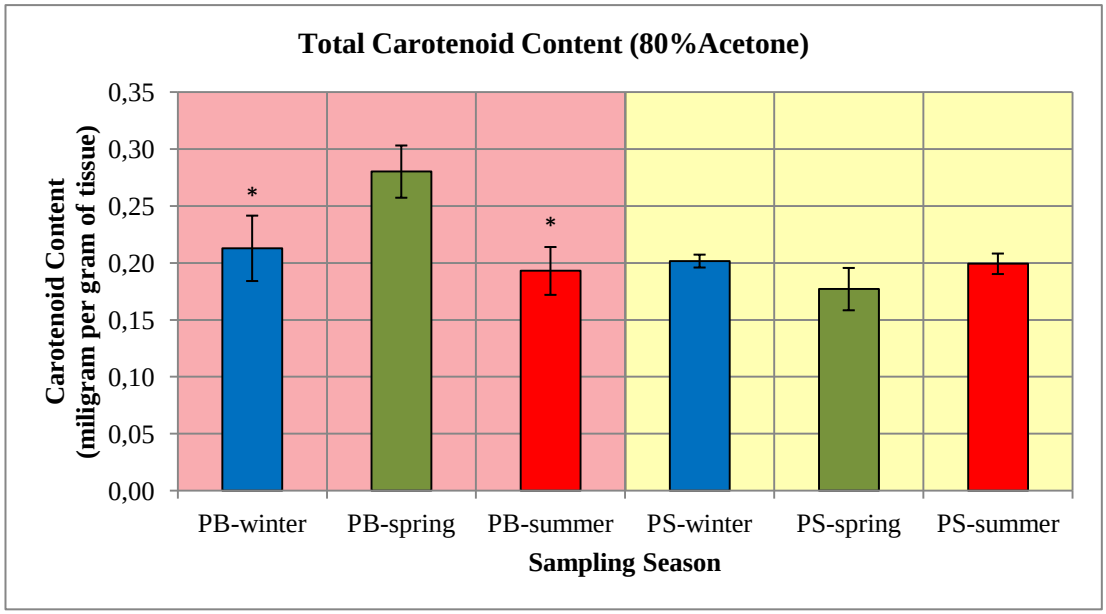

Figure 3.18 The total carotenoid amount of the needles collected in three different sampling seasons, for both of the species. 80% acetone was used for extraction procedure. Red area is for *P. brutia*, and yellow area is for *P. sylvestris*, and, standard deviation values are indicated as error bars. (*): p<0.05

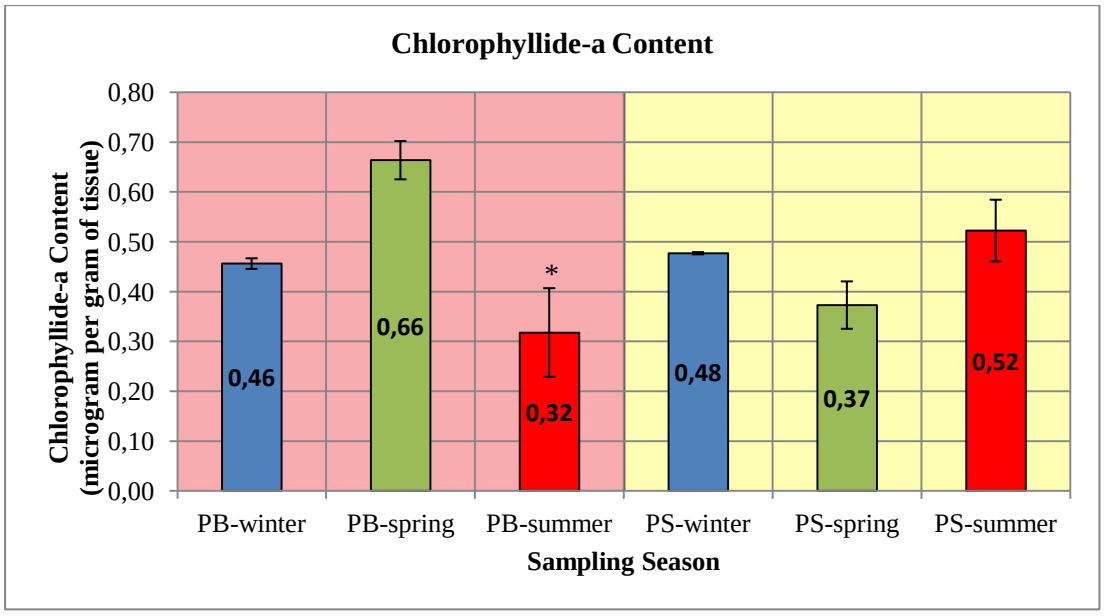

Figure 3.19 The chlorophyllide-a content of the needles collected in three different sampling seasons, for both of the species (red area is for *P. brutia*, and yellow area is for *P. sylvestris*). 80% acetone was used for extraction procedure. Standard deviation values are indicated as error bars. (*): $p<0.05$

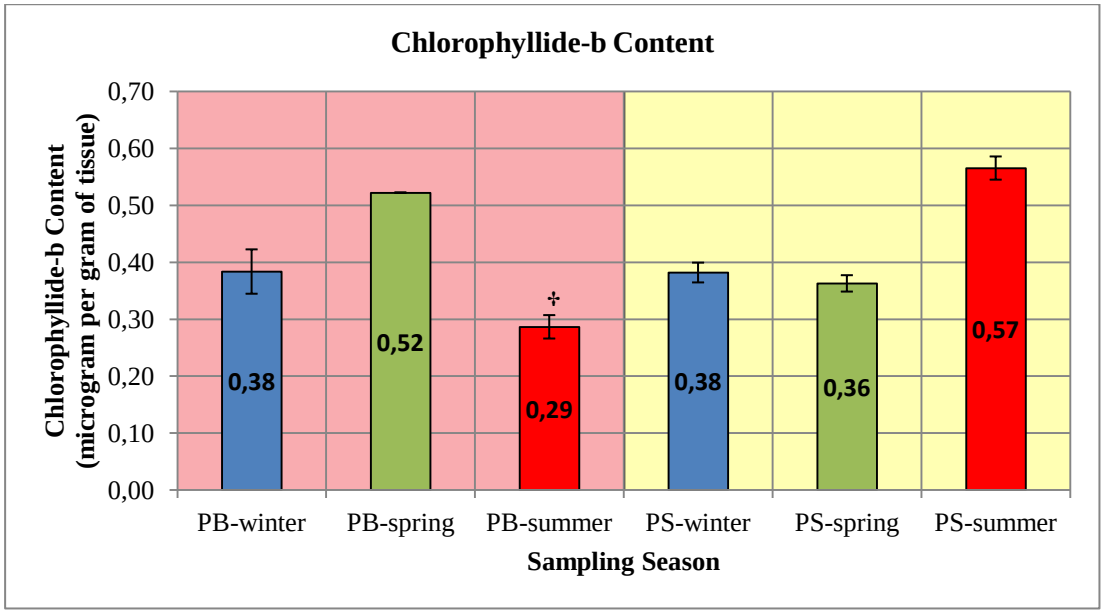

Figure 3.20 The chlorophyllide-b content of the needles collected in three different sampling seasons, for both of the species (red area is for *P. brutia*, and yellow area is for *P. sylvestris*). 80% acetone was used for extraction procedure. Standard deviation values are indicated as error bars. (†): $p<0,005$

Table 3.6 "Chlorophyll-(a+b) / Carotenoid Content" ratio of the needle extracts for *Pinus brutia* and *Pinus sylvestris* with respect to the sampling seasons. This ratio reached its minimal value in winter season for both of the species; however, Scots pine needles had their maximum value at summer season while the Turkish red pine needles provided the maximum value at spring time. (PB: *Pinus brutia*, PS: *Pinus sylvestris*)

	Chlorophyll-(a+b)/Carotenoid Ratio			
	95% EtOH	**100% Methanol**	**100% Acetone**	**80% Acetone**
PB-winter	3,90	3,75	3,44	3,27
PB-spring	4,21	4,53	3,98	4,17
PB-summer	3,62	3,97	3,76	3,67
PS-winter	3,29	3,46	2,77	3,15
PS-spring	4,74	5,14	4,33	4,27
PS-summer	5,13	5,42	4,26	4,54

Table 3.7 Rate of change in the chlorophyll a/b ratio for both pine species in winter and summer seasons (with respect to spring season). Minus sign (-) means a percentage decrease in the ratio with respect to the reference season. (PB: *Pinus brutia*, PS: *Pinus sylvestris*)

	Rate of change with respect to spring values (%)							
	95% EtOH		**100% Methanol**		**100% Acetone**		**80% Acetone**	
	winter	**summer**	**winter**	**summer**	**winter**	**summer**	**winter**	**summer**
PB	1,07	-3,76	9,26	3,06	20,62	7,65	0,83	-9,80
PS	-4,47	7,39	4,96	13,66	-3,55	6,79	-14,51	-6,54

The chlorophyll/carotenoid (xanthopyll) ratio was accepted as a tool to evaluate the presence and the effects of cold hardening in plant species (Ruelland *et al*, 2009). Table 3.6 summarizes the changes in this ration throughout the seasons for both pine species. The rate of changes in the chlorophyll a/b ratio for both species were also calculated (Table 3.7).

3.4. Malondialdehyde (MDA) Content

Malondialdehyde (MDA) is a widely used marker of oxidative lipid injury whose concentration varies in response to biotic and abiotic stress (Davey *et al*, 2005). The carbon-centered lipid radical of the fatty acid take oxygen in an aerobic medium to give rise to a $ROO^{\cdot}$ which propagates the peroxidation chain reaction by abstracting a hydrogen atom from adjacent poly unsaturated fatty acid side chains. The resulting lipid hydroperoxide can easily decompose into several reactive species including malonyldialdehyde with many other species (Gill & Tuteja, 2010).

Although there wasn't any statistically significant difference between the values of sampling seasons for both species (Figure 3.21), overall MDA amount measured for *Pinus brutia* was about 2.5 times higher with respect to *Pinus sylvestris*.

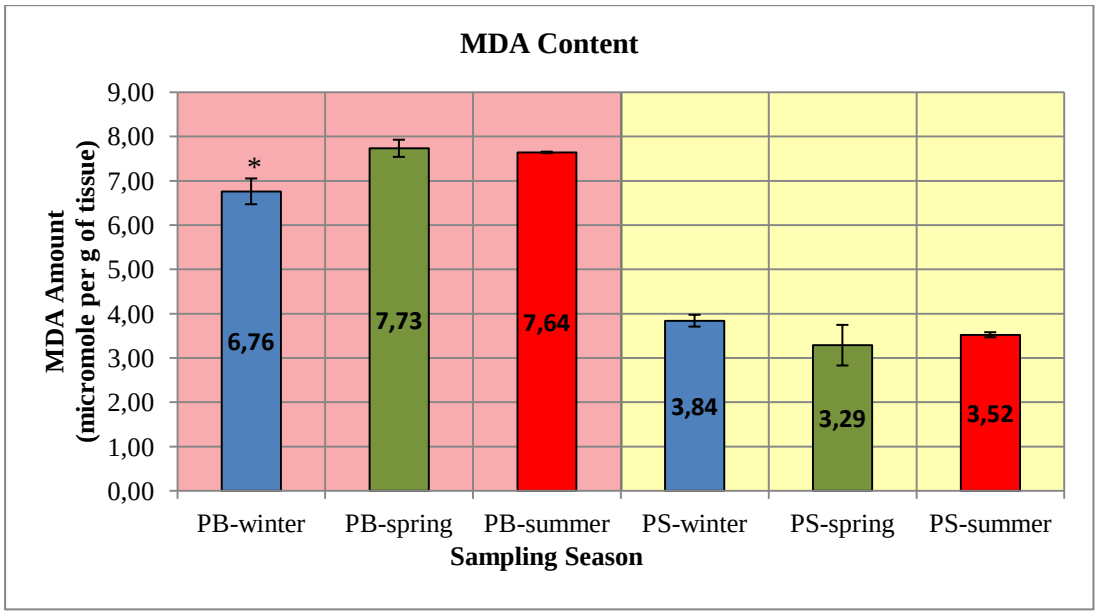

Figure 3.21 The results of MDA Assay. Red area is for *P. brutia*, and yellow area is for *P. sylvestris*, and, standard deviation values are indicated as error bars. (*): $p<0.05$

3.5. Proline Content

Proline is considered to be a compatible solute which accumulates in many plant species under a broad range of stress conditions such as water shortage, salinity, extreme temperatures, and high light intensity (Claussen, 2005) because it functions as an osmoprotectant, a protein stabilizer, a metal chelator, an inhibitor of LPO, and OH^* and $^1O_2$ scavenger (Gill & Tuteja, 2010). So, the changes in the amount of this molecule, in needle samples, could be used as an indicator of the physiological conditions of pine trees during all the sampling season (Figure 3.22).

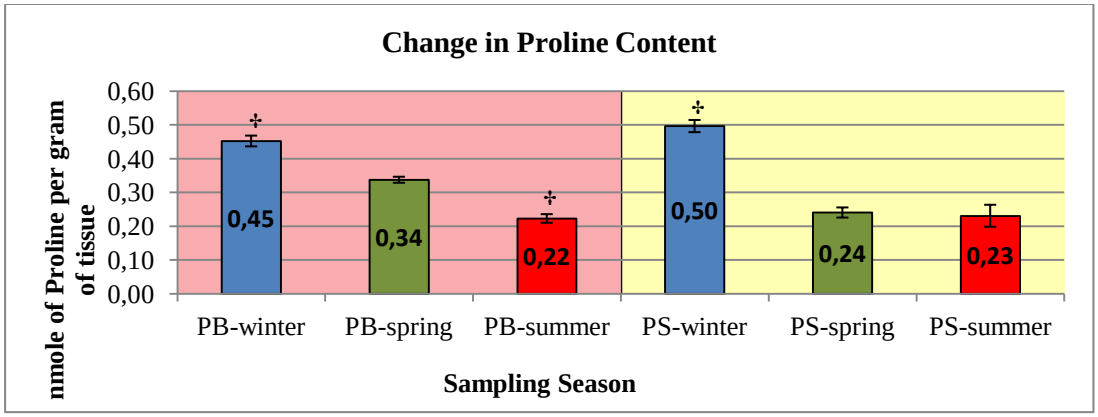

Figure 3.22 The changes in the amount of proline in the needles of both pine species throughout the sampling season. Red area is for *P. brutia*, and yellow area is for *P. sylvestris*, and, standard deviation values are indicated as error bars. (†): $p<0,005$

The levels of proline in the needles were highest in winter samples for *P. brutia* and *P.sylvestris* with values of 0.452 and 0.496 nmole/gr of tissue, respectively. At the end of the summer season, those values were decreased to 0.223 and 0.231 nmole/gr of tissue; almost the half of their maximum.

3.6. Amount of Total Thiol Groups in Needle Homogenates

Glutathione makes up more than 95 % of the water soluble thiol (-SH) content in needles of spruce (Grill *et al*, 1987); so the changes in thiol content can be considered as changes in glutathione in reduced form (GSH) (Pukacka & Pukacki, 2000).

The intracellular redox of the plants is open to any affect created by stressors such as extreme temperatures and drought, and, signalling pathways and the overall the fate of cells might be altered dramatically by those factors. For those plant cells, the production of glutathione (GSH), which acts as an antioxidant by quenching reactive oxygen species to eliminate damaging peroxides, is a natural response (Galant *et al*, 2011).

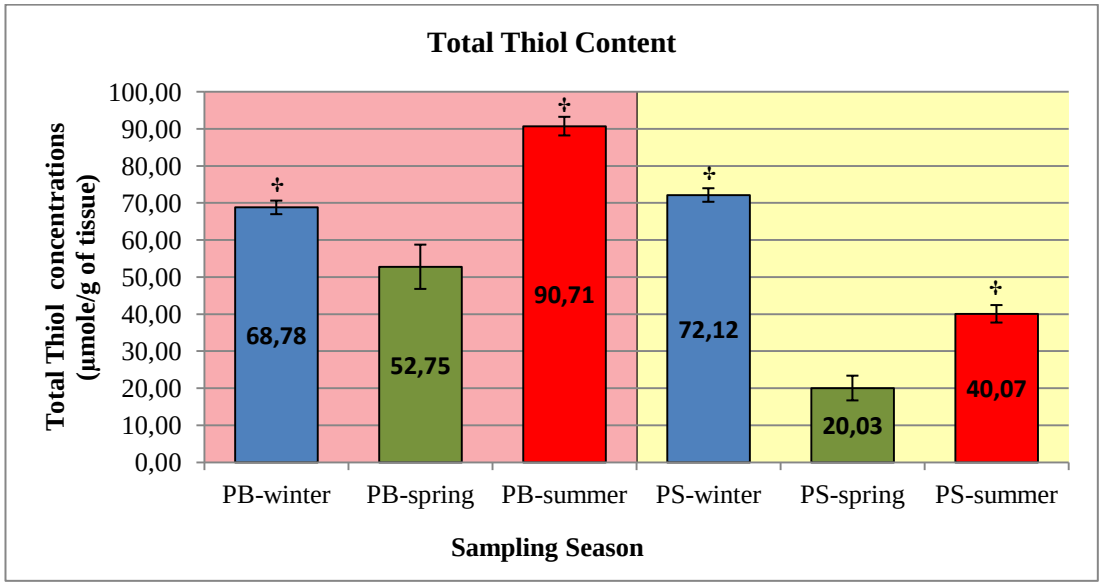

Figure 3.23 Total thiol amounts meeasured for needle homogenates of *Pinus brutia* and *Pinus sylvestris*. Red area is for *P. brutia*, and yellow area is for *P. sylvestris*, and, standard deviation values are indicated as error bars. (†): p<0,005

Table 3.8 Total thiol concentrations in the needle homogenates of both species, in all sampling seasons.

Sample	Total Thiol concentrations (µmole/g of tissue)	Standard Deviation
PB-Winter	68.78	±1.83
PB-Spring	52.75	±5.97
PB-Summer	90.71	±2.51
PS-Winter	72.12	±1.83
PS-Spring	20.03	±3.34
PS-Summer	40.07	±2.36

Pinus brutia and *Pinus sylvestris* showed similar patterns in the changes of total thiol content in the needle homogenates (Figure 3.23); a decrease in the spring season and an elevation in the summer season. The level of total thiol groups in the needle homogenates of *Pinus sylvestris* decreased by 70.3% at spring season, and elevated by a percentage of 84.2% at the end of summer season. For *Pinus brutia*, this level reduced by 15.3% from winter to spring season, and increased by 63.0% at the end of summer (Table 3.8).

3.7. GST Enzyme Activities of Needle Homogenates

Glutathione S-transferases (GSTs) have functions in detoxification of various xenobiotic compounds and oxygen radicals (Marrs, 1996) (Seppanen *et al*, 2000). Their roles in those biochemical pathways make them useful markers in the detection of stress in plant metabolism. Under extreme environmental conditions like very high or very low temperature and drought, severe membrane damage occurs (Yadav, 2010), which in turn, triggers a serious of transcriptional changes in the plant cells including an increase in the amount of GSH. Although it is not the only mechanism discovered, the elevated GSH levels induce transcription of defense genes such as GSTs (Marrs, 1996).

The total specific activity values of GSTs in *P.brutia* showed a decreasing pattern from winter season to summer with an approximatelly 35% of difference. On the contrary, the specific activity of GSTs in the needle homogenates of *P.sylvestris* increased almost twice in summer (Figure 3.24). An interesting outcome of those measurements was that the levels of the specific activities of *P. sylvestris* were considerably low with respect to the one of *P. brutia* (Table 3.9).

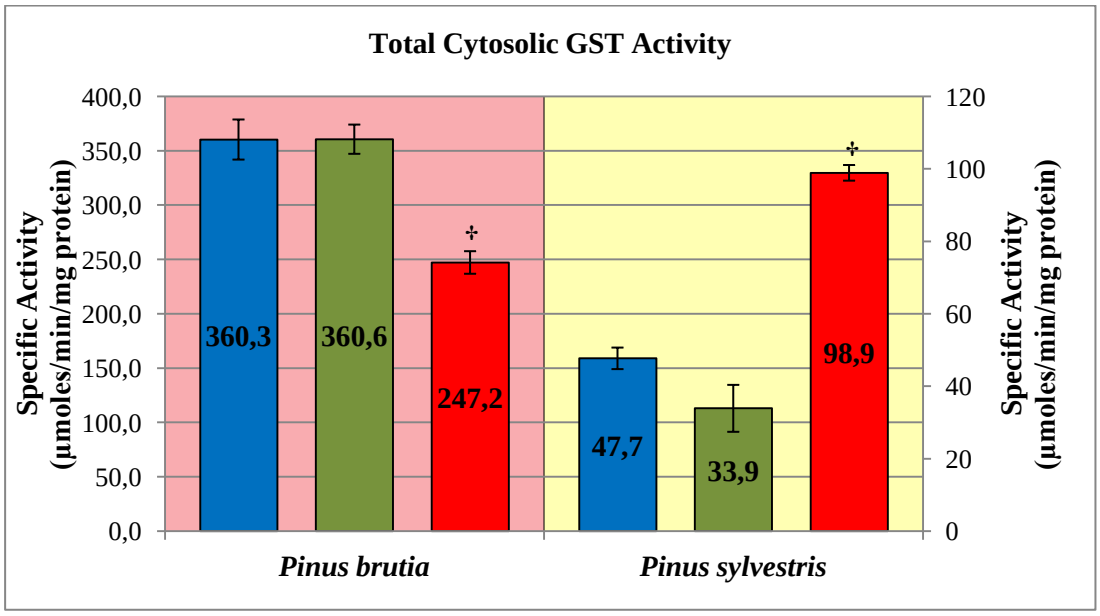

Figure 3.24 The specific activity of GST enzyme values of needle homogenates of both pine species in all three seasons (Colors of columns: green is for spring, red is for summer and blue is for Winter). Red area is for *P. brutia*, and yellow area is for *P. sylvestris*, and, standard deviation values are indicated as error bars. (†): p<0,005

Table 3.9 The specific activity of GST enzyme values measured against the common substrate CDNB. Needle homogenates of both pine species in all three seasons were used as the enzyme source.

Sample	Specific Activity (µmoles/min/mg protein)	Standard Deviation
PB-Winter	360,3	±18,44
PB-Spring	360,6	±13,46
PB-Summer	247,2	±10,39
PS-Winter	47,7	±2,97
PS-Spring	33,9	±6,48
PS-Summer	98,9	±2,16

3.8. Western Blot Anaylsis

Western Blot analysis of a set of antibodies representing some important members of the photosynthetic pathway and energy metabolism were performed. For some of the samples, there were doublets in western blot images. These were caused possibly by posttranslational modifications or simply by breaks in the protein structure because of extraction or dissolution procedure.

3.8.1. AtpB, beta subunit of ATP synthase

ATP synthase is the universal enzyme that synthesizes ATP from ADP and phosphate using the energy stored in a transmembrane ion gradient. This anti-AtpB antibody detects the mitochondrial form of the F1-ATP synthase subcomplex, as well as the chloroplastic CF1 Atp Synthase. For the production of this antibody, a peptide found in a beta sheet that wass close to the surface of AtpB protein was used.

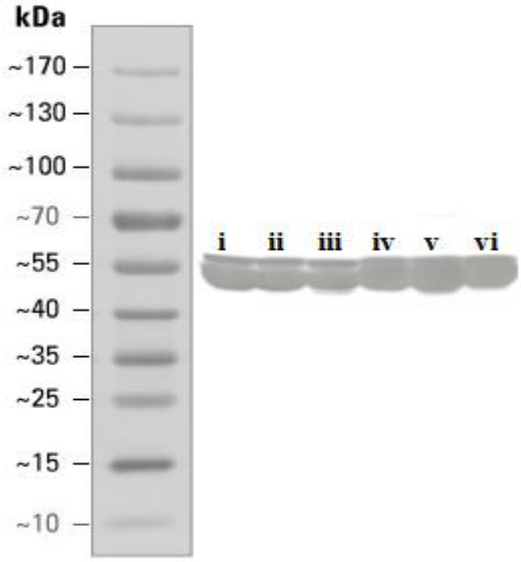

Figure 3.25 Lane analysis of the western blot image of six samples incubated for AtpB antibody diluted as 1:3000 in 2% non-fat dry milk solution prepared in phosphate buffered saline solution (PBS) at pH 7.4 containing 137mM NaCl, 2.7 mM KCl, 1,47 mM KH_2PO_4, 82 mM Na_2HPO_4. Bands were visualized by ECL method after 10 sec. of incubation in hypercasette. **(i)** *Pinus sylvestris*-summer, **(ii)** *Pinus sylvestris*-spring, **(iii)** *Pinus sylvestris*-winter, **(iv)** *Pinus brutia*-summer, **(v)** *Pinus brutia* -spring, **(vi)** *Pinus brutia*-winter.

After western blotting, the bands (Figure 3.25) were further analyzed by open-source software of ImageJ with gel analysis plug-ins (Figure 3.26) and the densities were compared as percentages by keeping the highest one as 100% (Table 3.8). The results showed that, there is an increased F1-ATP synthase subcomplex level for the spring season for *P.brutia* and in summer season for *P.sylvestris*.

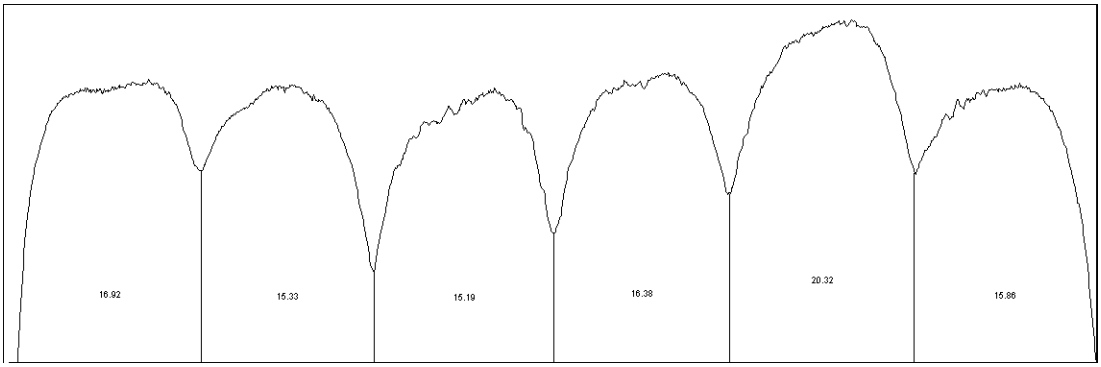

Figure 3.26 The resulting plots of the band analysis of samples after western blot analysis with AtpB antibody.

Table 3.10 Numerical values of the lane analysis of the bands for all six samples incubated for AtpB antibody and visualized by ECL method.

Sample	Area	Percentage (%)
PS-summer	49.056.744	83,26
PS-spring	44.448.794	75,44
PS-winter	44.044.865	74,75
PB-summer	47.495.037	80,61
PB-spring	58.920.108	100,00
PB-winter	45.997.986	78,07

3.8.2. LHCSR-III, Light Harvesting Complex Stress Related Protein-III

Light Harvesting Complex Stress Related proteins generally function in the modulation of excess light energy dissipation in most photosynthetic organisms (Bailleul, *et al*., 2010); moreover, they may have some other stress-related functions, especially, in Plantae.

After western blot analysis of the samples by using this antibody in 1:3000 diluted form, ECL method was applied and the membrane was kept in the hypercasette for 10 min. Figure 3.27 shows the binding pattern of the antibody to the bands. According to the results of lane analysis by ImageJ (Figure 3.28), for *P.brutia*, LHCSR-III expression seemed to be increased in spring time with respect to winter season and this amount appeared to be stable throughout the summer season. For *P.sylvestris*, level of this protein elevated from winter time till the end of summer season (Table 3.11).

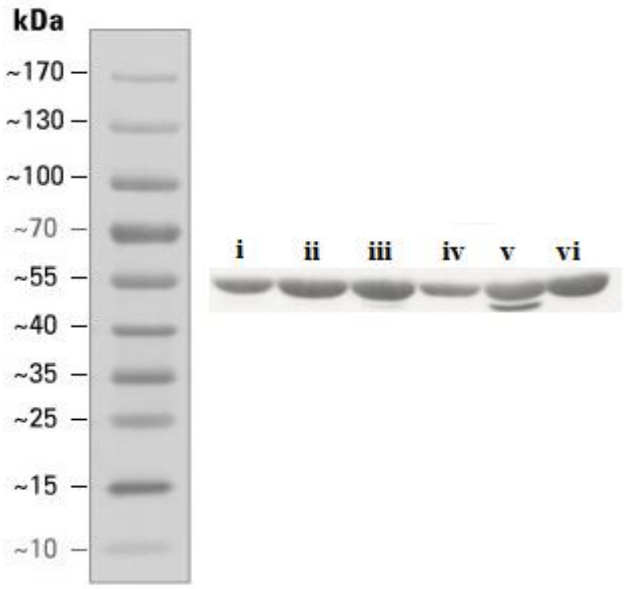

Figure 3.27 Lane analysis of the western blot image of six samples incubated for LHCSR-III antibody diluted as 1:3000 in 2% non-fat dry milk solution prepared in phosphate buffered saline solution (PBS) at pH 7.4 containing 137mM NaCl, 2.7 mM KCl, 1,47 mM KH_2PO_4, 82 mM Na_2HPO_4. Bands were visualized by ECL method after 10 sec. of incubation in hypercasette. **(i)** *Pinus brutia*-winter, **(ii)** *Pinus brutia* -spring, **(iii)** *Pinus brutia*-summer, **(iv)** *Pinus sylvestris*-winter, **(v)** *Pinus sylvestris*-spring, **(vi)** *Pinus sylvestris*-summer.

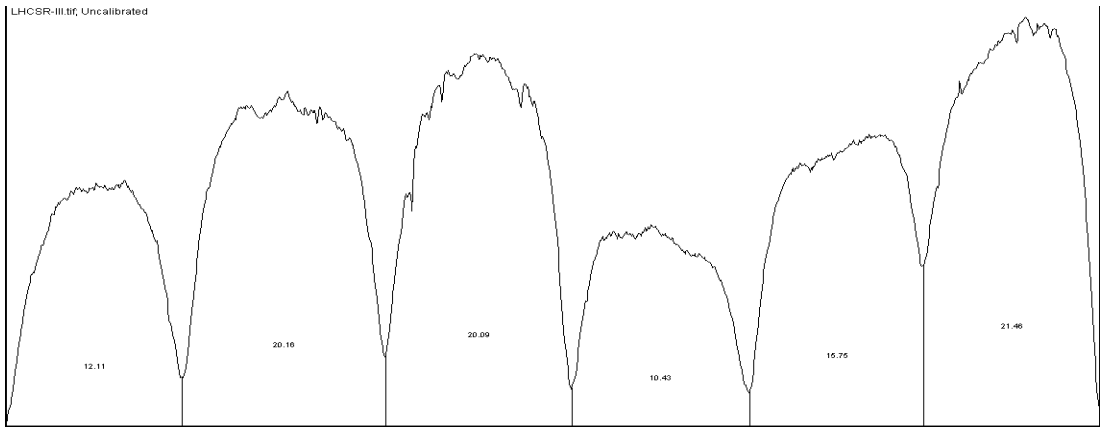

Figure 3.28 The resulting plots of the band analysis of samples after western blot analysis with LHCSR-III antibody.

Table 3.11 Numerical values of the lane analysis of the bands for all six samples incubated for LHCSR-III antibody and visualized by ECL method.

Sample	Area	Percentage (%)
PB-winter	47.030.401	56,43
PB-spring	78.265.371	93,91
PB-summer	78.020.179	93,62
PS-winter	40.506.815	48,61
PS-spring	61.145.865	73,37
PS-summer	83.340.693	100

3.8.3. PsbA-D1, D1 protein of PSII, C-terminal

The psbA gene, as a part of chloroplastic genome, is responsible for the production of D1 protein and this antibody reveals the functional content of the PSII in most photosynthetic organisms. Western blot analysis of the samples revealed a common pattern for the changes in the amount of this protein between the sampling periods (Figure 3.29). In winter time, for both of the species, the levels of expression for D1 protein appeared to be decreased (Figure 3.30) and the numerical values demonstrated that this change was more considerable for *Pinus sylvestris* with respect to *Pinus brutia* (Table 3.12).

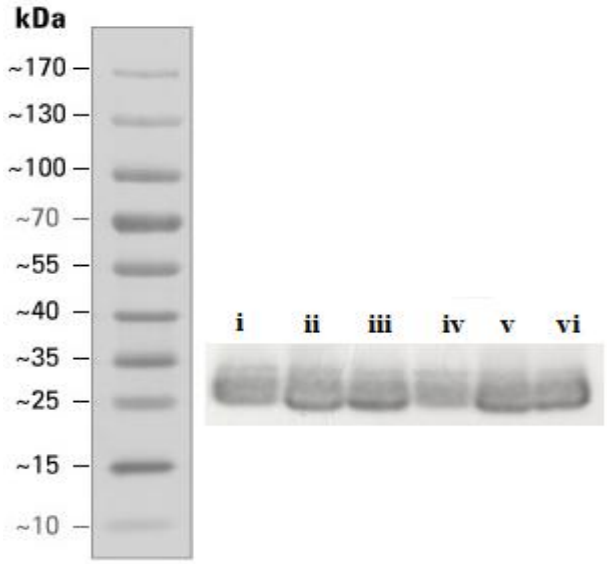

Figure 3.29 Lane analysis of the western blot image of six samples incubated for PsbA-D1 antibody diluted as 1:10000 in 2% non-fat dry milk solution prepared in phosphate buffered saline solution (PBS) at pH 7.4 containing 137mM NaCl, 2.7 mM KCl, 1,47 mM KH_2PO_4, 82 mM Na_2HPO_4. Bands were visualized by ECL method after 10 sec. of incubation in hypercasette. **(i)** *Pinus brutia*-winter, **(ii)** *Pinus brutia* -spring, **(iii)** *Pinus brutia*-summer, **(iv)** *Pinus sylvestris*-winter, **(v)** *Pinus sylvestris*-spring, **(vi)** *Pinus sylvestris*-summer.

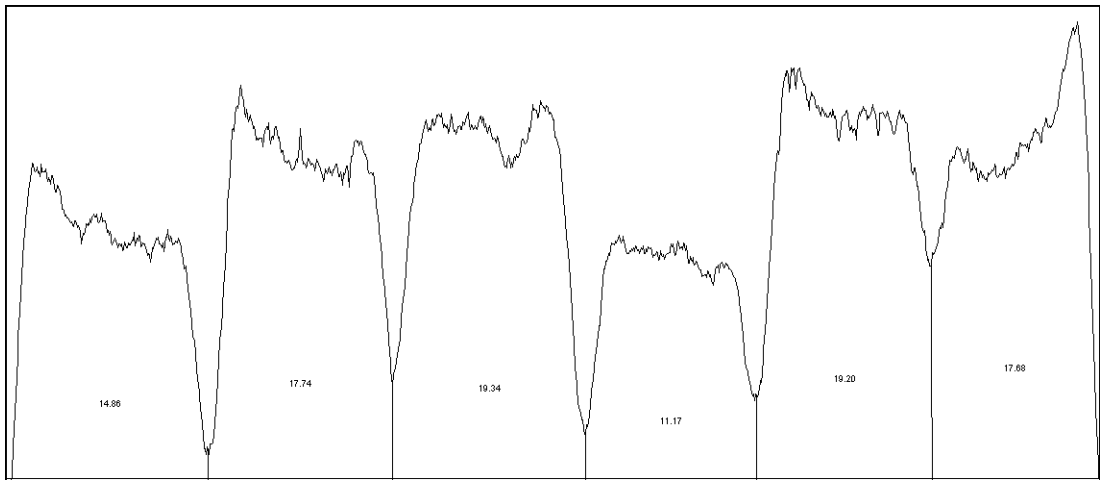

Figure 3.30 The resulting plots of the band analysis of samples after western blot analysis with PsbA-D1 antibody.

Table 3.12 Numerical values of the lane analysis of the bands for all six samples incubated for PsbA-D1 antibody and visualized by ECL method.

Sample	Area	Percentage (%)
PB-winter	48.899.421	76,83
PB-spring	58.383.472	91,73
PB-summer	63.644.836	100,00
PS-winter	36.743.158	57,73
PS-spring	63.175.693	99,26
PS-summer	58.171.744	91,40

3.9. Mass Spectrometry Analysis

Mass spectrometry techniques provide both quantitative and qualitative data for samples and today, there are a variety of procedures and equipments used for those purposes. In this study, among several systems, LC-MS/MS was used, which included the HPLC separation that was most often used for peptide fragments obtained from protease digestion of protein extracts like in our case. Trypsin-digested peptides were loaded into the Reverse Phase (RP) HPLC and via an ESI system used as ion source; they were analyzed in LTQ-Orbitrap MS/MS device. Then, Proteomatic software enabled us to run a set of programmes in a pipeline as shown in Figure 3.31.

Evaluation of the ion injection times, the number of averaged MS/MS scans and the number of averaged full scans are obligatory to produce favorable *b* and *y* ion coverage and high correlation to proteins using database searching algorithms (Wenner & Lynn, 2009). Three independent MS applications were performed (named as May-first set, July-second set and October-third set), and the number of Full scans and MS2 scans were calculated by using the software RawMeat (Table 3.13, Appendix D-I).

Table 3.13 Number of Full scans and MS2 scans for all mass spectrometric study.

Sample Sets	Full Scans	MS2 Scans
May-first set	115026	174207
July-second set	112748	169771
October-third set	141291	104427
TOTAL	**369065**	**448405**

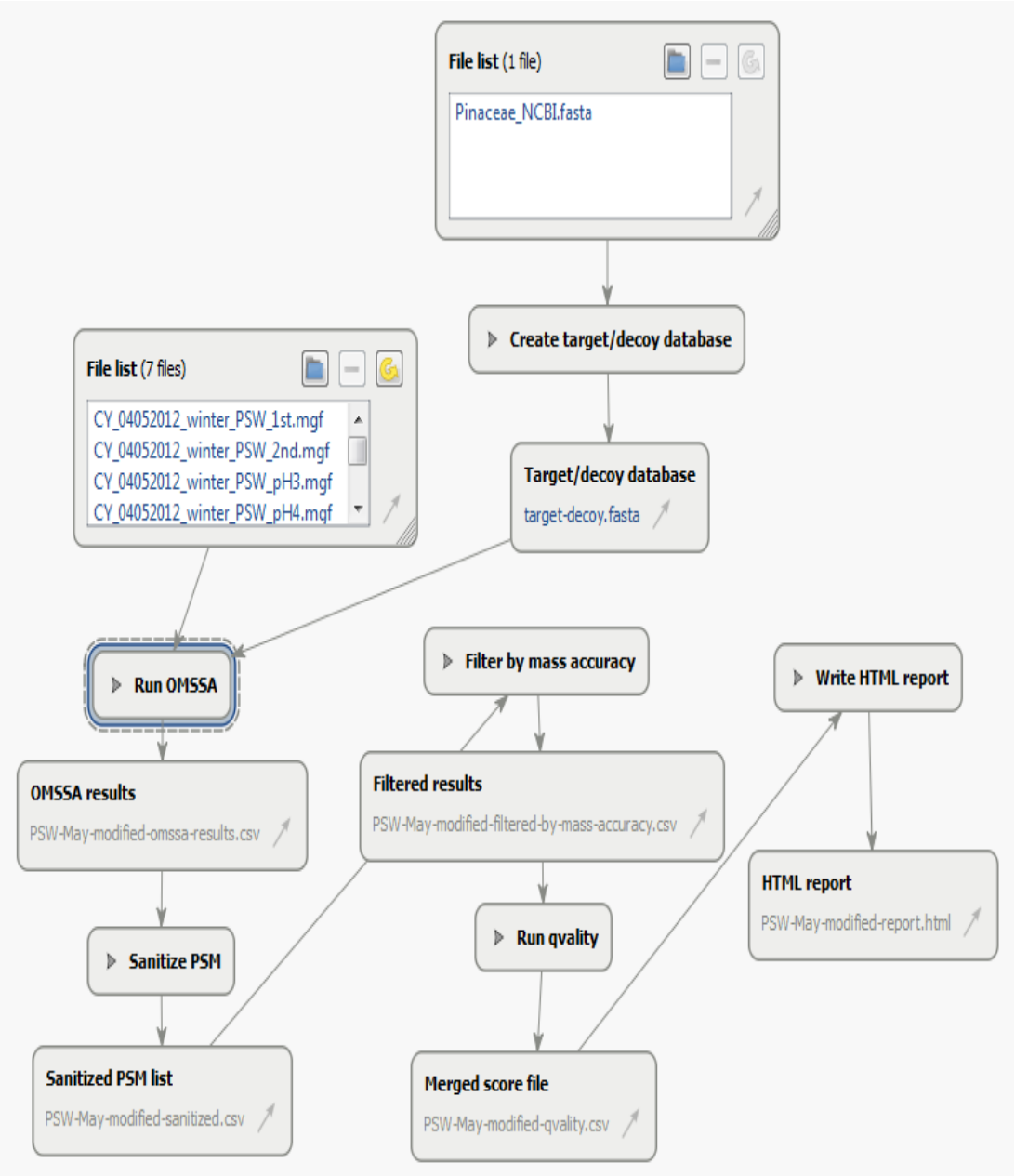

Figure 3.31 A sample Proteomatic pipeline used in the analysis of MS/MS results. Open Mass Spectrometry Search Algorithm (OMSSA) was used as the search engine, here.

OMSSA and X!Tandem engines identified 300-500 proteins for both species (Table 3.14, Appendix J). Spectral count values were accepted as an indicator for the abundance of proteins and so they were used as a tool to generate a quantitative approach for peptides and corresponding proteins (Terashima & Hippler, 2010). The spectral count calculation was carried out in a way that the OMSSA and X!Tandem peptide-spectrum matches were counted to reach peptide spectral counts, and then these values were added to produce the protein spectral count.

Table 3.14 The summary of the maximum (red in color) and the average (dark in color) protein and peptide numbers for all three MS applications. (i) Number of distinct peptides, (ii) Number of distinct peptides that unambiguously identify a gene model, (iii) Number of proteins identified

Pinus sylvestris	**OMSSA**			**X!Tandem**		
	spring	**summer**	**winter**	**summer**	**spring**	**winter**
(i)	1496	1387	1469	1409	1332	1362
	1975	**1760**	**1816**	**1839**	**1710**	**1671**
(ii)	623	582	645	590	561	598
	872	**771**	**825**	**805**	**744**	**749**
(iii)	362	342	380	335	326	343
	485	**435**	**473**	**435**	**409**	**423**
Pinus brutia	**OMSSA**			**X!Tandem**		
	spring	**summer**	**winter**	**summer**	**spring**	**winter**
(i)	1332	1364	1539	1272	1248	1458
	1762	**1762**	**1995**	**1634**	**1610**	**1929**
(ii)	569	589	710	556	539	675
	810	**802**	**947**	**756**	**730**	**923**
(iii)	336	352	400	325	317	379
	453	**463**	**508**	**425**	**411**	**489**

After identification process, samples of three seasons for *P.brutia* and *P.sylvestris*, were compared with each other for any possible overlaps; in other words, lists of identified proteins for all three seasons (for each species) were compared with each other by the software BioVenn to inspect any common protein members (Figure 3.32, Appendix K (i) and (ii))

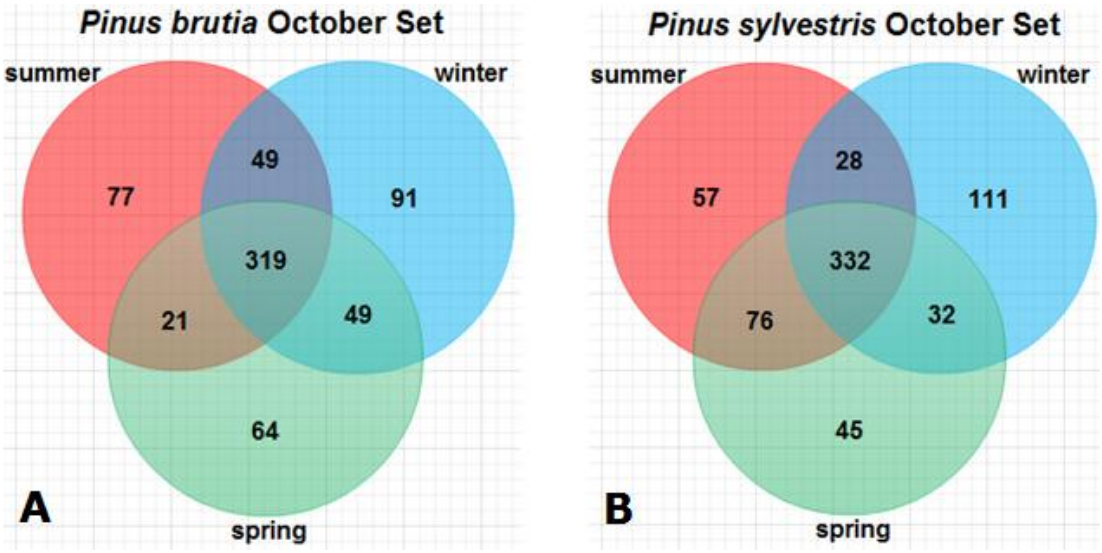

Figure 3.32 The total number of proteins which are/aren't common for all three sampling seasons of pine species: Pinus brutia (A), Pinus sylvestris (B). Blue color stands for winter, green for spring and red for summer. The results illustrated here were done by BioVenn for OMSSA results of October set for MS-MS/MS applications.

OMSSA and X!Tandem results were, also, compared with each other to find the common proteins identified by both of them, and to differentiate the ones detected by just one of the engines (Figure 3.33, Appendix L)

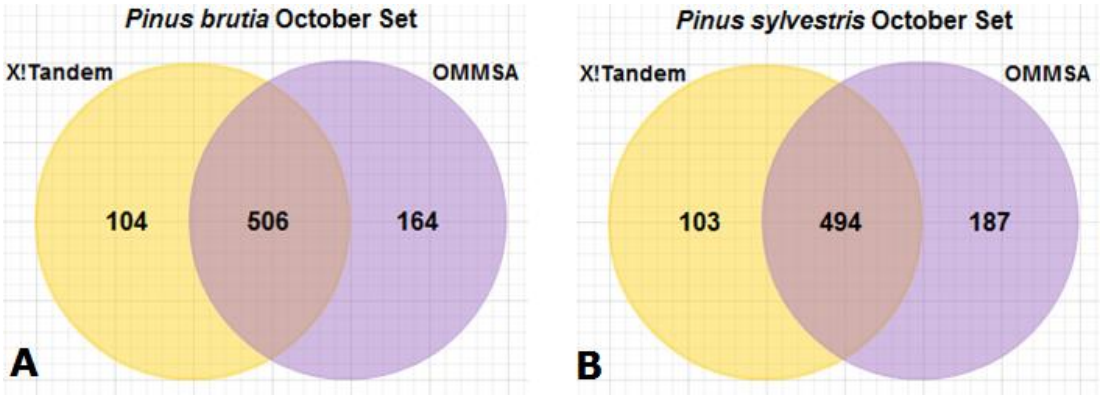

Figure 3.33 The total number of proteins which are/aren't common for search engines: Pinus brutia(A), Pinus sylvestris (B). Yellow color stands for X!Tandem and purple represents OMSSA.. The results illustrated here were done by BioVenn for October set for MS-MS/MS applications.

Comparison of total spectral counts between samples allowed the comparison of the expression of proteins in different seasons. Then, those proteins were grouped with respect to their functions in plant cell metabolism.

3.9.1. The Results of OMMSA Analysis

3.9.1.1. Photorespiration

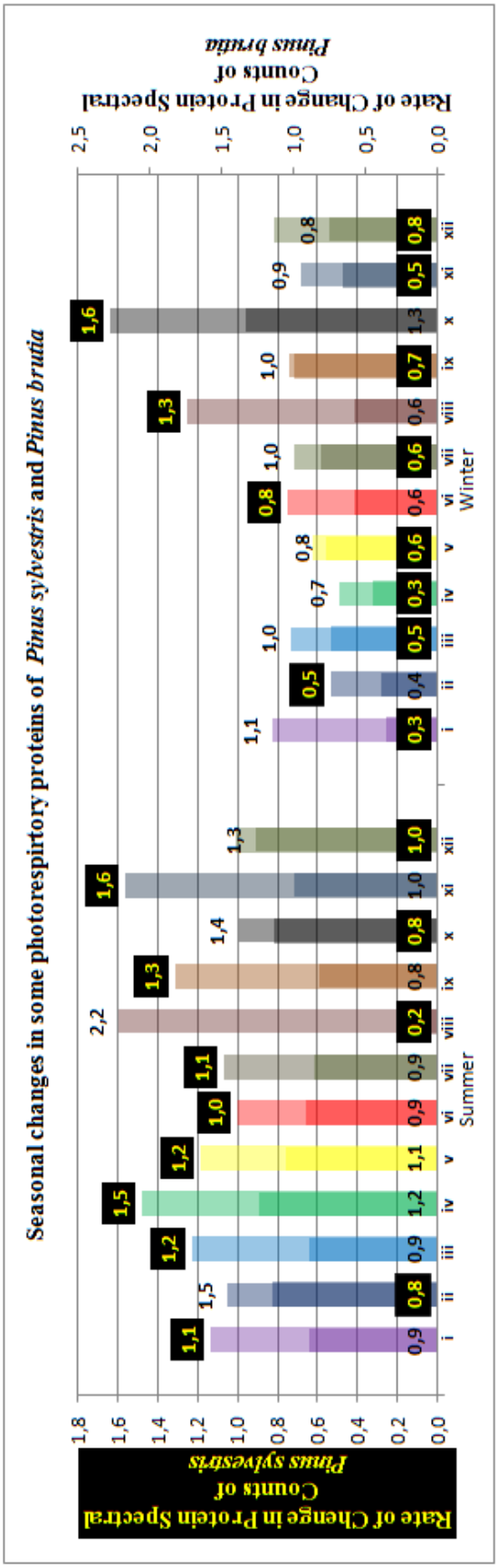

i	*361067753* alanine glyoxylate aminotransferase
ii	*gi|202188815|emb|CAC84492.1|* putative ribulose bisphosphate carboxylase small chain
iii	*116780244* glycolate oxidase
iv	*gi|14309928|emb|CAA56286.1|* glutamate synthase (ferredoxin)
v	*224284407* glycine dehydrogenase [decarboxylating] 1
vi	*294460278* aminomethyltransferase
vii	*116779353* hydroxypyruvate reductase
viii	*gi|148887789|gb|ABR15470.1|* sucrose synthase
ix	*116789369* NADP-Malate dehydrogenase
x	*gi|148887793|gb|ABR15472.1|* UDP-glucose pyrophosphorylase
xi	*gi|6967045|emb|CAB72439.1|* rubisco activase
xii	*gi|346452264|emb|CCC554419.1|* mitochondrial glycine decarboxylase complex H-protein

Figure 3.34 The rate of change in the protein spectral counts of both species according to the OMSSA results. The protein spectral count values of winter and summer seasons were compared with the spring that was accepted as the reference; so, the rate of change in the amount of proteins responsible in photorespiration metabolism were assigned.

3.9.1.2. Photosynthesis

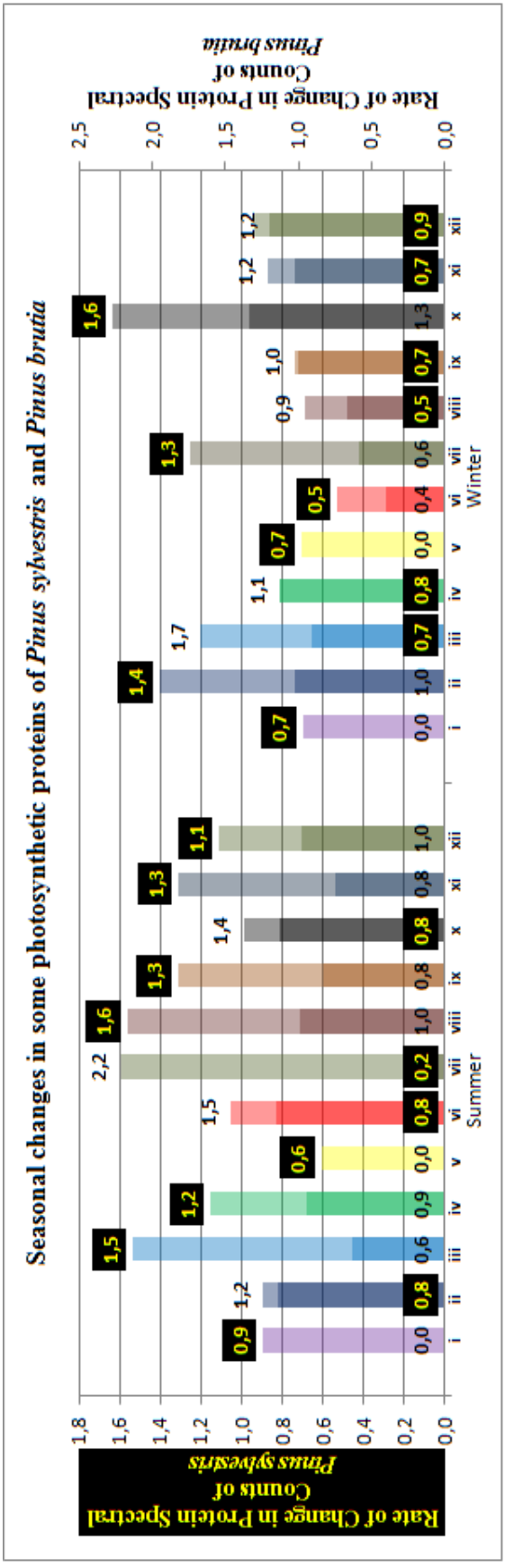

i	*361068437* photosystem II subunit29, Chlorophyll a-b binding protein	vii	*gi|148887789|gb|ABRI3470.1|* sucrose synthase
ii	*116794349* NADP-dependent glyceraldehyde-3-phosphate dehydrogenase-like	viii	*gi|69670451|emb|CAB72439.1|* rubisco activase
iii	*361068451* Transketolase	ix	*116789369* NADP-Malate dehydrogenase
iv	*224284456* chloroplast transketolase	x	*gi|148887793|gb|ABRI5472.1|* UDP-glucose pyrophosphorylase
v	*gi|20794|emb|CAA41407.1|* Type III chlorophyll a /b-binding protein	xi	*361069355* fructose-1,6-bisphosphatase
vi	*gi|20218815|emb|CAC84492.1|* putative ribulose bisphosphate carboxylase small chain	xii	*gi|332591479|emb|CBL95264.1|* phosphoglycerate kinase 1

Figure 3.35 The rate of change in the protein spectral counts of both species according to the OMSSA results. The protein spectral count values of winter and summer seasons were compared with the spring that was accepted as the reference; so, the rate of change in the amount of proteins responsible in photosynthesis metabolism were assigned.

3.9.1.3. Stress Resistance Metabolism

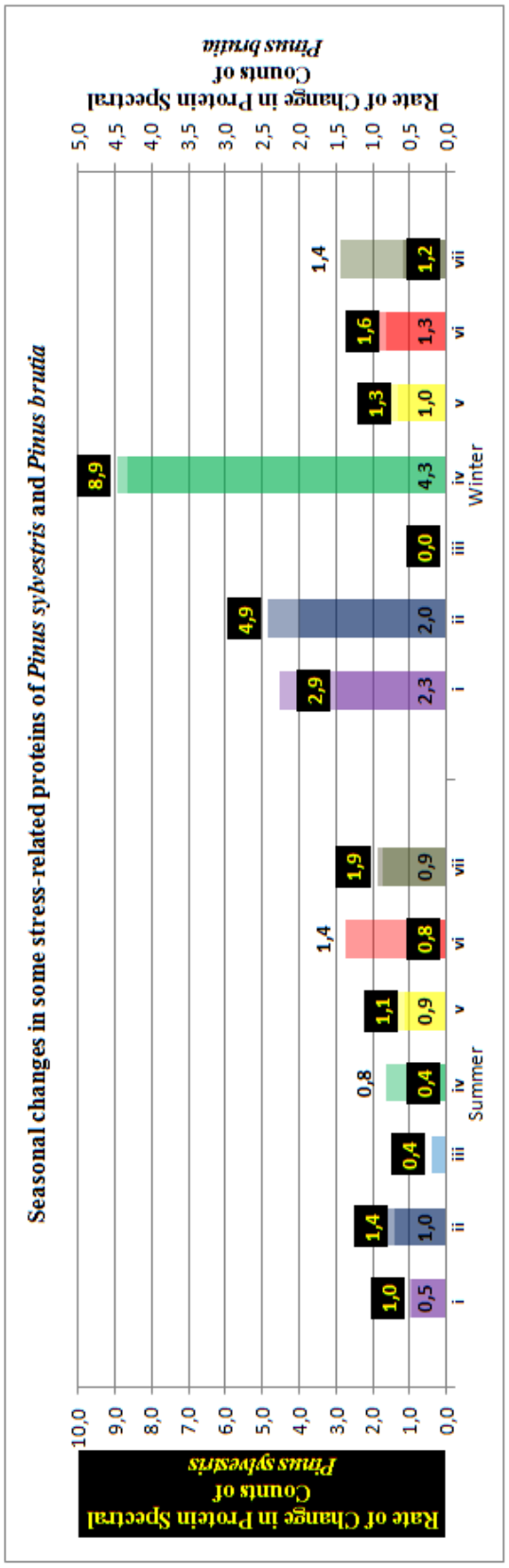

i	*gi|332391481|emb|CBL95265.1|* alcohol dehydrogenase
ii	*116790992* glutathione reductase
iii	*gi|28894490|gb|AAO61229.1|* monoterpene synthase-like protein
iv	*gi|52788398|gb|AAU87301.1|* cyclophilin
v	*116779823* peptidyl-prolyl cis-trans isomerase
vi	*gi|148887793|gb|ABR15472.1|* UDP-glucose pyrophosphorylase
vii	*116782122* D-ribulose-5-phosphate-3-epimerase

Figure 3.36 The rate of change in the protein spectral counts of both species according to the OMSSA results. The protein spectral count values of winter and summer seasons were compared with the spring that was accepted as the reference; so, the rate of change in the amount of proteins responsible in stress resistance metabolism were assigned.

3.9.1.4. Energy Metabolism

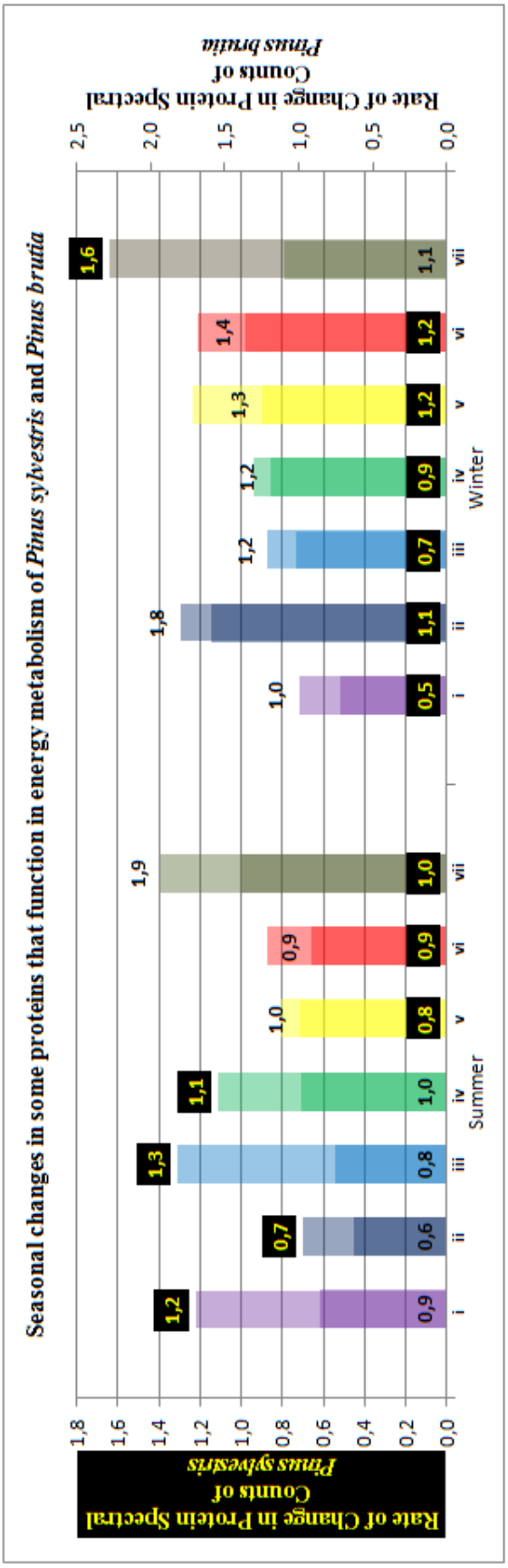

i	*148908831* ADP-glucose pyrophosphorylase large subunit 4	v	*294462280* citrate synthase 3
ii	*224285717* ATP-citrate synthase beta chain protein 1-like (XP_003546316.1)	vi	*148906790* citrate synthase
iii	*361069355* fructose-1,6-bisphosphatase	vii	*116789773* Phosphoglucomutase
iv	*gi|332591479|emb|CBL93264.1|* phosphoglycerate kinase 1		

Figure 3.37 The rate of change in the protein spectral counts of both species according to the OMSSA results. The protein spectral count values of winter and summer seasons were compared with the spring that was accepted as the reference; so, the rate of change in the amount of proteins responsible in energy metabolism were assigned.

3.9.1.5. Protein Folding Metabolism and Chaperone Function

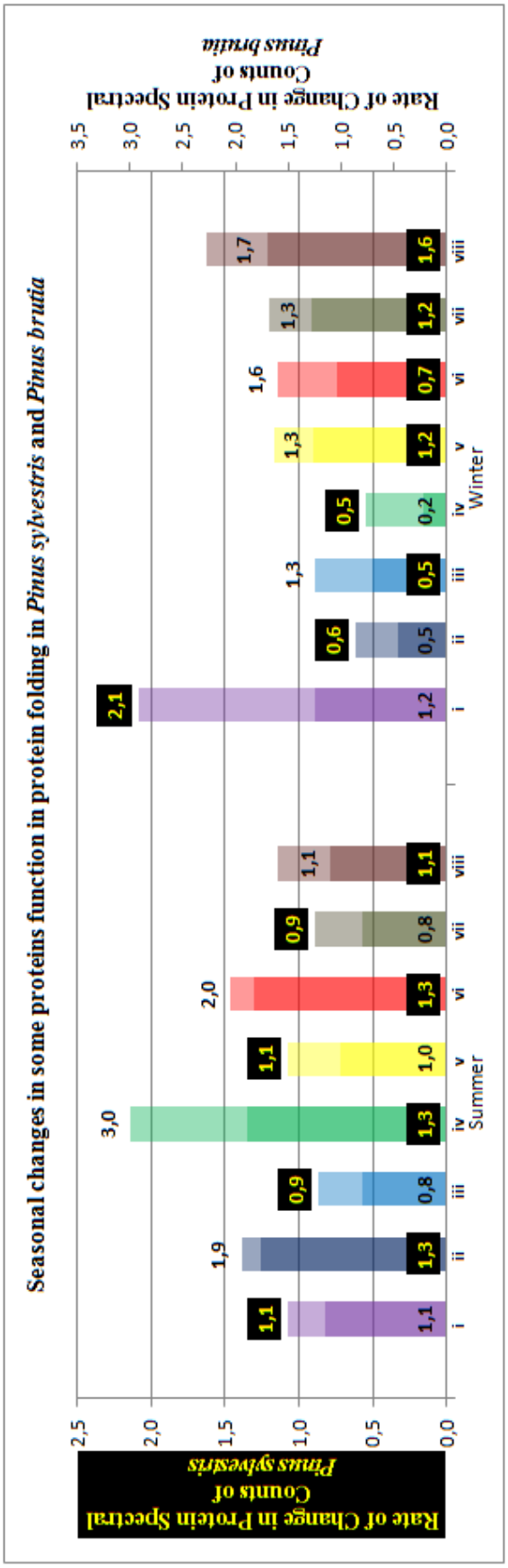

i	*224284462* filamentation temperature-sensitive H (FtsH)-like protein Pfff precursor
ii	*116783164* 101 kDa heat shock protein
iii	*294460912* T-complex protein 1 subunit alpha-like
iv	*148909835* 101 kDa heat shock protein
v	*294460598* heat shock protein, partial
vi	*gi|2982291|gb|AAC32731.1|* heat shock protein
vii	*294464851* ATP-dependent Clp protease ATP-binding subunit ClpC-Chaperone protein
viii	*116787373* chaperonin-60 beta subunit

Figure 3.38 The rate of change in the protein spectral counts of both species according to the OMSSA results. The protein spectral count values of winter and summer seasons were compared with the spring that was accepted as the reference; so, the rate of change in the amount of proteins responsible in protein folding and/or known as chaperon were assigned.

3.9.1.6. Chloroplastic Proteins

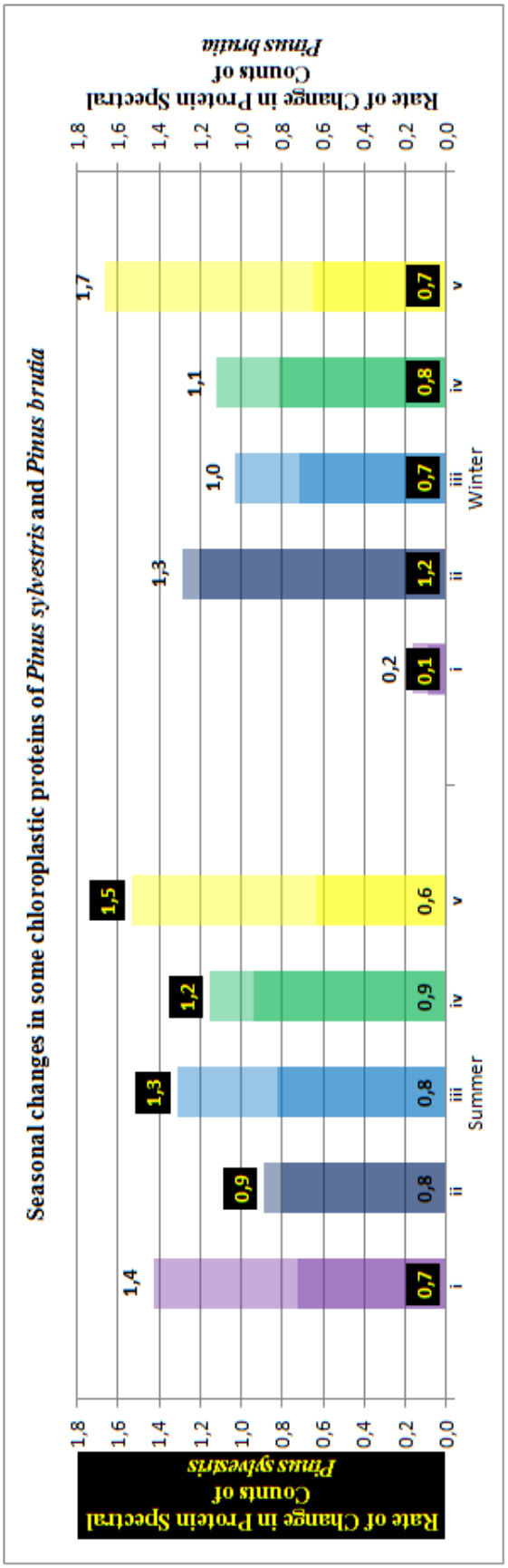

i	*148906778* lipoxygenase 2
ii	*294464851* ATP-dependent Clp protease ATP-binding subunit ClpC-Chaperone protein
iii	*116789369* NADP-Malate dehydrogenase
iv	*224284456* chloroplast transketolase
v	*361068451* Transketolase

Figure 3.39 The rate of change in the protein spectral counts of both species according to the OMSSA results. The protein spectral count values of winter and summer seasons were compared with the spring that was accepted as the reference; so, the rate of change in the amount of proteins found in the structure of chloroplasts were assigned.

3.9.1.7. Mitochondrial Proteins

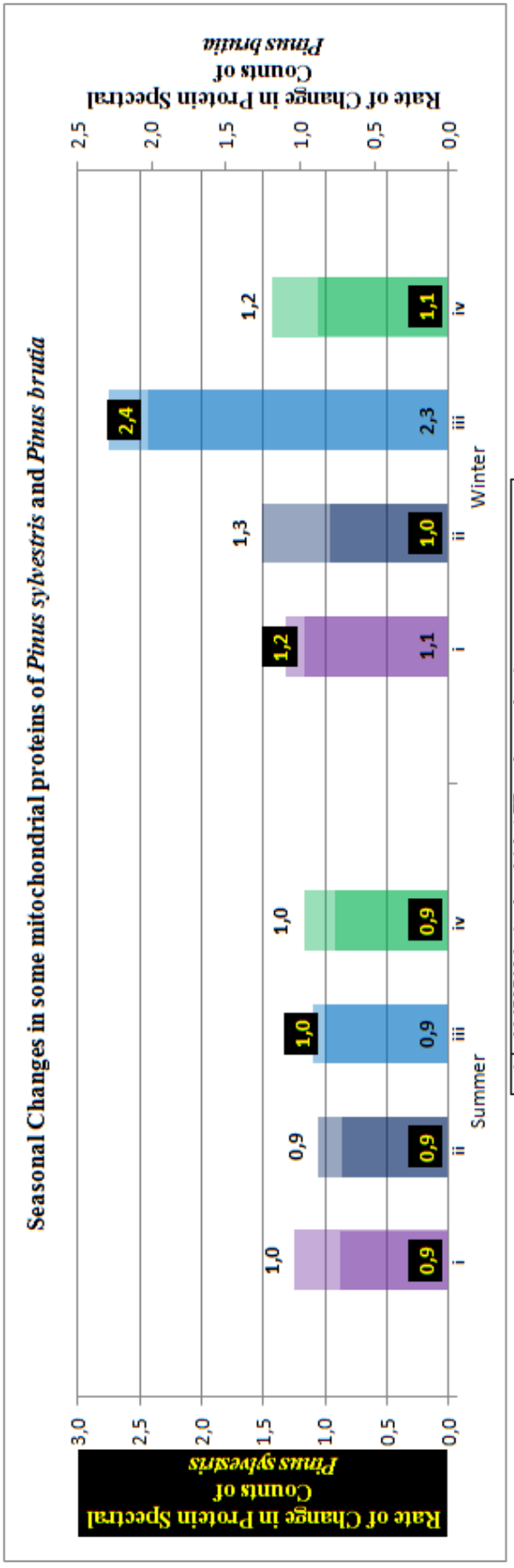

i	*116787106* mitochondrial ATPase beta subunit
ii	*294463383* mitochondrial-processing peptidase subunit alpha
iii	*148907636* NAD-dependent malic enzyme 1
iv	*116786682* porin/voltage-dependent anion-selective channel protein

Figure 3.40 The rate of change in the protein spectral counts of both species according to the OMSSA results. The protein spectral count values of winter and summer seasons were compared with the spring that was accepted as the reference; so, the rate of change in the amount of proteins found in the structure of mitochondria were assigned.

3.9.2. The Results of X!Tandem Analysis

3.9.2.1. Photorespiration

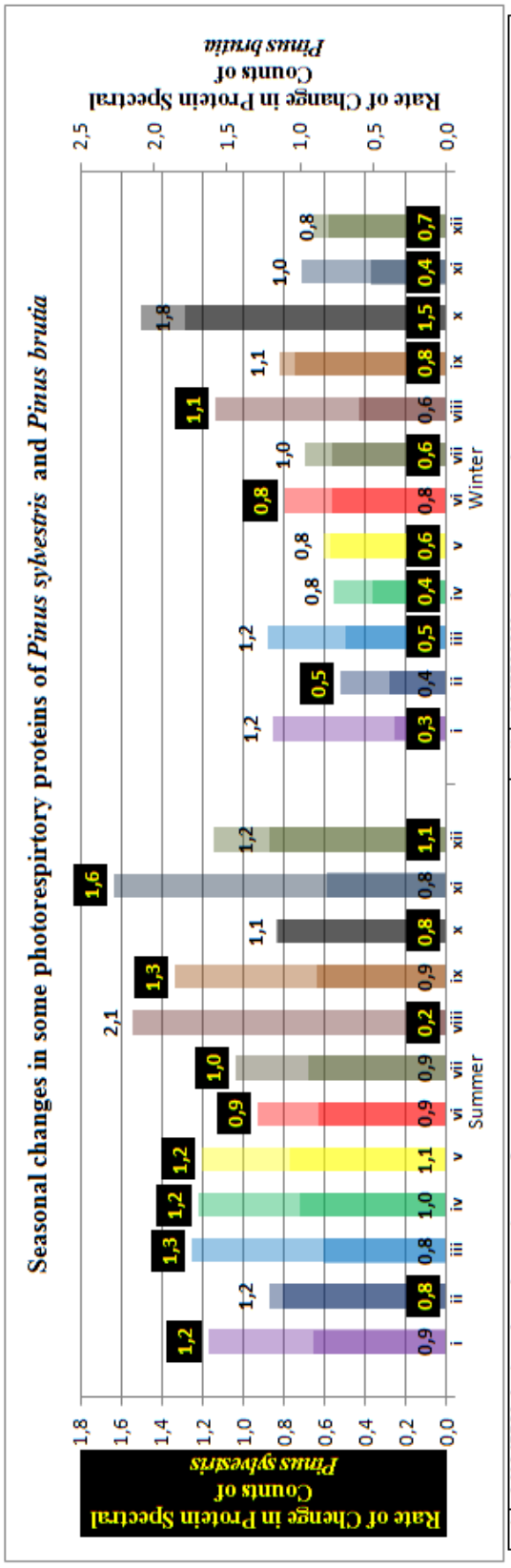

i	*3610677553* alanine glyoxylate aminotransferase	vii	*116779353* hydroxypyruvate reductase
ii	*gi|20218815|emb|CAC84492.1|* putative ribulose bisphosphate carboxylase small chain	viii	*gi|148887789|gb|ABR15470.1|* sucrose synthase
iii	*116780244* glycolate oxidase	ix	*116789369* NADP-Malate dehydrogenase
iv	*gi|1430928|emb|CAA56286.1|* glutamate synthase (ferredoxin)	x	*gi|148887793|gb|ABR15472.1|* UDP-glucose pyrophosphorylase
v	*224284407* glycine dehydrogenase [decarboxylating] 1	xi	*gi|6967045|emb|CAB72439.1|* rubisco activase
vi	*294460278* aminomethyltransferase	xii	*gi|346453264|emb|CCC55419.1|* mitochondrial glycine decarboxylase complex H-protein

Figure 3.41 The rate of change in the protein spectral counts of both species according to the X!Tandem results. The protein spectral count values of winter and summer seasons were compared with the spring that was accepted as the reference; so, the rate of change in the amount of proteins found in the photorespiration metabolism were assigned.

3.9.2.2. Photosynthesis

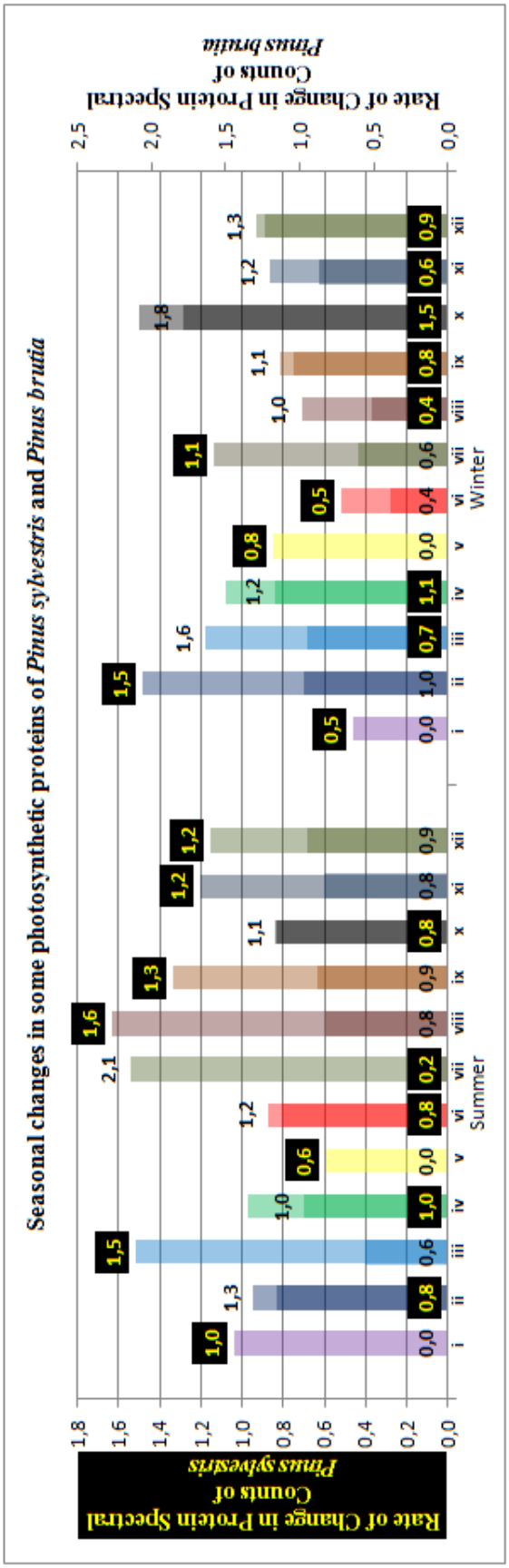

i	*361068437* photosystem II subunit29, Chlorophyll a-b binding protein	vii	*gi|148887789|gb|ABR15470.1|* sucrose synthase
ii	*116794349* NADP-dependent glyceraldehyde-3-phosphate dehydrogenase-like	viii	*gi|6967045|emb|CAB72439.1|* rubisco activase
iii	*361068431* Transketolase	ix	*116789369* NADP-Malate dehydrogenase
iv	*224284456* chloroplast transketolase	x	*gi|148887793|gb|ABR15472.1|* UDP-glucose pyrophosphorylase
v	*gi|20794|emb|CAA41407.1|* Type III chlorophyll a /b-binding protein	xi	*361069355* fructose-1,6-bisphosphatase
vi	*gi|20218815|emb|CAC84492.1|* putative ribulose bisphosphate carboxylase small chain	xii	*gi|332591479|emb|CBL95264.1|* phosphoglycerate kinase 1

Figure 3.42 The rate of change in the protein spectral counts of both species according to the X!Tandem results. The protein spectral count values of winter and summer seasons were compared with the spring that was accepted as the reference; so, the rate of change in the amount of proteins found in the photosynthesis metabolism were assigned.

3.9.2.3. Stress Resistance Metabolism

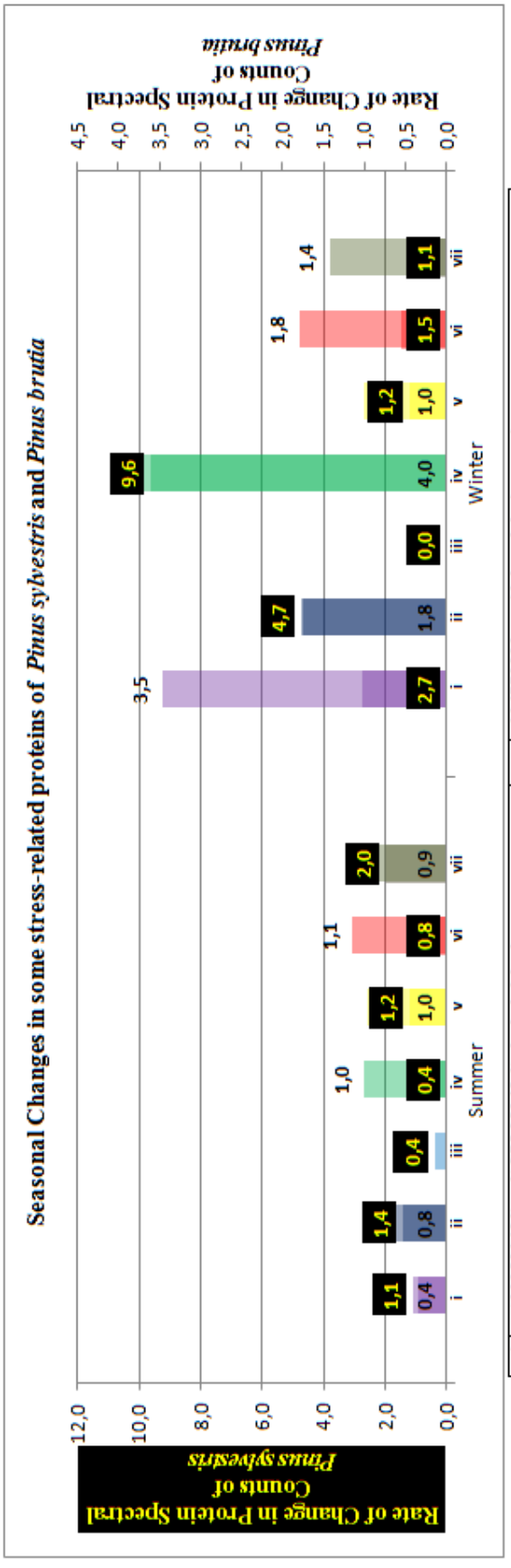

i	gi|332591481|emb|CBL95265.1| alcohol dehydrogenase
ii	*116790992* glutathione reductase
iii	gi|28894490|gb|AAO61229.1| monoterpene synthase-like protein
iv	gi|52788398|gb|AAU87301.1| cyclophilin
v	*116779823* peptidyl-prolyl cis-trans isomerase
vi	gi|148887793|gb|ABRI5472.1| UDP-glucose pyrophosphorylase
vii	*116782122* D-ribulose-5-phosphate-3-epimerase

Figure 3.43 The rate of change in the protein spectral counts of both species according to the X!Tandem results. The protein spectral count values of winter and summer seasons were compared with the spring that was accepted as the reference; so, the rate of change in the amount of proteins found in the stress resistance metabolism were assigned.

3.9.2.4. Energy Metabolism

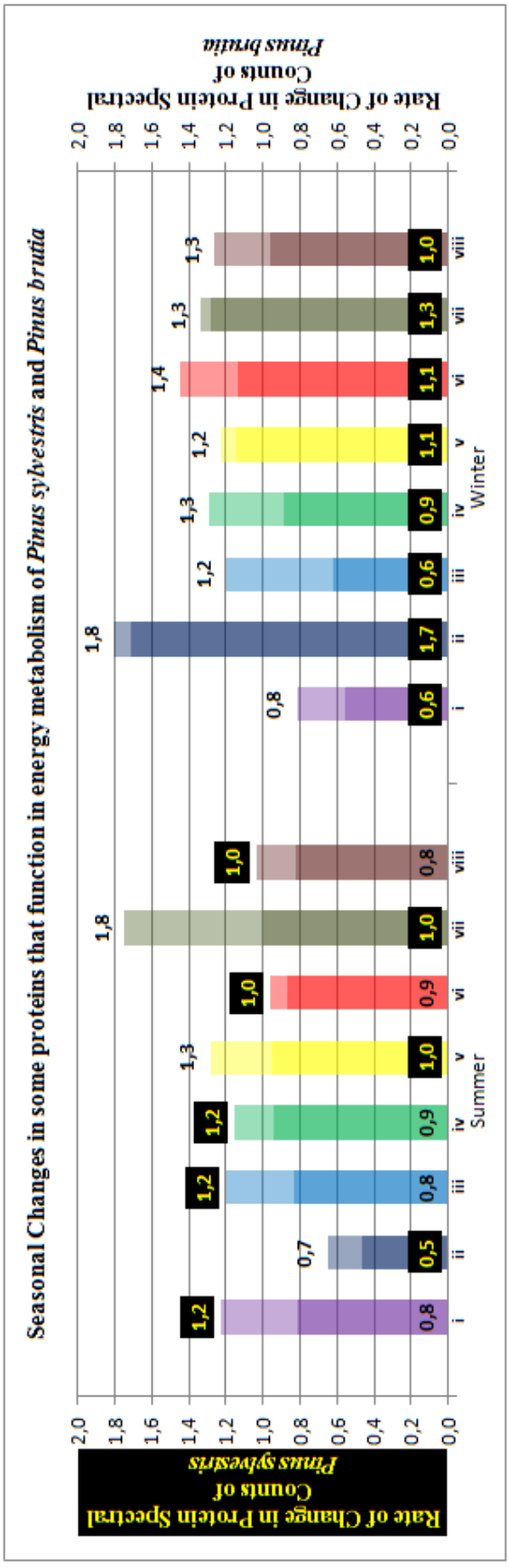

i	*148908831* ADP-glucose pyrophosphorylase large subunit 4	v	*294462280* citrate synthase 3
ii	*224285717* ATP-citrate synthase beta chain protein 1-like (XP_003546316.1)	vi	*148906790* citrate synthase
iii	*361069355* fructose-1,6-bisphosphatase	vii	*116789773* Phosphoglucomutase
iv	*gi|332591479|emb|CBL95264.1|* phosphoglycerate kinase 1	viii	*148906166* phosphoglucomutase (AAC00601.1)

Figure 3.44 The rate of change in the protein spectral counts of both species according to the X!Tandem results. The protein spectral count values of winter and summer seasons were compared with the spring that was accepted as the reference; so, the rate of change in the amount of proteins found in the energy metabolism were assigned.

3.9.2.5. Protein Folding Metabolism and Chaperone Function

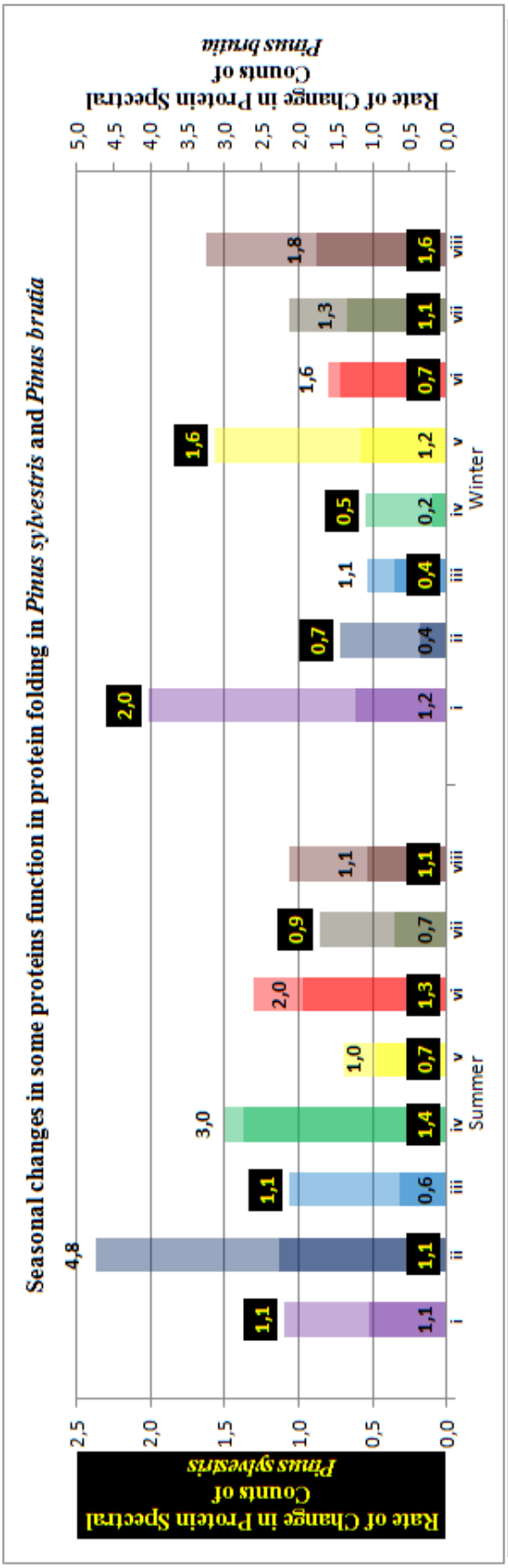

i	*224284462* filamentation temperature-sensitive H (FtsH)-like protein Pfff precursor
ii	*116783164* 101 kDa heat shock protein
iii	*294460912* T-complex protein 1 subunit alpha-like
iv	*148909835* 101 kDa heat shock protein
v	*294460598* heat shock protein, partial
vi	*gi|29829291|gb|AAC32131.1|* heat shock protein
vii	*294464851* ATP-dependent Clp protease ATP-binding subunit ClpC-Chaperone protein
viii	*116787373* chaperonin-60 beta subunit

Figure 3.45 The rate of change in the protein spectral counts of both species according to the X!Tandem results. The protein spectral count values of winter and summer seasons were compared with the spring that was accepted as the reference; so, the rate of change in the amount of proteins responsible in protein folding and/or known as chaperon were assigned.

3.9.2.6. Chloroplastic Proteins

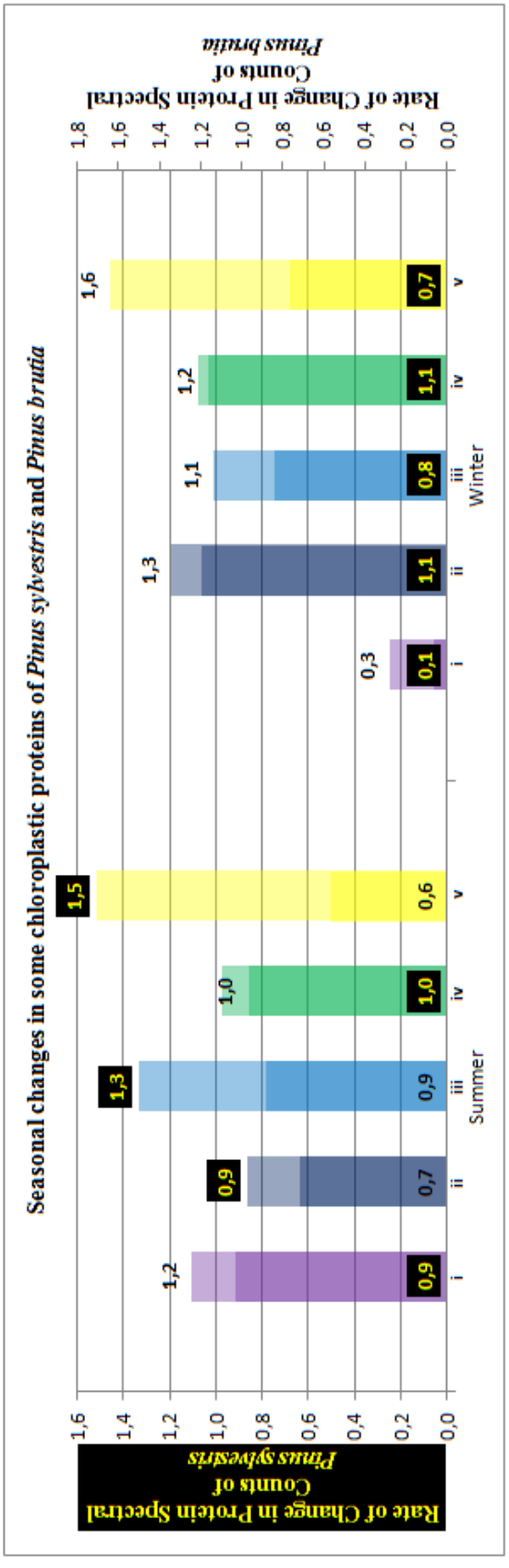

i	*148906778* lipoxygenase 2
ii	*294464851* ATP-dependent Clp protease ATP-binding subunit ClpC-Chaperone protein
iii	*116789369* NADP-Malate dehydrogenase
iv	*224284456* chloroplast transketolase
v	*361068451* Transketolase

Figure 3.46 The rate of change in the protein spectral counts of both species according to the X!Tandem results. The protein spectral count values of winter and summer seasons were compared with the spring that was accepted as the reference; so, the rate of change in the amount of proteins found in the structure of chloroplasts were assigned.

3.9.2.7. Mitochondrial Proteins

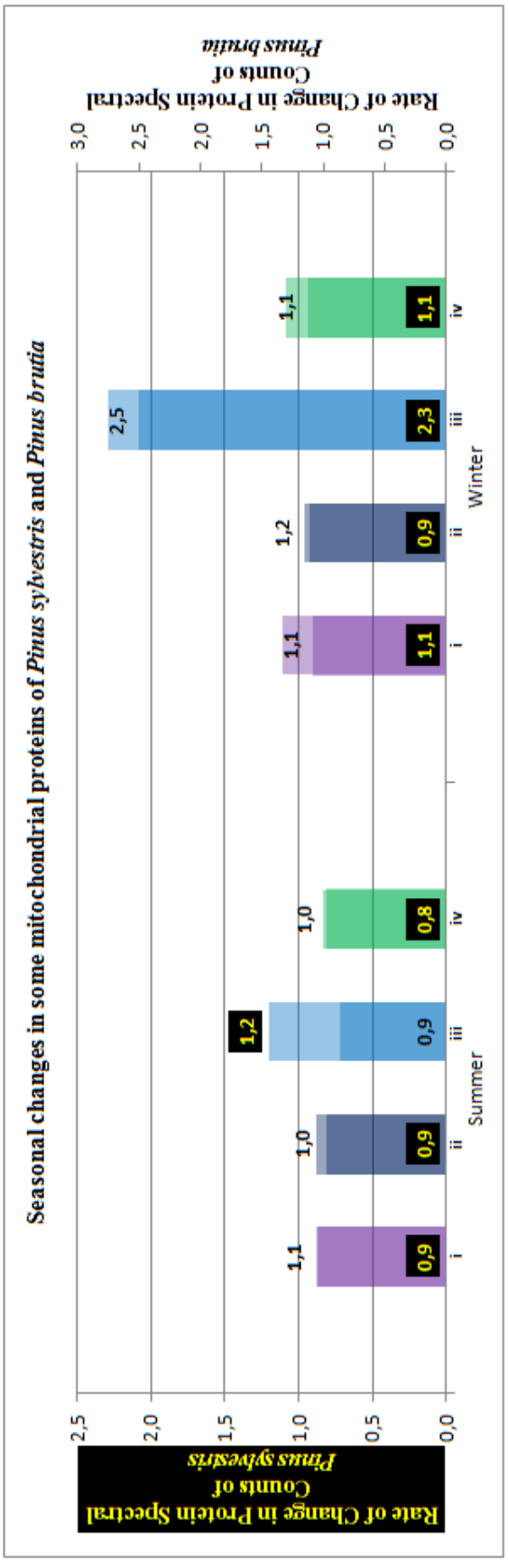

i	*116787106* mitochondrial ATPase beta subunit
ii	*294463383* mitochondrial-processing peptidase subunit alpha
iii	*148907636* NAD-dependent malic enzyme 1
iv	*116786682* porin/voltage-dependent anion-selective channel protein

Figure 3.47 The rate of change in the protein spectral counts of both species according to the X!Tandem results. The protein spectral count values of winter and summer seasons were compared with the spring that was accepted as the reference; so, the rate of change in the amount of proteins found in the structure of mitochondria were assigned.

CHAPTER IV

DISCUSSION

4.1. The evaluation of the photosynthetic capacities of the pine needles in different seasons

All organisms need an optimal temperature range to survive and, out of this range, growth begins to diminish. The divergence from the optimum range becomes more noxious with respect to the organism, or more specifically the plant in question (Strand, *et al*., 1999).

Richardson (Richardson, 1998) stated that the seasonal variations in the net photosynthetic rate of pine needles are formed by climate cycles, radiation and some genetically controlled responses. Photosynthetic light response curves of *Pinus brutia* and some other sun-adapted and early successional pine species is not saturated in growing season and it may reach to its maximal value late in the summer (Awada *et al*, 2003). *P. brutia* is a very shade-intolerant species and needs high radiation to reach the peak point in photosynthetic production. On the other hand, *P. sylvestris* performs about 65% of its all photosynthetic production in June, July and August (Korpilahti, 1990).

In winter time, like in most other plant species, photosynthetic capacity of *Pinus brutia* decreases (Awada, *et al*, 2003). Photosynthesis is inhibited during winter for *P. sylvestris*, too; it recovers slowly during spring, though it is enhanced on warm days (Hari & Nöjd, 2009).

Ruelland *et al* (Ruelland *et al*, 2009) and Vogg *et al* (Vogg *et al*, 1998) stated that frost hardening causes a decrease in the chlorophyll content (from 1,2 mg/g of fresh weight measured in August to 0,8 mg/g of fresh weight measured in January) and this change would lead the reduction in photosynthetic rate (Figure 4.1). The pattern of change in the chlorophyll content (even the measured values) of this study is all consistent with the results presented in our research; measured values were lower in winter time for both of the species as proposed. For *P. brutia*, there were 30-40% decreases in Chlorophyll-a amount in winter time (in different solvent systems) with respect to spring measurements. The rate of declines in Chlorophyll-b and Chlorophyll-(a+b) values were 30-43% and 30-40%, respectively. For the other pine species, the rate of reductions for Chlorophyll-a, Chlorophyll-b and Chlorophyll-(a+b) were 20-28%, 5-26% and 16-27%, respectively.

Hansen *et al* (Hansen *et al*, 1996) proposed that although the chlorophyll a/b ratio does not change considerably under severe cold stress, chlorophyll/carotenoid (xanthopyll) ratio wanes as a result of frost hardening. Ruelland *et al* (Ruelland *et al*, 2009) regarded that xanthophyll cycle in plants including conifers converts Photosystem-II (PSII) from a state of efficient light harvesting to a state of high thermal dissipation by making it unable to pass its energy to Chl-a. This process is called non-photochemical quenching and vital for lowering energy delivery to PSII. Table 3.6 and 3.7 summarizes the results of the calculations. For Scots pine, Chlorophyll-(a+b) / Carotenoid Content ratio was minimum in winter samples as it was defined in the literature and for the other species, the situation was the same. These findings pointed the presence of cold stress on the pine trees in winter time.

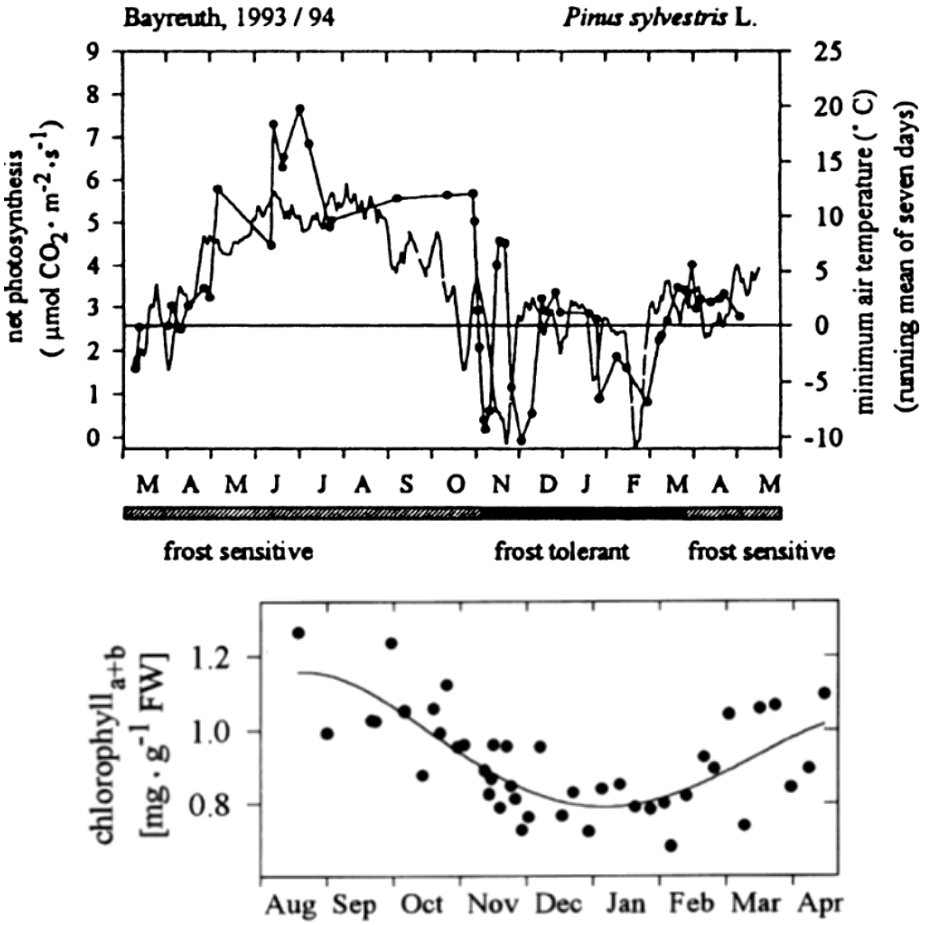

Figure 4.1 Seasonal changes in the photosynthetic rate and chlorophyll (a+b) content of the *Pinus sylvestris* trees grown outdoor. The graphs were derived from the study of Vogg *et al* (Vogg et al, 1998). In upper graph, the curve with dots indicates the minimum temperature values which were thought as the major parameter that the assimilation rate responds mainly.

The drop in the amount of chlorophyll-binding proteins was also charged as the reason of the decrement in chlorophyll content (Steponkus *et al*, 1990) (Vogg *et al*, 1998). The same type of changes were observed in the amounts of photosystem II subunit-29 (as a chlorophyll a-b binding protein) (gi: 361068437) and Type III chlorophyll a /b-binding protein (gi: 20794) for *Pinus sylvestris* after LC-MS/MS analysis. Both of them showed decreases in winter time as their proportions to spring samples were 0.7.

The main factors affecting the photosynthetic metabolism and the overall response of the pine species to environmental conditions of winter time are the low and even sub-freezing temperatures and low/high radiation. Peers *et al* (Peers, *et al*., 2009) stated that Light Harvesting Complex Stress Related Protein (LHCSR) is a light-induced transcript, and it accumulates under environmental conditions known to induce photo-oxidative stress, including deprivation of carbon dioxide, sulphur, or iron, as well as high light. Moreover the accumulation of LHCSR3 protein was claimed to be correlated with quenching capacity. In our study, LHCSR-III antibodies produced for *Chlamydomnas reinhardtii* was used to check the levels of this protein in needle protein extracts. Results proposed a significant increase from winter to summer for *Pinus sylvestris* in a way that it reached highest value at summer samplings. This might be an indicator of the exalted light stress and possibly photorespiration for that season. A similar result was observed for *Pinus brutia*, but interestingly, expression of this special protein reached its maximum at the end of spring (pointing this species' early demand for maximum photosynthetic rate).

For evergreen conifers such as *Pinus sylvestris*, cold acclimation induces cessation of primary growth and a resultant decrease in the sink demand for photoassimilates. The cessation of growth decreases the capacity for energy utilization and this, in turn, results in feedback inhibition of photosynthesis (Ensminger *et al*, 2006) (Hjelm & Ogren, 2003) (Savitch, *et al*., 2002). Huner *et al* (Huner *et al*, 1993) notified that there should be a balance between the reduction of $NADP^+$ and the production of triose-phosphate compounds in overall photosynthesis mechanism. However, low temperatures causes an imbalance by increasing membrane viscosity and changing biophysical properties which in turn inhibit electron transfer through in/out thylakoid membranes, and by decreasing the rate of enzymatic reactions in Calvin cycle more than light-dependent ones. In those cases evergreen trees down-regulate photosynthesis by inactivation of PSII reaction centers and re-organization of the light harvesting complexes (LHCs) into "energy quenching complexes" (Ensminger *et al*, 2006) (Savitch, *et al*., 2002). Ensminger *et al* (Ensminger *et al*, 2006) proved this hypothesis by screening the changes in the PSII Reaction Centre Protein D1 (PsbA D1) which was degraded under low temperature conditions, in Scots pine seedlings. Such a change was also measured in western blot analysis of our own samples: the amount of this protein was 16% less in winter samples with respect to spring samples, for *Pinus brutia*. This difference was measured as 42% for *Pinus sylvestris*. The studies on the natural populations of Scots pine supported such a change indicating the general behaviour of frost acclimation in this pine species as suppression of photosynthetic mechanism (Hjelm & Ogren, 2003). LC-MS/MS results provided supportive data for this situation. FtsH protein catalyses the proteolytic degradation of D1 proteins of PSII (Yu *et al*, 2004). Filamentation temperature-sensitive H (FtsH)-like protein Pftf precursor (accession number: 224284462) increased in winter samples (especially for *Pinus sylvestris*).

The MS results of Rubisco activase (RCA), mitochondrial glycine decarboxylase complex H-protein, glycine dehydrogenase [decarboxylating], glutamate synthase (ferredoxin) and glycolate oxidase supports this hypothesis. All those proteins were considerably down-regulated in winter samplings of both species and significantly up-regulated in summer samplings. This means both species aimed to reduce the rate of photorespiration in winter time.

Rubisco is a haloenzyme composed of 8 large (LSUs; 55 kD) and 8 small subunits (SSU; 15–18 kD) among which large ones are encoded by the chloroplast large subunit of Rubisco

(*rbcL*) gene and SSU precursors are produced by a nuclear family of small subunit of Rubisco (*rbcS*) genes (Chen & Spreitzer, 1993). All 16 subunit forms the complex in the chloroplast and there is a control mechanism settled upon the conditional synthesis of the subunits with each other. In other words, in the absence of one subunit in the complex, synthesis of another subunit of the complex decreases. Cohen *et al* (Cohen *et al*, 2006) reported that translational arrest of LSU or any other factor inhibiting the assembly process might cease the Rubisco activity. Rubisco SSU amount in winter samples of scots pine and brutia pine were almost half of the values measured for spring samplings, which supports the argument on decreased photosynthetic facilities under cold stress. Nominal ADP-glucose pyrophosphorylase content in winter (almost half of the values measured for spring samplings) for scots pine pointed the drop in photosynthetic rate, too (Ballicora *et al*, 2004) because this enzyme is highly correlated with the members of Calvin cycle, especially 3PGA which was down-regulated at this season.

Rubisco gains its catalysing ability by carbamylation of a specific lysine amino acid which binds to Ribulose 1,5 bisphosphate (RuBP). When phosphorylated by the increased ATP concentration in the stroma, RCA removes one proton from this lysine and makes it possible for the CO_2 molecule to attach that site.

In summer, exalted air temperature and attenuate humidity in soil and air compels plants to raise the rate of photorespiration. Drought stress causes stomata to be closed to reduce further water loss because of excessive respiration and this phenomena decreases intercellular CO_2 concentrations which in turn elevates the rate of photorespiration. In drought-stressed leaves, photorespiration protects the photosynthetic apparatus against photoinhibition by sustaining photon utilization during reduced electron consumption when CO_2 assimilation decreases (Osmond & Grace, 1995) (Bonhomme, *et al.*, 2009). Ristic *et al* (Ristic, *et al*., 2009) stated that because of its low temperature optimum for ATPase activity and an inherent thermal instability, RCA is unable to keep pace with the rate of Rubisco deactivation during periods of moderate heat stress. Because of this fact, changes in the levels of RCA could serve as an important determinant of plant productivity under elevated temperatures. Under moderate heat stress, accumulation of a new putative RCA of 45-46 kDa was pronounced (Ristic, *et al*., 2009) (Weston *et al*, 2007). Mass spectrometry analysis of the pine samples revealed an increase of RCA in summer samples of *Pinus sylvestris* and a significant decrease was detected for the winter samples of the same species. Those changes could be interpreted as an elevated photorespiration in summer season and a possible heat stress on pine trees. Increased levels of mitochondrial glycine decarboxylase complex H-protein, glycine dehydrogenase [decarboxylating], glutamate synthase (ferredoxin) and glycolate oxidase strenghten this hypothesis. In short, scots pine derogated photosynthetic units to avoid photoinhibition and excessive ROS formation under cold stress. On the other hand, to cope with the high radiation and low carbon dioxide levels in photosynthetic units (as a result of closed stomata by drought conditions), it up-regulated the members of photorespiration. *Pinus brutia*, also, responded in the same way but in a lower magnitude.

4.2. The changes in some stress parameters as a response to environmental stress

GSH accumulation was observed in all stress conditions; not just because of cold stress, but also high temperature and drought stress (Noctor, *et al*., 2012), because it is involved in ascorbate-glutathione cycle and performs the quenching of ROS as an anti-oxidant to eliminate damaging peroxides (Galant *et al*, 2011). This molecule has many other functions in plant cells including even the induction of the transcription of *gst* genes (Marrs, 1996). According to these findings, the elevated GSH levels in winter and summer samples for both of the pine species might be a sign of the presence of high stress possibly created by cold/heat and drought. Kawamura *et al* (Kawamura *et al*, 2003) and Kosmala *et al* (Kosmala *et al*, 2009) affirmed that the cold stress causes the accumulation of ROS in plant cells which in turn invites an elevation in the amount of scavenging enzymes especially functioning in ascorbate and glutathione metabolisms such as superoxide dismutase (SOD), ascorbate peroxidase (APX), glutathione reductase (GR) and glutathione S-transferase (GST). Drought and heat generated by the climatic conditions of the summer season, also, generates an increase in the amount and specific activities of those enzymes, especially GSTs and GRs (Davis & Swanson, 2001) (Marrs, 1996) (Hausladen & Alscher, 1994). Specific activity values of GSTs measured for Scots pine peaked at the end of summer season. This might be a result of its being in-tolerant to drought and heat stresses; studies on *P. sylvestris* indicated a relatively high mortality in drought stress conditions (Rigling *et al*, 2003) (Gruber *et al*, 2012) (Bigler *et al*, 2006). Contrarily, the highest values of total GST activity were measured at winter time for brutia pine. As it was mentioned in Introduction part in detail, *Pinus brutia* prefers Mediterranean climate which have mild winter conditions and hot summers. As a partially drought and heat resistant species, Turkish red pine was actually expected to have such high GST activities under cold stress. On the other hand, mass spectrometry results didn't help in explaining a possible relationship between the increased/decreased activities of the GST enzymes and their expressions (or amount) in the total protein extracts of the samples. There were no detected peptides of the tryptic digest of any GST protein. However, another enzyme that operates in the same protective team of enzymes processing against the harmful effects of ROS in the cell was found: GR regenerates the GSH pool by catalysing the NADPH-dependent reduction of GSSG (Hausladen & Alscher, 1994). Although the total protein spectral count values for GR were very low that made it statistically incoherent to take into consideration, winter samples of scots pine showed an acceptable value indicating a possible upregulation of this enzyme with respect to other two seasons. This fact also helps us to explain why it had largest GSH pool in winter when the GST activity was still high. Increased reduction of GSSG by GR might make it possible.

Gardner (Gardner, 1995) stated that there were various services of lipid peroxidation to the plant cell such as contribution to development, generation of volatile substances, production of jasmonic acid and senescence. This means that it is vital for the plants if it could be kept under control; because stress conditions could also create excessive lipid peroxidation that might end the whole metabolism. Cold, heat and drought stresses induce high degree of lipid peroxidation which produces malondialdehyde (MDA). MDA reacts with thiobarbituric acid (TBA) and yield a pink colored condensation product which could be detected at 532 nm.

MDA values didn't fit the expected profile; there were no significant changes between seasons, although there were stress conditions and possibly high levels of lipid peroxidation. One explanation of such a situation might be settled upon the fact that this universal method

might not work well for plant species. Wang *et al* (Wang, *et al*., 2013) and Hodges *et al* (Hodges *et al*, 1999) proposed that there were interfering substances, which cause false positive or false negative results. These are sugars such as sucrose, glucose and fructose, phenylpropanoid-type pigments like anthocyanin and some aldehyde compounds which are produced in higher amounts in the cases of severe stress conditions.

As another important indicator of the presence of stress, proline accumulation in the pine needles were measured. Claussen (Claussen, 2005) and Borsani *et al* (Borsani *et al*, 1999) reported that proline has many functions in the plant cells such as protection of the folding of proteins against denaturation, serving as an nitrogen and energy storage, stabilisation of the membranes, working as a hydroxyl radical scavenger and finally adjustment of osmotic balance in the cell. They, also, added that the stress-related changes in the proline pool of the cell might affect the expression of genes governing the stress-regulatory mechanisms.

Duncan *et al* (Duncan & Widholm, 1987), Yumiko *et al* (Yumiko *et al*, 1997), Bohnert *et al* (Bohnert *et al*, 1995) and Ito *et al* (Ito, *et al*., 2006) stated that proline amount increaess in the cases of chilling and water stress to drive influx of water or reduce the efflux. Meteorological data proved that there were frosty days during the winter season (Appendix N-R) and both pine species were under drastic cold stress which generated changes in their proteomes possibly by affecting energy metabolism and by decreasing water uptake. Steponkus *et al* (Steponkus *et al*, 1990) proposed that sub-freezing temperatures causes extracellular ice formation which in turn yields a severe dehydration of the tissues because almost 80% of all water in the cells may be in frozen form (Hansen & Beck, 1988). Actually, the only freezing tolerance developed by a plant is tolerance of the secondary freezing stress - the water stress induced by freezing.

Pinus brutia and *Pinus sylvestris* needle samples had approximately 35% and 105% (about 2 times) more proline in winter with respect to spring samplings, respectively. Proline content of the brutia pine continued to decrease by 50% from spring till the end of summer season; but, Scots pine didn't represent such a considerable fall with 5%. This decrease in the amount of proline might be controversial if a possible drought stress was in the case at that period. However, besides being a member of anti-stress mechanism, proline has many other usages as explained before: high demand for nitrogen in summer season when the growth was being continued might be an explanation for low proline levels for both pine species.

Bedell *et al* (Bedell *et al*, 1995) stated that acidic soil, secondary products of the trees and high lignin in the soil of pine forests force this species to use ammonium as the predominant nitrogen source and moreover, unlike herbaceous plants, conifers prefer ammonium over nitrate. Suarez *et al* (Suárez, *et al*., 2002) affirmed that plants handle this ammonium need by also protein/nucleic acid breakdown, photorespiration, the biosynthesis of phenylpropanoids and amino acid/nucleotide catabolism which includes the usage of proline with some other amino acids.

There are two members of the glutamate-glutamine cycle in the plant cells: Glutamine synthase (GS) and Glutamate synthase (GOGAT) which have two classes among that the Ferrodoxin-glutamate synthase (Fd-GOGAT) is the major one in photosynthetic tissues (Temple *et al*, 1998). Mass spectrometry results showed an increase in the amount of Fd-GOGAT in summer season (1.2 times for *Pinus brutia* and 1.5 times for *Pinus sylvestris*) which might support the idea of a higher production of glutamate from glutamine. Glutamate

is one of the primary sources of proline in plant cells, so, this situation generates a proposition of increased proline production although it couldn't be detected by chemical way. High rate of photorespiration is a reason for relatively high expression of Fd-GOGAT measured in summer samplings, but still, there might be some other points to mention.

Hare *et al* (Hare *et al*, 1999) informed that most of the proline in plant tissues is produced from glutamate in two steps catalysed by the enzymes P5C synthetase (P5CS; EC 2.7.2.11/1.2.1.41) and P5C reductase (P5CR; EC 1.5.1.2). In the first step glutamate is converted into D1-pyrroline-5-carboxylate (P5C) in chloroplast, and then P5C is used for proline generation (Figure 4.3).

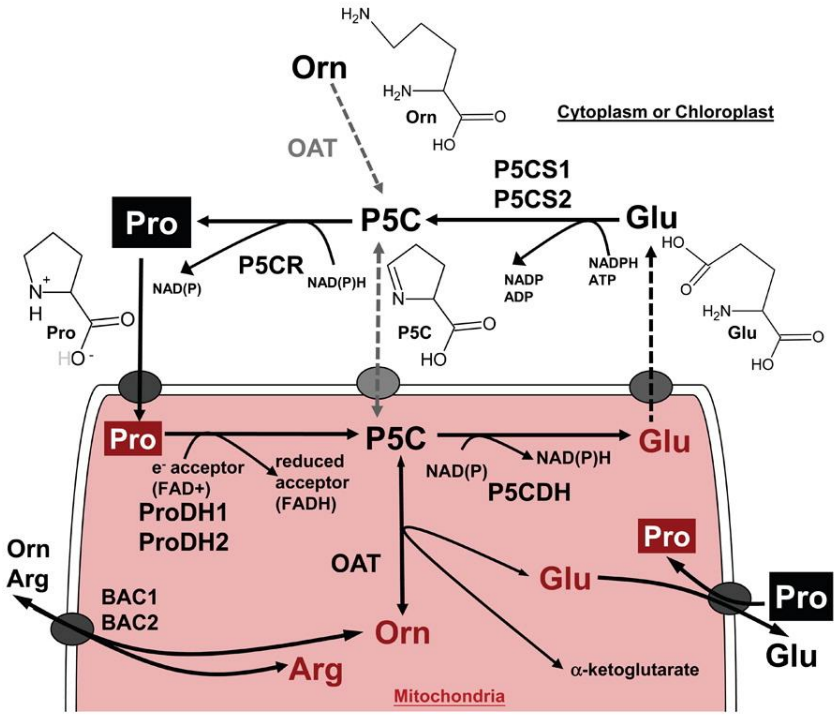

Figure 4.2 Proline metabolism in plants (Verslues & Sharma, 2010)

Figure 4.2 demonstrates the interaction of proline metabolism with other metabolic pathways. Its role in preserving the $NAD(P)^+$/NAD(P)H ratios is critical in the case of the maintaining of photosynthesis and respiration. The cycle of proline synthesis and degradation provides $NAD(P)^+$ and NAD(P)H, respectively; and, this is very important in plant antioxidant defence mechanisms under stress conditions (Sivakumar *et al*, 2000) (Alia & Mohanty, 1991).

All those information on the cellular fate of proline in different compartments might draw pictures for *Pinus brutia* and *Pinus sylvestris*. In one of them, low photosynthetic rate, high ROS production and water stress caused by sub-freezing temperatures possibly needed a large proline pool in the samples, at winter time. The measurements were done for the samples collected at the end of this season, so, this might explain why Fd-GOGAT amount was smaller with respect to other two seasons: cold hardening needs an elevation in the amount and activity of this enzyme at the beginning of the winter season. By this way, needles would be ready for sub-freezing temperatures with increased proline concentration. Moreover, there wasn't a need in the photorespiratory pathway, as explained before. In the other picture, at summer, under drought stress, those pine species would probably needed a

large proline pool, again. However, there were some other metabolic needs for the same molecule; such as elevated $NAD(P)^+$ need because of high photosynthesis, respiration and photorespiration, higher nitrogen need in other parts such as roots and shoots (Figure 4.3). In other words, in summer season, proline produced in the needles might be used or transported from the needles to the other parts of the trees at a very fast rate with respect to its production that might cause low measured proline: The faster the cycle turned, the higher the production of those metabolites produced.

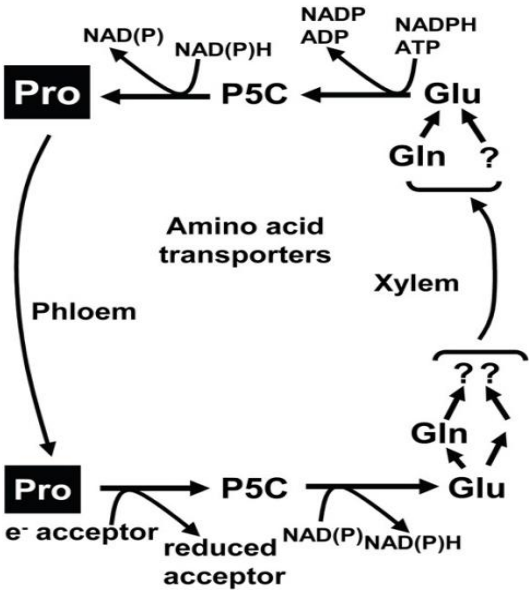

Figure 4.3 Proline transport pathway in plants proposed by Verslues *et al* (Verslues & Sharma, 2010)

Another important enzyme in chloroplast homeostasis, NADP-Malate dehydrogenase (NADP-MDH) increased in summer and decreased in winter samples of *Pinus sylvestris*. This enzyme converts oxaloacetate to malate using NADPH, and by this way, it facilitates the regeneration of the electron acceptor $NADP^+$ in the chloroplasts, particularly when CO_2 assimilation is restricted (Hebbelmann, 2011). So, although the differences between the protein spectral count values of this enzyme measured for *Pinus brutia* were not noteworthy, *Pinus sylvestris* might tend to balance electron transfer in chloroplast by altering the amount of NAD-MDH.

4.3. Seasonal changes in carbohydrate and energy metabolisms

In our study, carbohydrate content, specifically the starch and sucrose contents, of the samples were not measured; however, LC/MS-MS results suggested a proposal about the total sugar/energy metabolism in the needles with respect to seasonal stress conditions. In general sense, starch bodies in the plant cells was used up for the generation of sucrose to provide this osmoprotectant for the sake of protection against water stress created by sub-freezing temparatures (Fischer & Höll, 1992). Moreover, overall energy metabolism is also modified for stress resistance and a higher survival rate.

Desiccation created by drought stress yields an up-regulation in the enzymes such as sucrose phosphate synthase (SPS) and sucrose synthase (SuSy) that increase sucrose concentration in the cytoplasm. SuSy performs the production of sucrose:

UDP-Glucose + Fructose → Sucrose + UDP + H^+

and SPS catalyses the reaction:

UDP-Glucose + Fructose-6-P → Sucrose-6-P + UDP + H^+

SuSy and SPS are located in the cytoplasm and they catalyze freely reversible reactions. However, *sucrose phosphatase(SPP)* removes sucrose-6-P in a relatively higher rate that keeps the cytosolic sucrose-P concentration low. As a result, SPS reaction is essentially irreversible (Figure 4.4). Huber *et al* (Huber & Huber, 1996) suggested that SPS and SPP might actually form a complex in vivo and by this way, sucrose synthesis could be claimed to be catalyzed by SPS (in conjunction with SPP), whereas sucrose breakdown was largely catalyzed by SuSy.

For *Pinus brutia*, there was 2,2 times increase in SuSy amount in summer samples but it was decreased about half (0,6 times) in winter with respect to spring time. For *Pinus sylvestris*, there was almost 0,2 times (80%) less SuSy in summer and it was 1,3 times more in winter samples. On the other hand, as expected, total protein spectral count values for SPS enzyme were very low in both species when evaluated by both engines (of OMSSA and X!Tandem), because this enzyme is a low-abundance protein (<0.1% of leaf soluble protein) and is also relatively unstable (Huber & Huber, 1996). Still, for brutia pine, there was a slight increase in winter with respect to other two seasons at which values were almost the same (OMSSA: 19, 18, 28 and X!Tandem: 14, 15, 22 for spring, summer, winter respectively). The change was less discernible for scots pine (OMSSA: 8, 11, 10 and X!Tandem: 8, 12, 16 for spring, summer and winter, respectively).

Those results for sucrose synthase and sucrose phosphate synthase propose a case for the pine species: In winter time, under cold stress conditions, relatively higher expression of SPS and lower SuSy amount in *Pinus brutia* needles suggested an increase in the sucrose concentration in the cytoplasm. This is an acceptable idea with the fact that sucrose function as an osmoprotectant. In summer time, increased SuSy activity may be a result of increased rate of energy metabolism. For *Pinus sylvestris*, there was an opposite situation: SuSy levels were high in winter and significantly lower in summer time. This might be a natural result of this species' being able to succeed cold-acclimation earlier (and even better) than Turkish red pine. It might continue to produce ATP by using its starch depots in winter time and contrarily, it might tend to increase starch storages while it reached to its maximum photosynthetic rate in summer.

This proposition needs to be evaluated by comparing the changes in the expressions of the other enzymes located in the energy and carbohydrate metabolism (Appendix M). Kosova *et al* (Kosova *et al*, 2011) proposed that under cold stress conditions, glyceraldehyde 3-phosphate dehydrogenase (GAPDH), phosphoglycerate kinase (PGK) and UDP-Glucose Pyrophosphate (UDPGP) were up-regulated to create an up-regulation in catabolic pathways together with a down-regulation in anabolic pathways. Like cold stress, heat and drought stresses, also, subjected for the same type of changes in the amount of those enzymes in the cell: heat causes up-regulation of UDPGP and transketolase (TK). It was declared that

drought stress caused up-regulation of the ATP synthase β-subunit, ATPase α-subunit, GAPDH and PGK (Kosova *et al*, 2011) (Singh & Jwa, 2013).

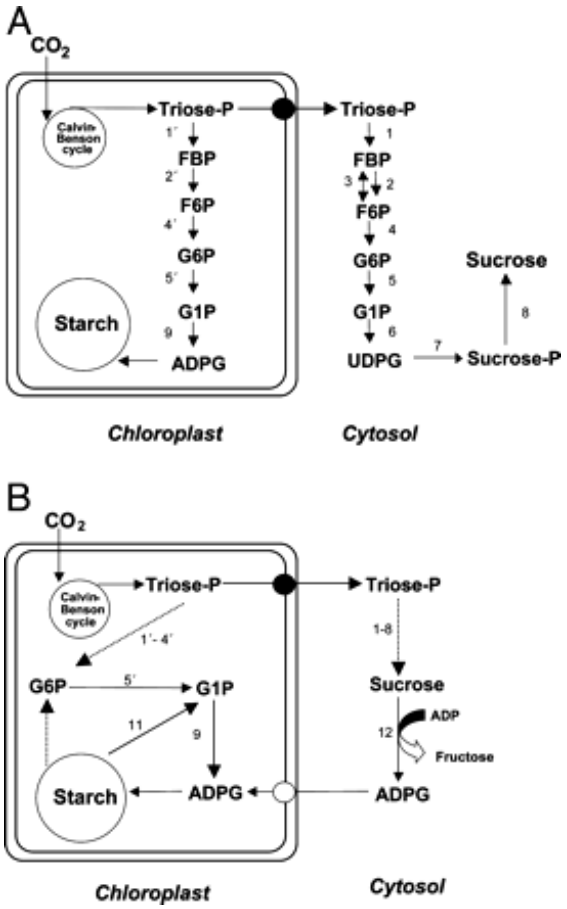

Figure 4.4 Fernández *et al* (Fernández, *et al*., 2004) suggested pathways of starch synthesis in leaves. (*A*) "Classic model" claims that the starch biosynthesis occurs completely in the chloroplast and sucrose biosynthesis is in the cytosol of the plant cell. (*B*) The alternative model, on the other hand, states that both processes are interconnected by means of the ADPG-synthesizing activity of SuSy. (*ADPG*, ADP-glucose, *G1P*, glucose-1-phosphate, *G6P*, glucose-6-phosphate, *UDPG*, UDP-glucose):

1 and 1′ fructose-1,6-bisphosphate aldolase;
2 and 2′ fructose 1,6-bisphosphatase;
3 PPi:fructose-6-phosphate phosphotransferase;
4 and 4′ phosphoglucoisomerase;
5 and 5′ phosphoglucomutase;
6 UGP; UDPG pyrophosphorylase
7 SPS; sucrose-phosphate synthase
8 sucrose phosphate phosphatase;
9 AGP; ADPG pyrophosphorylase
10 SS; starch synthase
11 SP; starch phosphorylase
12 SuSy; sucrose synthase

Transketolases catalyse the reversible transfer of an activated two-carbon glyco-aldehyde from a ketose to an aldose. They are key enzymes in the non-oxidative part of the pentose phosphate cycle and Calvin cycle in photosynthetic tissues; and because of this property, they form the link between sugar, nucleic acid and amino acid metabolisms. In other words, they control the flux of carbon from the Calvin cycle to biosynthetic pathways of phosphate sugars (Bemacchia *et al*, 1995). Ozdemir *et al* (Ozdemir, *et al*., 2009) informed that

transketolases play an important role in the stress-induced production of cytosolic NADPH in plants and a moderate increase in the activity of transketolase was detected in maize under salt and oxidative stresses.

Pinus sylvestris and *Pinus brutia* showed different patterns of change in their transketolase amount between the seasons. Turkish red pine had maximum amount in winter time when it was probably suffered from the harmful effects of cold stress. Plant species produces phenylpropanoids under such stress conditions and TK provides the necessary precursors for the production of those complexes (Henkes *et al*, 2001). Christie *et al* (Christie *et al*, 1994) affirmed that the increase in the phenylpropanoid content might reach to 10 fold upon exposure to elongated chilling and cold stresses. Contrarily, TK expression for this species was low in summer samples with respect to other sampling periods. *Pinus brutia* is an early-successional species and growing season was stated as spring time; so, the operations over pentose phosphate pathway might be maximum at this period which needed high TK activity than any other time. In summary, brutia pine might increase TK amount in winter for stress management and kept it relatively high during spring for sustainable growth. *Pinus sylvestris*, as being a more resistant species against cold stress, didn't performed a considerable change in TK expression in winter; however, in summer season, it might need the elevated TK levels for stress resistance mechanism or simply to meet the needs of amino acid and nucleic acid metabolisms via pentose phosphate pathway. Elevated TK in photosynthetic tissues, also, provides the substrate for Rubisco by regenerating ribulose 1,5 bisphosphate (Skylas *et al*, 2005) which is vital for photorespiration.

In accordance with the increased UDPGP, NAD-dependent malic enzyme 1 and PGK expression in the winter season, brutia pine might increase energy production by respiratory metabolism to cope with the oxidative stress created by sub-freezing temperatures and decreased enzyme activities because of low temperature values. Elevated expressions of ATP-citrate synthase beta chain protein 1-like (XP_003546316.1), citrate synthase (148906790) and citrate synthase 3(294462280) in winter samples of both species, also, proved the enhancement in respiratory pathway for more ATP production with respect to winter values proposing a decrease in energy derivation in this system. Alcohol dehydrogenase, (ADH) which function in anaerobic part of whole energy derivating mechanism of the plant cells, was considerably up-regulated in both species, too (2.3 times for brutia pine and 2.9 times for scots pine). Jarillo *et al* (Jarillo *et al*, 1993) notified that low temperatures cause alterations in membrane structure which in turn affect the membrane-bound processes such as oxidative respiration. As a result, in plants under cold stress, there exists an inbalance between glycolysis and ETS; and plants lean to glycolysis as much as possible to meet the ATP need. In short, up-regulation of ADH might be a result of increased ATP demand of those pine species under cold-stress, which also caused those other enzymes mentioned to be up-regulated.

The source of this energy was hard to guess with respect to the fluctuations in the amounts of enzymes, however, it might be possible that brutia pine used its starch storage in two ways: by decreased SuSy activity, it increased the concentration of sucrose in the cytoplasm against water stress, and at the same time, by increasing respiratory enzymes, it spent this depot as glucose. In other saying, starch might be converted into sucrose (to be used as osmoprotectant) and glucose (to be used as energy source). The changes in UDPGP and PGK levels in Scots pine needles were consistent with the expected ones in cold winter conditions and summer time; although there was an insignificant decrease in UDPGP.

4.4. The changes in the protein folding and chaperon networks

Temperature and drought stresses also cause protein misfolding except their effects on elevated ROS production. Plants have a wide diversity of heat stress proteins (HSP) and chaperones in chloroplasts, mitochondria and cytosol to deal with this problem (Figure 4.5). One of those protein groups is peptidyl-prolyl *cis-trans* isomerases (PPIases) that catalyse the reversible conversion of peptidyl prolyl bond from *cis* to *trans* in protein folding. Cyclophilin forms one of three major classes of PPIases and take responsibilities in both protein folding and chaperonic issues (Sharma *et al*, 2003). LC-MS/MS analysis revealed remarkable increases in cyclophilin amount in winter samplings of *Pinus brutia* and *Pinus sylvestris*; and such high values never measured so far for pinus species.

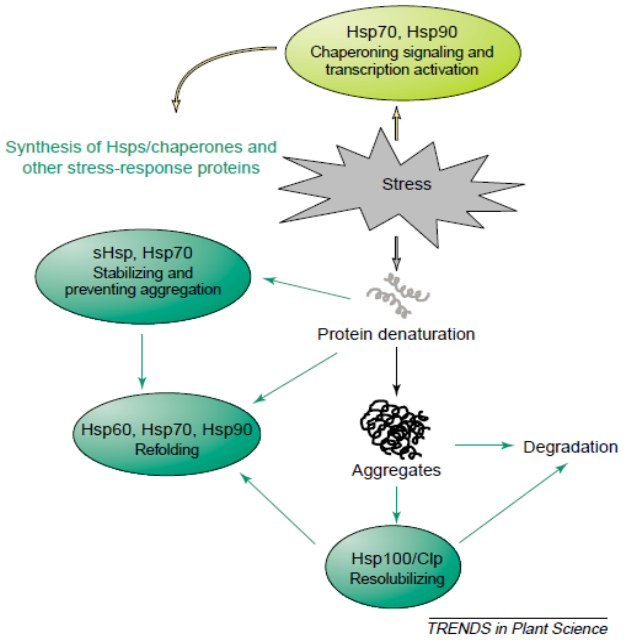

Figure 4.5 HSP and chaperone network against abiotic stress (Wang *et al*,2004)

101 kD Heat Shock Protein (HSP101) was measured as 2-3 times more for *Pinus brutia* and 1.3 times more for *Pinus sylvestris* in winter samples. Wang *et al* (Wang *et al*, 2004) informed that HSP101 performs the dissolution of electron-dense granules during the post-stress phase. This might be an acceptable reason for those very high amounts measured at the end of winter season.

HSP60 β subunit is a chaperonin which support Rubisco folding and its binding to the substrates; and also its amount increases under heat stress conditions (Holland *et al*, 1998) (Salvucci, 2008). In this study, an opposite situation was observed for both of the species: although there were insignificant increases in summer time, the major raise was measured for winter samples. This is a challenging result which needs to be supported by some other tests, because the number of studies on this specific molecule is still low.

CHAPTER V

CONCLUSION

This study provided the first proteomic data for *Pinus brutia* by defining more than 300 proteins. Moreover, by comparing with a relatively well-studied pine species, *Pinus sylvestris*, the responses of important biochemical pathways like photosynthesis, photorespiration, energy production and protein folding/chaperonin were explained. In spite of being unable to proceed with further MALDI-TOF MS/MS applications, we succeeded in handling a 2D-PAGE gel image comparison for three seasons of both species.

The optimization issues on the protein extraction method did not affect the number of bands on SDS-PAGE gels. However, the new "combined" method increases the performance of IEF procedure and yielded better gel images after 2D-PAGE. Moreover, the final product of this protein extraction was clear enough to be analyzed in LC-MS/MS system. After FASP and anion exchange column applications, the noise levels for all samples were in acceptable range (though pine needles contains a huge amount of interfering substances) which was one of the advantages allowed us to use LC-MS efficiently.

Although they were grown in the same area with the same climatic conditions, these two pine species showed a tendency to respond to different abiotic stress conditions as they were in their natural habitats. This behavior invited a serious level of stress on *Pinus sylvestris* in summer and *Pinus brutia* in winter.

Rubisco amount reached its minimum values in winter time for both of the species as stated by the information on photosynthetic units, LC-MS/MS results and a huge pile of literature sources. As being the most abundant protein in photosynthetic tissues of plants, decrease in the amount of Rubisco might create an elevated chance to observe less abundant ones in the analysis. The average numbers of defined proteins in winter samples of both pine species were higher than those of other seasons.

Its being successful in cold acclimation metabolism as stated in literature many times was proved once again for *Pinus sylvestris*; decreased photosynthetic machinery, exalted chlorophyll-(a+b)/carotenoid ratio and significantly increased HSPs and chaperonin levels were all consistent with this fact. On the other hand, as expected, *Pinus brutia* trees were not as successful as scots pine in management of sub-freezing temperatures. This Mediterranean pine species decreased its chlorophyll (a+b) content almost 25-30% in winter like scots pine and reached to its maximum level in spring time. *P. sylvestris* reached to this highest level in

summer season. If we consider the number of cold, even sub-freezing, daily temperatures (especially in March) of spring season, this early response might cause the oxidative stress that red pine suffered from.

The degradation of the PSII system as a precaution of unmanageable photorespiration was observed in both pine species in different dimensions. D1 protein was the target of this process and western blot analysis of all samples braced this idea.

The changes in the GSH pool were purposeful with respect to the specific activity values of the total GST in both species: when the enzymatic activity rose, the pool was waned because of increased demand. Moreover, this relationship strengthens the proposition of higher oxidative stress in summer for *Pinus sylvestris* and in winter for *Pinus brutia*.

Under cold stress conditions both of the species tend to increase the rate or the dimension of energy harvesting mechanism to meet the ATP need. Up-regulated respiratory system enzymes such as UDPGP, PGK, ATP-citrate synthase beta chain protein 1-like, citrate synthase, citrate synthase 3, NAD-dependent malic enzyme 1 pointed an increased ATP production. Moreover, the increase in the amount of ADH, which protects the sustainable proceeding of glycolysis, might be an indicator of this exalted need for energy because it seemed that it forced needle cells to gather energy even from anaerobic respiration. Elevated SuSy levels in winter samples of scots pine might be used to explicate the source of this energy: starch stored before winter was used by converting it to sucrose molecules, first. Conversely, *Pinus brutia* might tent to increase cytosolic sucrose level high enough to protect cells against water stress by decreasing SuSy levels. This species might, also, use glucose-1-P (after converting into glucose-6-p by elevated phosphoglucomutase content) as the energy source instead of sucrose, unlike *Pinus sylvestris* that might use both the sucrose and glucose-1-P "ways" at the same time.

As stated in many studies, proline content of both pine species were relatively higher in winter season to protect osmotic balance against increased water stress created by sub-freezing temperatures. The fate of this molecule in summer season might be shaped by the elevated Fd-GOGAT enzyme that might direct proline into nitrogen metabolism.

REFERENCES

Agrawal, G. K., & Randeep, R. (2008). *Plant proteomics: technologies, strategies, and applications.* John Wiley & Sons, Inc.

Alan, G., & Marshall, C. (1998). Fourier transform ion cyclotron resonance mass spectrometry: A primer. *Mass Spectrometry Reviews , 17*, 1-35.

Alia, P. S., & Mohanty, P. (1991). Proline enhances primary photochemical activities in isolated thylakoid membranes of Brassica juncea by arresting photoinhibitory damage. *Biochemical and Biophysical Research Communications , 181*, 1238-1244.

Andrecht, S., & von Hagen, J. (2008). General Aspects of Sample Preparation for Comprehensive Proteome Analysis. In J. von Hagen, *Proteomics Sample Preparation* (pp. 5-17). Darmstadt.

Awada, T., Radoglou, K., Fotelli, M. N., & Constantinidou, H. I. (2003). Ecophysiology of seedlings of three Mediterranean pine species in contrasting light regimes. *Tree Physiology , 23* (1), 33-41.

Baettig, M. B. (2007). A climate change index: Where climate change may be most prominent in the 21st century. *Geophysical Research Letters* , L01705.

Bailleul, B., Rogato, A., de Martino, A., Coesel, S., Cardol, P., Bowler, C., et al. (2010). An atypical member of the light-harvesting complex stress-related protein family modulates diatom responses to light. *PNAS , 107* (42), 18214-18219.

Ballicora, M. A., Iglesias, A. A., & Preiss, J. (2004). ADP-glucose pyrophosphorylase: a regulatory enzyme for plant starch synthesis. *Photosynthesis Research , 79*, 1-24.

Bedell, J.-P., Chalot, M., Brun, A., & Botton, B. (1995). Purification and properties of glutamine synthetase from Douglas-fir roots. *Physiologia Plantarum , 94* (4), 597-604.

Bernacchia, G., Schwall, G., Lottspeich, F., Salamini, F., & Bartels, D. (1995). The transketolase gene family of the resurrection plant Craterostigma plantagineum: differential expression during the rehydration phase. *The EMBO Journal , 14* (3), 610-618.

Bigler, C., Bräker, O., Bugmann, H., Dobbertin, M., & Rigling, A. (2006). Drought as an inciting mortality factor in Scots pine stands of the Valais, Switzerland. *Ecosystems , 9*, 330-343.

Bjellqvist, B., Ek, K., Righetti, P., Gianazza, E., Görg, A., Westermeier, R., et al. (1982). Isoelectric focusing in immobilized pH gradients: principle, methodology and some applications. *Journal of Biochemical and Biophysical Methods , 6* (4), 317-339.

Bohnert, H. J., Nelson, D. E., & Jensen, R. G. (1995). Adaptations to Environmental Stresses. *The Plant Cell , 7*, 1099-1111.

Bonhomme, L., Monclus, R., Vincent, D., Carpin, S., Lomenech, A.-M., Plomion, C., et al. (2009). Genetic variation in drought response and in water-use efficiency involves photosynthesis-related proteins. *Proteomics , 9*, 4121-4142.

Borsani, O., Diaz, P., & Monza, J. (1999). Proline is Involved in Water Stress Responses of Lotus corniculatus Nitrogen Fixing and Nitrate Fed Plants. *Journal of Plant Physiology , 155*, 269-273.

Boydak. (2003). Effects of Water Stress on Germination in Six Provenances of Pinus brutia Seeds from Different Bioclimatic Zones in Turkey. *Turkish Journal of Agriculture and Forestry , 27*, 91-97.

Chen, Z., & Spreitzer, R. (1993). Thermal Instability of Ribulose-1,5-Bisphosphate Carboxylase/Oxygenase from a Temperature-Conditional Chloroplast Mutant of Chlamydomonas reinhardtii. *Plant Physiology , 101* (4), 1189-1194.

Christie, P. J., Alfenito, M. R., & Walbot, V. (1994). Impact of low-temperature stress on general phenylpropanoid and anthocyanin pathways: Enhancement of transcript abundance and anthocyanin pigmentation in maize seedlings. *Planta , 194* (4), 541-549.

Claussen, W. (2005). Proline as a measure of stress in tomato plants. *Plant Science , 168* (1), 241–248.

Cohen, I., Sapir, Y., & Shapira, M. (2006). A Conserved Mechanism Controls Translation of Rubisco Large Subunit in Different Photosynthetic Organisms. *Plant Physiology , 141*, 1089-1097.

Costa, P., Pionneau, C., Bauw, G., Dubos, C., Bahrmann, N., Kremer, A., et al. (1999). Separation and characterisation of needle and xylem maritime pine proteins. *Electrophoresis, 20*, 1098-1108.

Craig, R., & Beavis, R. C. (2004). TANDEM: matching proteins with mass spectra. *Bioinformatics , 20*, 1466-1467.

Davey, M., Stals, E., Panis, B., Keulemans, J., & Swennen, R. (2005). High-throughput determination of malondialdehyde in plant tissues. *Analytical Biochemistry , 347* (2), 201-207.

Davis, D. G., & Swanson, H. R. (2001). Activity of stress-related enzymes in the perennial weed leafy spurge (Euphorbia esula L.). *Environmental and Experimental Botany , 46*, 95-108.

Duncan, D. R., & Widholm, J. M. (1987). Proline Accumulation and Its Implication in Cold Tolerance of Regenerable Maize Callus. *Plant Physiology , 83*, 703-708.

Eidhammer, I., Flikka, K., Martens, L., & Mikalsen, S. (2007). *Computational Methods for Mass Spectrometry Proteomics.* John Wiley & Sons, Ltd.

Ekramoddoullah, A. (1993). Analysis of needle proteins and N-terminal amino acid sequences of two photosystem II proteins of western white pine (Pinus monticola D. Don). *Tree Physiology , 12* (1), 101-106.

Eng, J., McCormack, A., & Yates, J. 3. (1994). An Approach to Correlate Tandem Mass Spectral Data of Peptides with Amino Acid Sequences in a Protein Database. *Journal of American Society of Mass Spectrometry , 5*, 976-989.

Ensminger, I., Busch, F., & Huner, N. (2006). Photostasis and cold acclimation: Sensing low temperature through photosynthesis. *Physiologia Plantarum , 126*, 28-44.

EuropeanEnvironmentAgency. (2010). *Climate change mitigation (Turkey).* European Environment Agency.

Fernández, E. B., Muñoz, F. J., Criado, A. Z., Zorzano, M. T., Viale, A. M., Casajús, N. A., et al. (2004). Most of ADP-glucose linked to starch biosynthesis occurs outside the chloroplast in source leaves. *PNAS , 101* (35), 13080-13085.

Fischer, C., & Höll, W. (1992). Food reserves of scots pine (P. sylvetris): II: Seasonal changes and radial distribution of carbohydrate and fat reserves in pine wood. *Trees , 6*, 147-155.

Flengsrud, R. (2008). Protein Extraction from Green Plant Tissue. In R. Flengsrud, *2D PAGE: Sample Preparation and Fractionation Volume:2.* Humana Press.

Galant, A., Preuss, M. L., Cameron, J. C., & Joseph, M. J. (2011). Plant glutathione biosynthesis: diversity in biochemical regulation and reaction products. *Frontiers in Plant Metabolism and Chemodiversity , 2* (45).

Gardner, H. W. (1995). Biological Roles and Biochemistry of the Lipoxygenase Pathway. *Horticultural Science , 30* (2).

Geer, L. Y. (2004). Open Mass Spectrometry Search Algorithm. *Journal of Proteome Research , 3*, 958-964.

Gezer, A. (1986). *The Sylviculture of Pinus brutia in Turkey.* Paris: CIHEAM.

Gill, S., & Tuteja, N. (2010). Reactive oxygen species and antioxidant machinery in abiotic stress tolerance in crop plants. *Plant Physiology and Biochemistry , 48* (12), 909-930.

Gion, J.-M. G., Lalanne, C., Le Provost, G., Dumazet, H. F., Paiva, J., Chaumeil, P., et al. (2005). The proteome of maritime pine wood forming tissue. *Proteomics , 5* (14), 3731-3751.

Grill, D., Pfeifhofer, H., & Esterbauer, H. (1987). Further investigations on the thiol content of Norway spruce needles. *Phyton (Austria) , 27* (2), 311-317.

Grivet, D., Climent, J., Zabal-Aguirre, M., Neale, D. B., Vendramin, G. G., & González-Martínez, S. C. (2013). Adaptive evolution of Mediterranean pines. *Molecular Phylogenetics and Evolution , 68*, 555-566.

Grotkopp, E., Rejmánek, M., Sanderson, M., & Rost, T. (2004). Evolution of Genome Size in Pines (Pinus) and its life-history correlates: supertree analyses. *Evolution , 58*, 1705-1729.

Gruber, A., Pirkebner, D., Florian, C., & Oberhuber, W. (2012). No evidence for depletion of carbohydrate pools in Scots pine (Pinus sylvestris L.) under drought stress. *Plant Biology , 14* (1), 142-148.

Habig, W., Pabst, M., & Jakoby, W. (1974). Glutathione S-transferases. The first enzymatic step in mercapturic acid formation. *Journal of Biological Chemistry , 249* (22), 7130-7139.

Hansen, J., & Beck, E., 1988, Evidence for ideal and non-ideal equilibrium freezing of leaf water in frost-hardy ivy (*Hedera helix*) and winter barley (*Hordeum vulgare*). *Botanica Acta, 101*, 76-82.

Hansen, J., Vogg, G., & Beck, E. (1996). Assimilation, allocation and utilization of carbon by three-year-old Scots pine (Pinus sylvestris L.) trees during winter and early spring. *Trees , 11*, 83-90.

Hardman, M., & Makarov, A. (2003). Interfacing the orbitrap mass analyzer to an electrospray ion source. *Analytical Chemistry , 75*, 1699-1705.

Hare, P., Cress, W., & van Staden, J. (1999). Proline synthesis and degradation: a model system for elucidating stress-related signal transduction. *Journal of Experimental Botany , 50* (333), 413-434.

Hari, P., & Nöjd, P. (2009). The effect of temperature and PAR on the annual photosynthetic production of Scots pine in northern Finland during 1906-2002. *Boreal Environment Research , 14*, 5-18.

Hausladen, A., & Alscher, R. G. (1994). Cold-Hardiness-Specific Glutathione Reductase lsozymes in Red Spruce-Thermal Dependence of Kinetic Parameters and Possible Regulatory Mechanisms-. *Plant Physiology , 105*, 215-223.

Havaux, M. (1998). Carotenoids as membrane stabilizers in chloroplasts. *CarotenoidTrends in Plant Science , 3* (4), 147-151.

Hebbelmann, I. (2011). Multiple strategies to prevent oxidative stress in Arabidopsis plants lacking the malate valve enzyme NADP-malate dehydrogenase. *Journal of Experimental Botany*.

Henkes, S., Sonnewald, U., Badur, R., Flachmann, R., & Stitt, M. (2001). A Small Decrease of Plastid Transketolase Activity in Antisense Tobacco Transformants Has Dramatic Effects on Photosynthesis and Phenylpropanoid Metabolism. *The Plant Cell , 13*, 535-551.

Hjelm, U., & Ogren, E. (2003). Is photosynthetic acclimation to low temperature controlled by capacities for storage and growth at low temperature? Results from comparative studies of grasses and trees. *Physiologia Plantarum , 119*, 113-120.

Hodges, D. M., DeLong, J. M., Forney, C. F., & Prange, R. K. (1999). Improving the thiobarbituric acid-reactive-substances assay for estimating lipid peroxidation in plant tissues containing anthocyanin and other interfering compounds. *Planta , 207*, 604-611.

Holland, N., Belkind, A., Holland, D., Pick, U., & Edelman, M. (1998). Stress-responsive accumulation of plastid chaperonin 60 during seedling development. *The Plant Journal , 13* (3), 311-316.

Hu, Q. (2005). The Orbitrap: a new mass spectrometer. *Journal of Mass Spectrometry , 40*, 430-443.

Huber, S., & Huber, J. (1996). Role and Regulation of Sucrose-Phosphate Synthase in Higher Plants. *Annual Review of Plant Physiology and Plant Molecular Biology , 47*, 431-444.

Huner, N., Öquist, G., Hurry, V., Krol, M., Falk, S., & Griffith, M. (1993). Photosynthesis, photoinhibition and low temperature acclimation in cold tolerant plants. *Photosynthesis Research, 37*, 19-39.

IPCC. (1996). *Intergovermental Panel on Climate Change.*

Ito, Y., Katsura, K., Maruyama, K., Taji, T., kobayashi, M., Seki, M., et al. (2006). Functional Analysis of Rice DREB1/CBF-type Transcription Factors Involved in Cold-responsive Gene Expression in Transgenic Rice. *Plant Cell Physiology , 47* (1), 141-153.

Jarillo, J. A., Leyva, A., Salinas, J., & Zapater, J. M. (1993). Low Temperature lnduces the Accumulation of Alcohol Dehydrogenase mRNA in Arabidopsis fhaliana, a Chilling-Tolerant Plant. *Plant Physiology , 101*, 833-837.

Johnson, R. S., & Taylor, J. A., 1998, Sequence database searches via de novo peptide sequencing by tandem mass spectrometry, Rapid Communications in Mass Spectrometry, 11,9, 1067-1075.

Kandemir, G. E., Kaya, Z., Temel, F., & Önde, S. (2010). Genetic Variation in Cold Hardiness and Phenology Between and Within Turkish Red Pine (Pinus brutia Ten.) Populations: Implications for Seed Transfer. *Silvae Genetica , 59*, 2-3.

Karaca, M. (2008). Potential implications of accelerated sea-level rise for Turkey. *Journal of Coastal Research , 24* (2), 288-298.

Kawamura, Y., & Uemura, M. (2003). Mass spectrometric approach for identifying putative plasma membrane proteins of Arabidopsis leaves associated with cold acclimation. *Plant Journal, 36*, 141-154.

Kaya, Z. (2001). Biodiversity and conservation of Turkish forests. *Biological Conservation , 97*, 131-141.

Kinter, M., & Sherman, N. E. (2000). *Protein Sequencing and IdentiJication Using Tandem Mass Spectrometry.* John Wiley & Sons Inc Publication.

Korpilahti, E. (1990). Seasonal and annual photosynthetic production of Pinus sylvestris estimated for a period of 20 years. *Scandinavian Journal of Forest Research , 5*, 1-4.

Kosmala, A., Bocian, A., Rapacz, M., Jurczyk, B., & Zwierzykowski, Z. (2009). Identification of leaf proteins differentially accumulated during cold acclimation between

Festuca pratensis plants with distinct levels of frost tolerance. *Journal of Experimental Botany , 60*, 3595-3609.

Kosová, K., Vítámvás, P., Prášil, I. T., & Renaut, J. (2011). Plant proteome changes under abiotic stress- Contribution of proteomics studies to understanding plant stress response. *Journal of Proteomics , 74*, 1301-1322.

Kurt, Y., Bilgen, B. B., Kaya, N., & Işık, K. (2011). Genetic Comparison of Pinus brutia Ten. Populations from Different Elevations by RAPD Markers. *Notulae Botanicae Horti Agrobotanici , 39* (2), 299-304.

Labra. (2006). Distribution of genetic variability in southern populations of Scots pine (Pinus sylvestris L.) from the Alps to the Apennines. *Flora , 201*, 468-476.

Linnaei, C. (1753). *Species plantarum: exhibentes plantas rite cognitas, ad genera relatas, cum differentiis specificis, nominibus trivialibus, synonymis selectis, locis natalibus, secundum systema sexuale digestas.* Stockholm.

Lowry, O., Rosebrough, N., Farr, A., & Randall, R. (1951). Protein measurement with the Folin phenol reagent. *Journal of Biological Chemistry , 193* (1), 265-275.

Marrs, K. A. (1996). The functions and regulation of Glutathione S-transferases in plants. *Annual Review of Plant Physiology and Plant Molecular Biology , 47*, 127-158.

McNulty, G. S. (1996). Potential Climate Change Effects on Loblolly Pine Forest Productivity and Drainage across the Southern United States. *AMBIO: A Journal of the Human Environment , 25*, 7.

Mencarelli, F., & Saltveit, M. (1988). Ripening of mature-green tomato fruit slices. *Journal of the American Society for Horticultural Science , 113* (5), 742-745.

Morse, A. M., Peterson, D. G., Islam-Faridi, M. N., Smith, K., Magbanua, Z., Garcia, S. A., et al. (2009). Evolution of Genome Size and Complexity in Pinus. *PLOS One , 4* (2), 4332.

Noctor, G., Mhamdi, A., Chaouch, S., Han, Y., Neukermans, J., Garcia, B. M., et al. (2012). Glutathione in plants: an integrated overview. *Plant, Cell and Environment , 35* (2), 454-484.

Osmond, C., & Grace, S. (1995). Perspectives on photoinhibition and photorespiration in the field: quintessential inefficiencies of the light and dark reactions of photosynthesis? *Journal of Experimetal Botany , 46*, 1351-1362.

Ozdemir, M. T., Miller, G., Luhua, S., Kim, J., Sodek, A., Koussevitzky, S., et al. (2009). Thiamin Confers Enhanced Tolerance to Oxidative Stress in Arabidopsis. *Plant Physiology , 151* (1), 421-432.

Peers, G., Truong, T. B., Ostendorf, E., Busch, A., Elrad, D., Grossman, A. R., et al. (2009). An ancient light-harvesting protein is critical for the regulation of algal photosynthesis. *Nature , 462*, 518-521.

Perkins, D. (1999). Probability-based protein identification by searching sequence databases using mass spectrometry data. *Electrophoresis , 20*, 3551-3567.

Pukacka, S., & Pukacki, P. M. (2000). Seasonal changes in antioxidant level of Scots pine (*Pinus sylvestris* L.) needles exposed to industrial pollution. I. Ascorbate and thiol content. *Acta Physiologiae Plantarum , 22* (4), 451-456.

Rehm, H. (2006). *Protein Biochemistry and Proteomics.* California: Elsevier.

Richardson, D. M. (1998). *Ecology and biography of Pinus* (Vol. 527). Cambridge: Cambridge University Press.

Rigling, A., Brühlhart, H., Bräker, O. U., Forater, T., & Schweingruber, F. H. (2003). Effects of irrigation on diameter growth and vertical resin duct production in Pinus sylvestris L. on dry sites in the central Alps, Switzerland. *Forest Ecology and Management* .

Ristic, Z., Momcilovic, I., Bukovnik, U., Prasad, P. V., Fu, J., DeRidder, B. P., et al. (2009). Rubisco activase and wheat productivity under heat-stress conditions. *Journal of Experimental Botany , 60* (14), 4003-4014.

Ruelland, E., Vaultier, M.-N., Zachowski, A., & Hurry, V. (2009). Cold Signalling and Cold Acclimation in Plants. *Advances in Botanical Research , 49*.

Salvucci, M. (2008). Association of Rubisco activase with chaperonin-60beta: a possible mechanism for protecting photosynthesis during heat stress. *Journal of Experimental Botany, 59* (7), 1923-1933.

Saravanan, R., & Rose, J. (2004). A critical evaluation of sample extraction techniques for enhanced proteomic analysis of recalcitrant plant tissues. *Proteomics , 4* (9), 2522-2532.

Savitch, L., Leonardos, E., Krol, M., Jansson, S., Grodzinski, B., Huner, N., et al. (2002). Two different strategies for light utilization in photosynthesis in relation to growth and cold acclimation. *Plant, Cell and Environment , 25*, 761-771.

Schröder P., Berkau, C., 1993, Characterization of cytosolic glutathione S-transferase in spruce needles, Botanica Acta, 106:301-306

Sedlak, J., & Lindsay, R. (1968). Estimation of total, protein-bound, and nonprotein sulfhydryl groups in tissue with Ellman's reagent. *Analytical Biochemistry , 25* (1), 192-205.

Seppanen, M., Cardi, T., Hyökki, B. M., & Pehu, E. (2000). Characterization and expression of cold-induced glutathione S-transferase in freezing tolerant Solanum commersonii, sensitive S. tuberosum and their interspecific somatic hybrids. *Plant Science , 153* (2), 125–133.

Sharma, A., Wajapeyee, N., Yadav, V., & Singh, P. (2003). Stress-induced changes in peptidyl-prolyl cis-trans isomerase activity of Sorghum bicolor seedlings. *Biologia Plantarum , 47* (3), 367-371.

Singh, R., & Jwa, N.-S. (2013). Understanding the Responses of Rice to Environmental Stress Using Proteomics. *Journal of Proteome Research* .

Sivakumar, P., Sharmila, P., & Saradhi, P. (2000). Proline alleviates salt-stress induced enhancement in ribulose-1,5-bisphosphate oxygenase activity. *Biochemical and Biophysical Research Communications , 279*, 512-515.

Skylas, D., Cordwell, S., Hains, P., Larsen, M., Basseal, D., & Wash, B. (2005). Heat shock of wheat during grain filling: proteins associated with heat-tolerance. *Journal of Cereal Science , 35*, 175-188.

Specht, M., Kuhlgert, S., Fufezan, C., & Hippler, M. (2011). Proteomics to go: Proteomatic enables the user-friendly creation of versatile MS/MS data evaluation workflows. *Bioinformatics , 27* (8), 1183-1184.

Steponkus, P., Lynch, D., & Uemura, M. (1990). The influence of cold acclimation on the lipid composition and cryobehaviour of the plasma membrane of isolated rye protoplasts. *Philosophical Transactions of the Royal Society of London. Series B, Biological Sciences , 326*, 571-583.

Strand, A., Hurry, V., Henkes, S., Huner, N., Gustafsson, P., Gardestorm, P., et al. (1999). Acclimation of Arabidopsis leaves developing at low temperatures-Increasing cytoplasmic volume accompanies increased activities of enzymes in the Calvin cycle and in the sucrose-biosynthesis pathway. *Plant Physiology , 119*, 1387-1398.

Suárez, M. F., Avila, C., Gallardo, F., Canton, F. R., Gutierrez, A. G., Claros, M. G., et al. (2002). Molecular and enzymatic analysis of ammonium assimilation in woody plants. *Journal of Experimental Botany , 53* (370), 891-904.

TC-Çevre_ve_Orman_Bakanlığı. (2010). *2010 yılı iklim verilerinin değerlendirilmesi.* Ankara: TC Çevre ve Orman Bakanlığı, Devlet Meteoroloji İşleri Genel Müdürlüğü, Zirai Meteoroloji ve İklim Rasatları Dairesi Başkanlığı.

Temple, S., Vance, C., & Gantt, J. (1998). Glutamate synthase and nitrogen assimilation. *Trends in Plant Science , 3*, 51-56.

Tenore, M. (1811). *Flora Napolitana-Tipografia del Giornale Enciclopedico* (Vol. 1). Napoli: Stamperia Reale.

Terashima, M., & Hippler, M. (2010). Characterizing the anaerobic response of Chlamydomonas reinhardtii by quantitative proteomics. *Molecular & Cellular Proteomics , 9*, 9.7.

The_Ministery_of_Environment_and_Forestry. (2010). *National Activities of Turkey on Climate Change.*

TheWorldBank. (2009). *Adapting to Climate Change in Europe and Central Asia.* Adapting to Climate Change in Europe and CThe staff of the International Bank for Reconstruction and Development.

Türkiye Çevre Atlası. (2004).

Valledor, L., Castillejo, M. A., Lenz, C., Rodriguez, R., Canal, M. J., & Jorrin, J. (2008). Proteomic Analysis of Pinus radiata Needles: 2-DE Map and Protein Identification by LC/MS/MS and Substitution-Tolerant Database Searching. *Journal of Proteome Research , 7* (7), 2616-2631.

Verslues, P. E., & Sharma, S. (2010). Proline Metabolism and Its Implications for Plant-Environment Interaction. *The Arabidopsis Book , 8*, Verslues, Paul E., Sharma, Sandeep, 2010, Proline Metabolism and Its Implicationse0140.

Vogg, G., Heim, R., Hansen, J., Schafer, C., & Beck, E. (1998). Frost hardening and photosynthetic performance of Scots pine (Pinus sylvestris L.) needles. I. Seasonal changes in the photosynthetic apparatus and its function. *Planta , 204*, 193-200.

Wang, W., Vignani, R., Scali, M., & Cresti, M. (1996). A universal and rapid protocol for protein extraction from recalcitrant plant tissues for proteomic analysis. *Electrophoresis , 27*, 2782–2786.

Wang, W., Vinocur, B., Shoseyov, O., & Altman, A. (2004). Role of plant heat-shock proteins and molecular chaperones in the abiotic stress response. *Trends in Plant Science , 9* (5).

Wang, Y., Ding, M., Gu, X., Wang, J., Pang, Y., Gao, L., et al. (2013). Analysis of Interfering Substances in the Measurement of Malondialdehyde Content in Plant Leaves. *American Journal of Biochemistry and Biotechnology , 9* (3), 235-242.

Wenner, B. R., & Lynn, B. C. (2009). Factors that Affect Ion Trap Data-Dependent MS/MS in Proteomics. *Journal of American society of Mass Spectrometry , 15* (2), 150-157.

Weston, D. J., Bauerle, W. L., Clark, G. A., Moore, B. d., & Baird, V. W. (2007). Characterization of Rubisco Activase from thermally contrasting genotypes of Acer Rubrum (Aceraceae). *American Journal of Botany , 94* (6), 926-934.

Wilkins, M. R., & Appel, R. D. (2007). 1 Ten Years of the Proteome. In *Proteome Research: Concepts, Technology and Application.* Heidelberg: Springer.

Wiśniewski, J. R., Zougman, A., Nagaraj, N., & Mann, M. (2009). Universal sample preparation method for proteome analysis. *Nature Methods , 6*, 359-362.

www.conifers.org. Retrieved from (derived from http://www.conifers.org/pi/pin/sylvestris.htm)

Yadav, S. K. (2010). Cold stress tolerance mechanisms in plants. A review. *Agronomy for Sustainable Development , 30* (3), 515-527.

Yu, F., Park, S., & Rodermel, S. R. (2004). The Arabidopsis FtsH metalloprotease gene family: interchangeability of subunits in chloroplast oligomeric complexes. *The Plant Journal , 37*, 864-876.

Yumiko, I., Yoshiba, Y., Sanada, Y., Yamaguchi, S. K., Wada, K., & Shinozaki, K. (1997). Characterization of the gene for 1-pyrroline-5-carboxylate synthetase and correlation between the expression of the gene and salt tolerance in Oryza sativa L. *Plant Molecular Biology , 33*, 857-865.

APPENDIX A

Formulations used in the Calculation of Chlorophyll and Carotenoid Content in Needles of *Pinus brutia* and *Pinus sylvestris*

95%EtOH

Chlorophyll-a	$(ABS_{664} \times 13,36) - (ABS_{648} \times 5,19)$
Chlorophyll-b	$(ABS_{648} \times 27,43) - (ABS_{664} \times 8,12)$
Chlorophyll-(a+b)	$(ABS_{664} \times 5,24) + (ABS_{648} \times 22,24)$

100%MeOH

Chlorophyll-a	$(ABS_{665} \times 16,72) - (ABS_{652} \times 9,16)$
Chlorophyll-b	$(ABS_{652} \times 34,09) - (ABS_{665} \times 15,28)$
Chlorophyll-(a+b)	$(ABS_{665} \times 1,44) + (ABS_{652} \times 24,93)$

100% Acetone

Chlorophyll-a	$(ABS_{661} \times 11,24) - (ABS_{645} \times 2,04)$
Chlorophyll-b	$(ABS_{645} \times 20,13) - (ABS_{661} \times 4,19)$
Chlorophyll-(a+b)	$(ABS_{661} \times 7,05) - (ABS_{645} \times 18,09)$

80% Acetone

Chlorophyll-a	$(ABS_{661} \times 11,24) - (ABS_{645} \times 2,04)$
Chlorophyll-b	$(ABS_{645} \times 20,13) - (ABS_{661} \times 4,19)$
Chlorophyll-(a+b)	$(ABS_{661} \times 7,05) - (ABS_{645} \times 18,09)$
Carotenoid	$[(1000 \times ABS_{470}) - (1,9 \times \text{Chl-a}) - (63,14 \times \text{Chl-b})] /214$
Chlorophllide-a	$(ABS_{667} / 74,9)$
Chlorophllide-b	$(ABS_{650} / 47,2)$

APPENDIX B

Sucrose Method of Protein Extraction

Comparison of Methods for Protein Extraction from Pine Needles
He Cai-yun *et al*, Forestry Studies in China, 7(4): 20–23, 2005

1. One gram of needle powder with the addition of 0.1 g of PVPP is extracted with 10 mL of extraction buffer (5% sucrose, 4% SDS and 5% 2-ME) for 10 min at room temperature with gentle stirring (*in 15 ml falcon tube*),
2. Centrifugation is applied at 15,000 g (30 min) (*in metal tubes*),
3. The clear supernatant is heated at 100°C for 3 min and then cooled at room temperature (*in ordinary glass tubes*),
4. Proteins are precipitated by 8 volumes of cold acetone (*in metal tubes*)
5. After at least 1 h at –20°C, the mixture is centrifuged at 10,000 g (20 min) (*in metal tubes*)
6. The pellet is re-suspended in 5 mL of extraction buffer and centrifuged at 10,000 g (15 min) (*in metal tubes*)*—by the help of a teflon covered homogenizator—*
7. The supernatant is transferred into a glass tube, first; and then 4 ml of it is used in next step (*in metal tubes*)
8. 4 volumes (4x4=16 ml) of cold acetone is added into the tube and mixed for a while
9. The mixture is centrifuged at 10,000 g (15 min) (*in metal tubes*)
10. The pellet is washed once or twice with 80% cold acetone (centrifuge is applied at 10000g for 10 min) (*in metal tubes*)
11. The pellet is dissolved in cold, pure acetone and transferred into capped glass tube
12. The mixture is centrifuged to gather the precipitate at the bottom (10 min at 250g)
13. Place the tube as its cap oppened in laminar hood (in an inclined position to dry the sample)
14. Store at -20^0C (or preferably at -70^0C)

APPENDIX C

Wang's Method of Protein Extraction

A universal and rapid protocol for protein extraction from recalcitrant plant tissues for proteomic analysis
Wei Wang *et al Electrophoresis* 2006, *27,* 2782–2786

1. 0.1-0.3 gram of needle powder is weighed into 2 ml eppendorf tube and it is filled with 10% TCA/Acetone.
2. The mixture is vortexed well, and centrifuged at 16000g for 3 min (at 4^{o}C). Then, supernatant is removed.
3. The tube is filled with 80%methanol containing 0.1 M ammonium acetate, vortexed well and centrifuged at 16000g for 3 min (at 4^{o}C).
4. Pellet is washed with 80% acetone in the same way.
5. After centrifugation and decanting supernatant, pellet is air-dried to remove residual acetone.
6. 0.4-0.8ml/0.1 g starting material of 1:1 phenol (pH 8.0)/SDS buffer is added and tube is incubated for 5 min after mixing thoroughly.
7. Tube is centrifuged at 16000g for 3 min (at 4^{o}C) and the upper phenol layer is transported into a new 2ml-eppendorf tube.
8. Then, tube is filled with 80%methanol containing 0.1 M ammonium acetate, vortexed well and centrifuged at 16000g for 5 min (at 4^{o}C).
9. The pellet is washed with 100% methanol and 80% acetone once, in the same way.
10. Proteins are allowed to be air-dried.

APPENDIX D

Chromatogram by Raw Meat

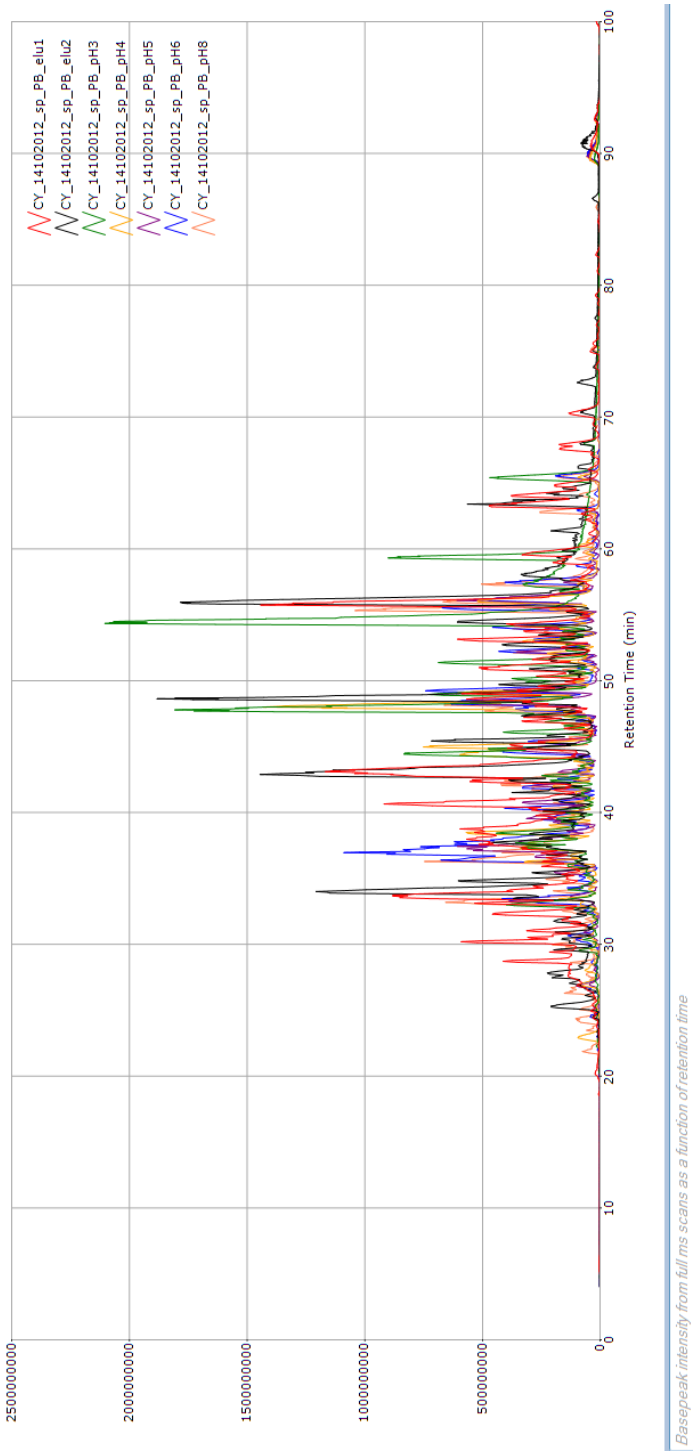

Figure D.1: Chromatogram drawn by Raw Meat Software for *Pinus brutia* spring sample

APPENDIX E

MS2 Charge Distribution

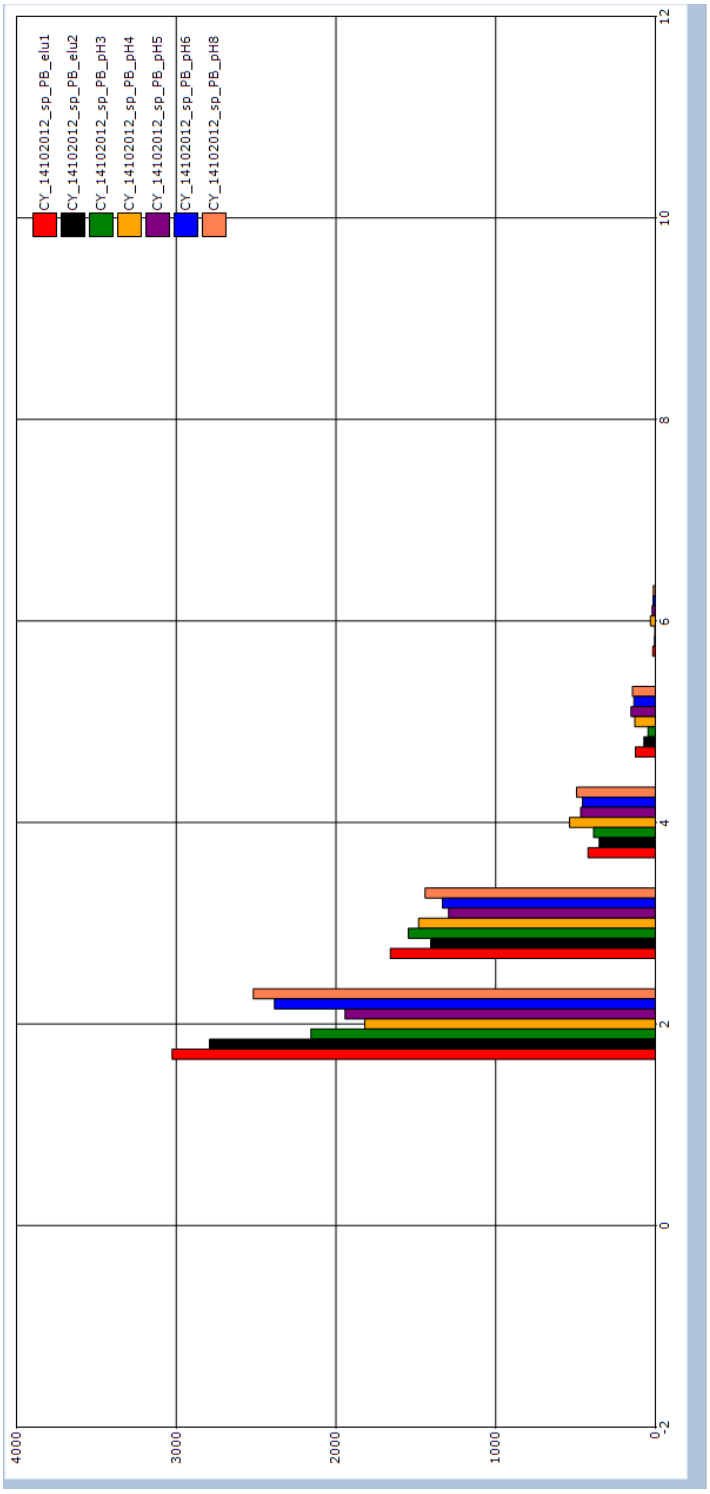

Figure E.1: MS2 charge distribution of *Pinus brutia* spring sample

APPENDIX F

MZ Distribution of Selected Monitored Ion

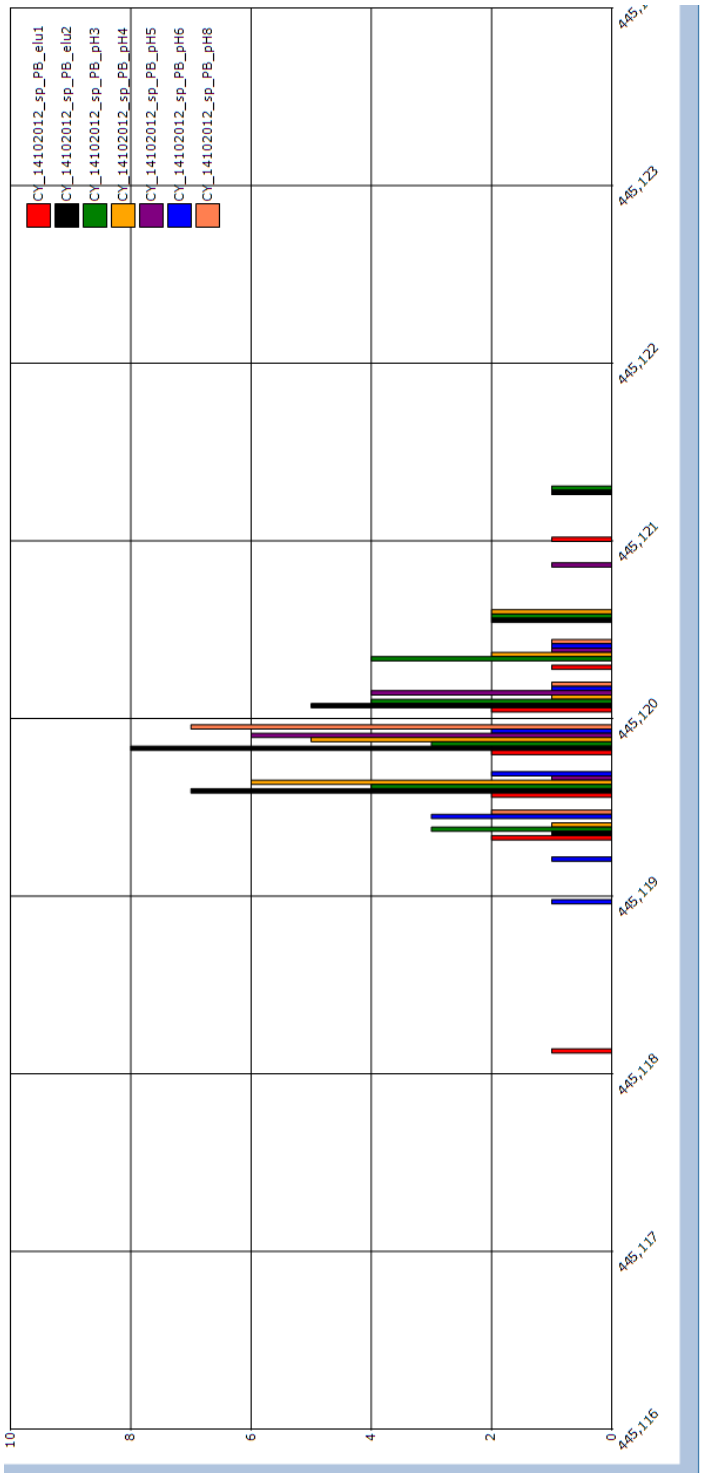

Figure F.1: MZ distribution of selected monitored ion for *Pinus brutia* spring sample

APPENDIX G

Chromatogram created by RawMeat Software

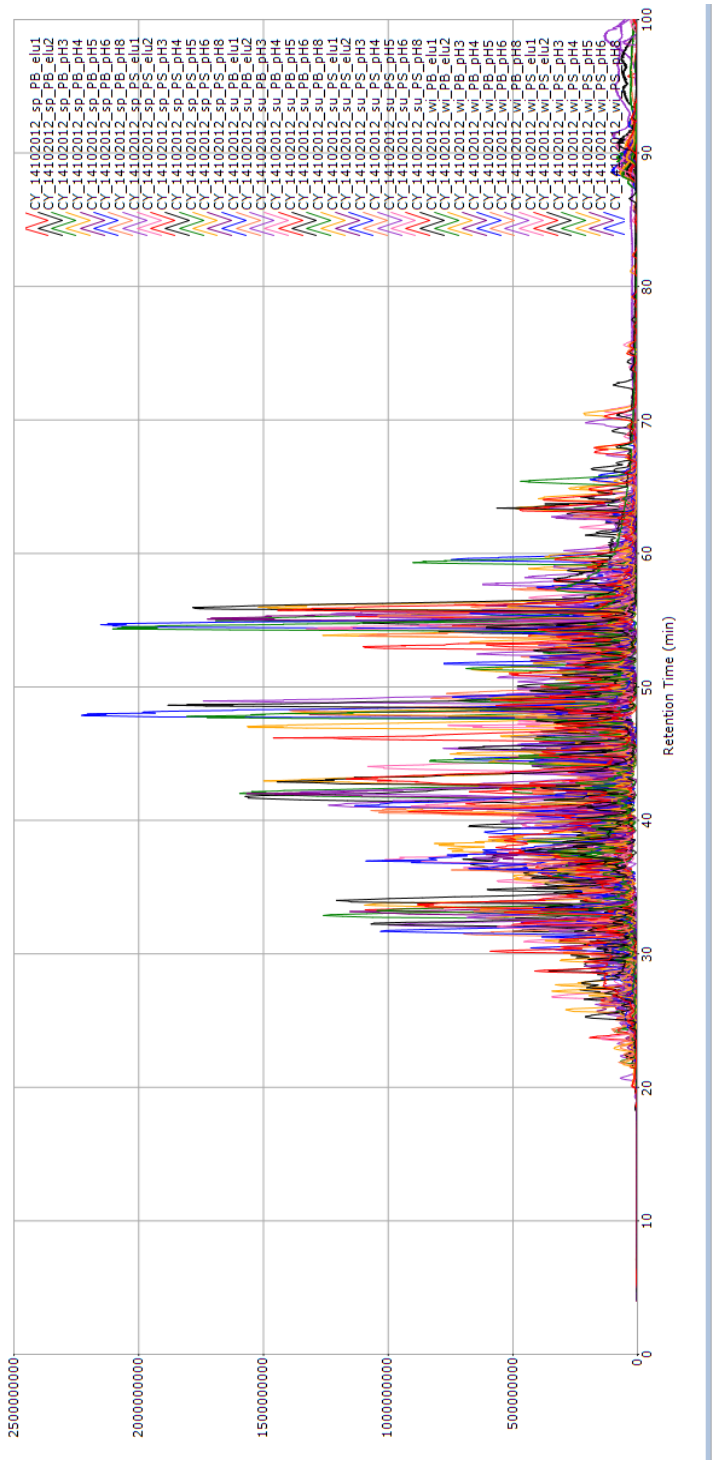

Figure G.1: Chromatogram created by RawMeat Software demonstrating the full set of samples for *Pinus brutia*

APPENDIX H

MS2 Charge Distribution of the Full Set of Samples

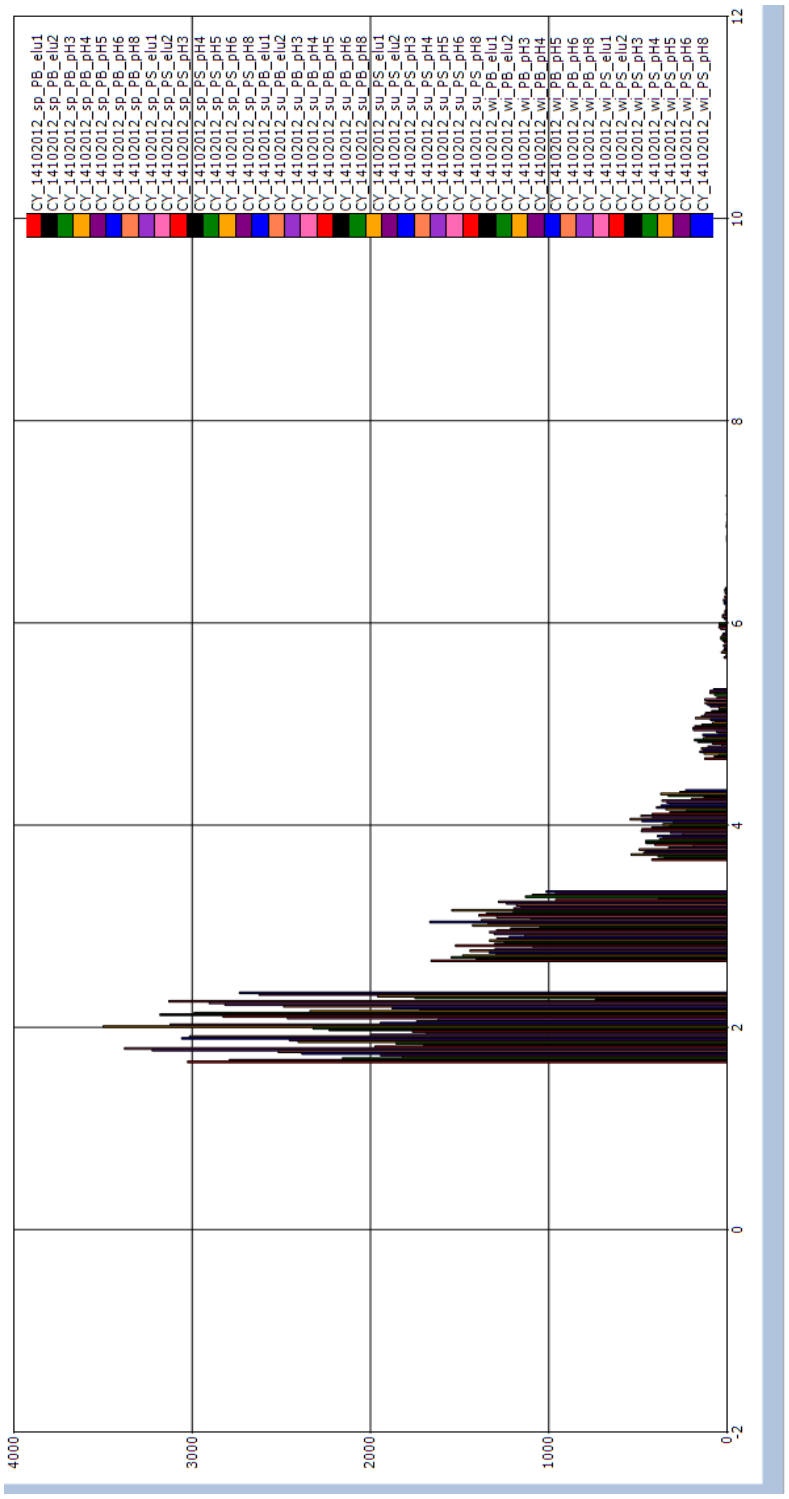

Figure H.1: MS2 charge distribution of the full set of samples for *Pinus brutia*.

APPENDIX I

MZ Distribution of Selected Monitored Ion of the Full Set of Samples

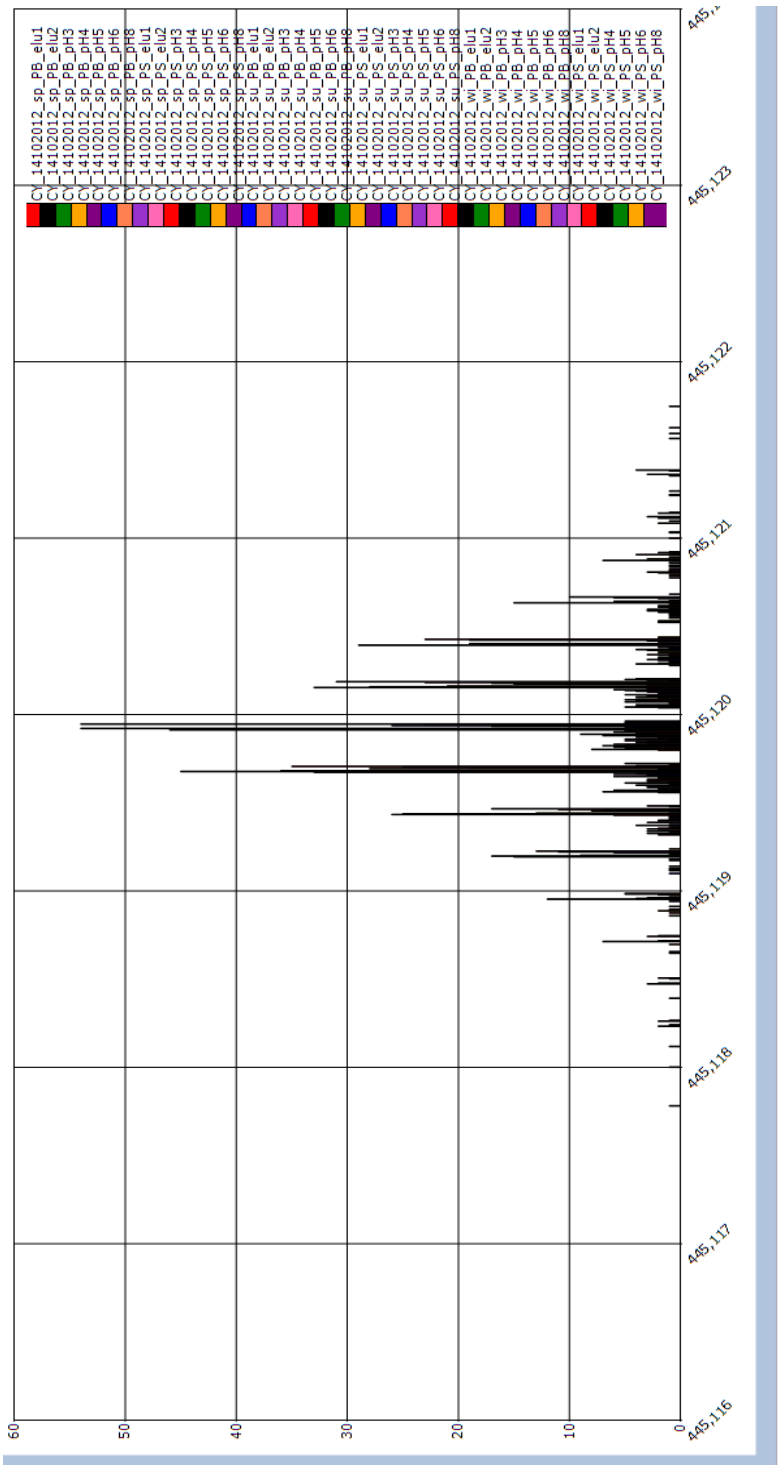

Figure I.1: MZ distribution of selected monitored ion of the full set of samples for *Pinus brutia*

APPENDIX J

A Summary of the Peptide and Protein Numbers Calculated by Search Engines

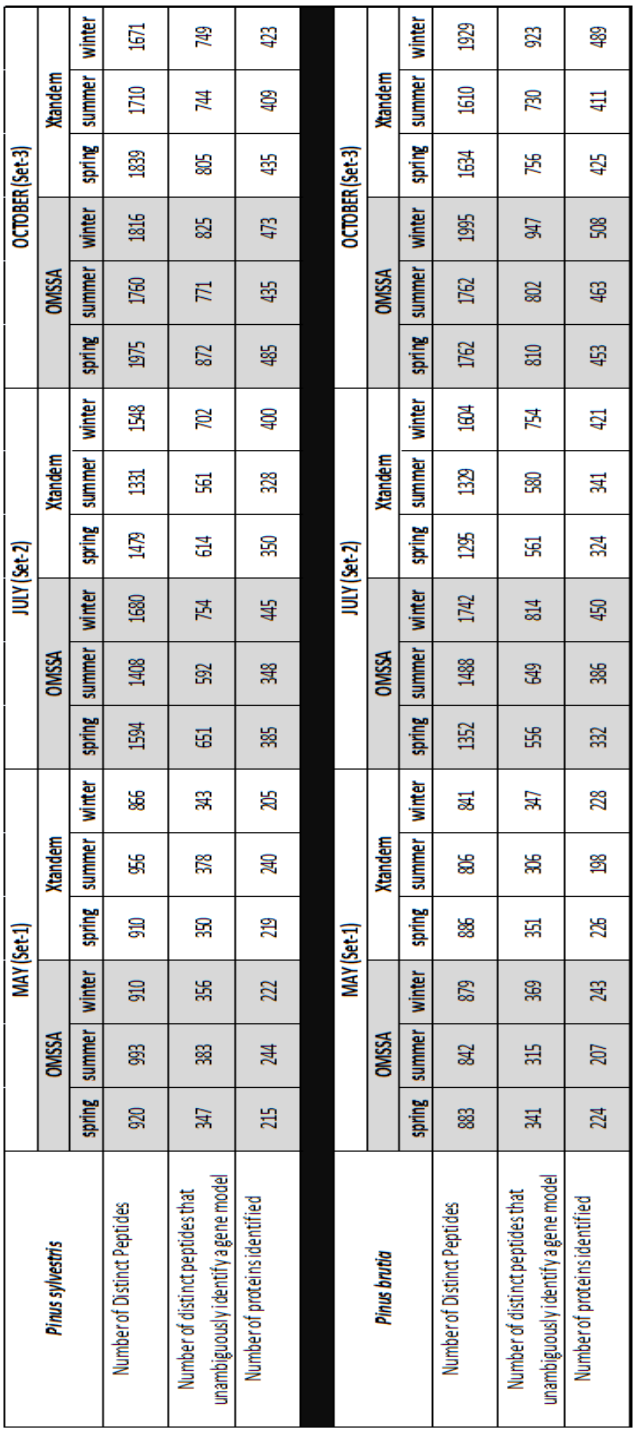

Pinus sylvestris	MAY (Set-1)						JULY (Set-2)						OCTOBER (Set-3)					
	OMSSA			Xtandem			OMSSA			Xtandem			OMSSA			Xtandem		
	spring	summer	winter	spring	summer	winter	spring	summer	winter	spring	summer	winter	spring	summer	winter	spring	summer	winter
Number of Distinct Peptides	920	993	910	910	956	866	1594	1408	1680	1479	1331	1548	1975	1760	1816	1839	1710	1671
Number of distinct peptides that unambiguously identify a gene model	347	383	356	350	378	343	651	592	754	614	561	702	872	771	825	805	744	749
Number of proteins identified	215	244	222	219	240	205	385	348	445	350	328	400	485	435	473	435	409	423

Pinus brutia	MAY (Set-1)						JULY (Set-2)						OCTOBER (Set-3)					
	OMSSA			Xtandem			OMSSA			Xtandem			OMSSA			Xtandem		
	spring	summer	winter	spring	summer	winter	spring	summer	winter	spring	summer	winter	spring	summer	winter	spring	summer	winter
Number of Distinct Peptides	883	842	879	886	806	841	1352	1488	1742	1295	1329	1604	1762	1762	1995	1634	1610	1929
Number of distinct peptides that unambiguously identify a gene model	341	315	369	351	306	347	556	649	814	561	580	754	810	802	947	756	730	923
Number of proteins identified	224	207	243	226	198	228	332	386	450	324	341	421	453	463	508	425	411	489

Figure J.1: Number of distinct peptides, distinct peptides that unambiguously identify a gene model and proteins identified after OMMSA and X!Tandem analysis

APPENDIX K

BioVenn Diagrams of OMSSA and X!Tandem Results

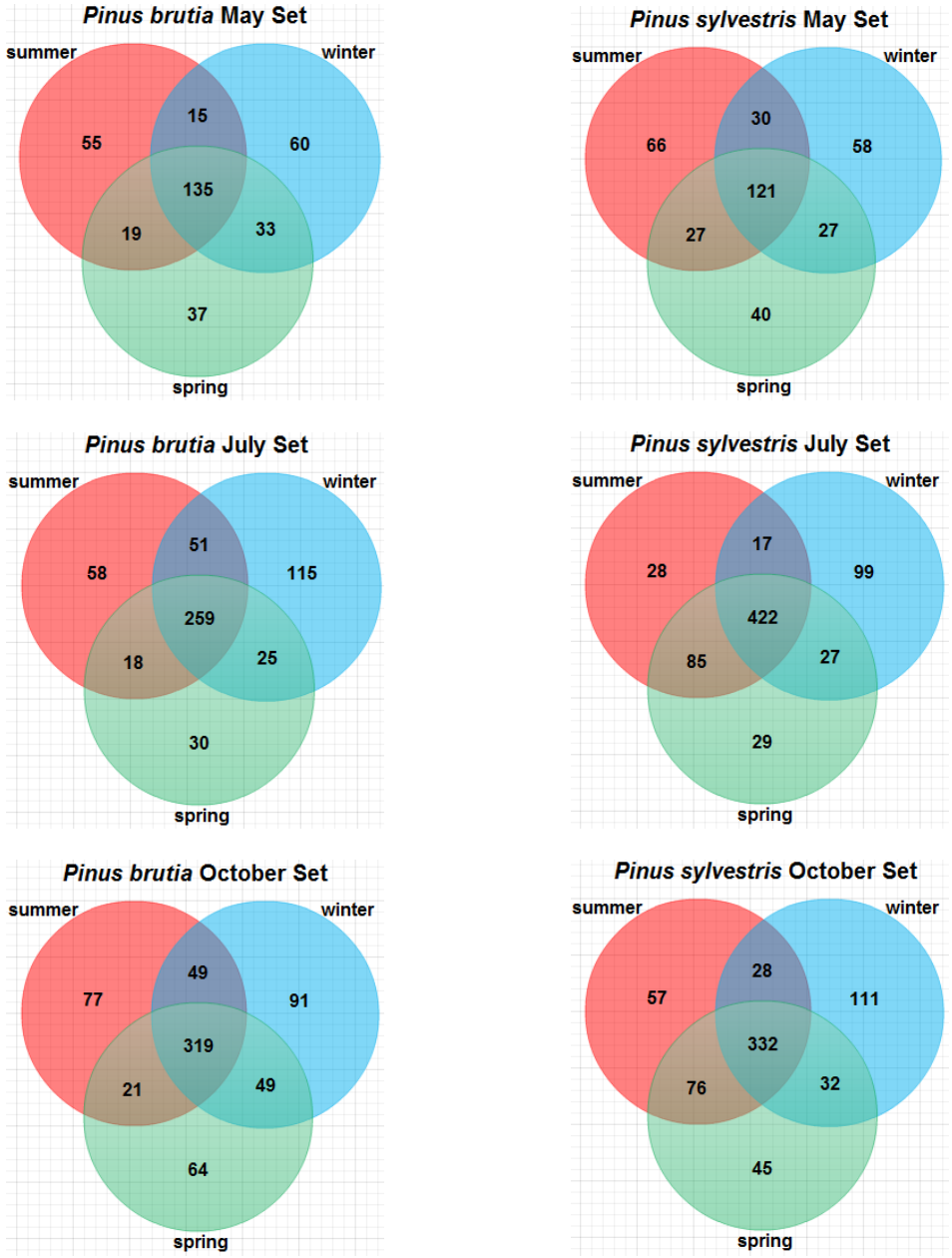

Figure K.1: Venn diagrams of OMMSA results for all MS applications

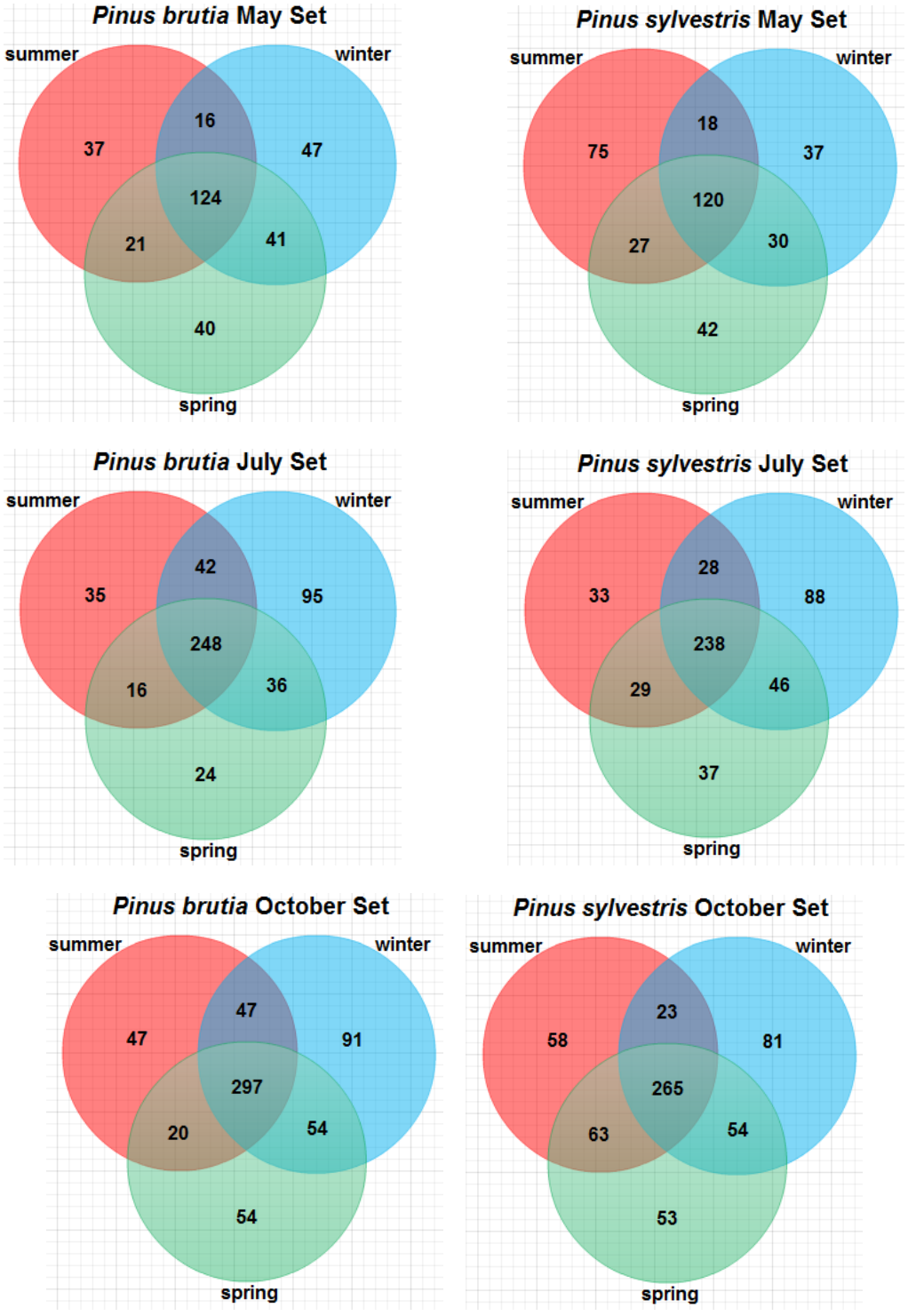

Figure K.2: Venn diagrams of X!Tandem results for all MS applications

APPENDIX L

Comparison of OMMSA vs X!Tandem

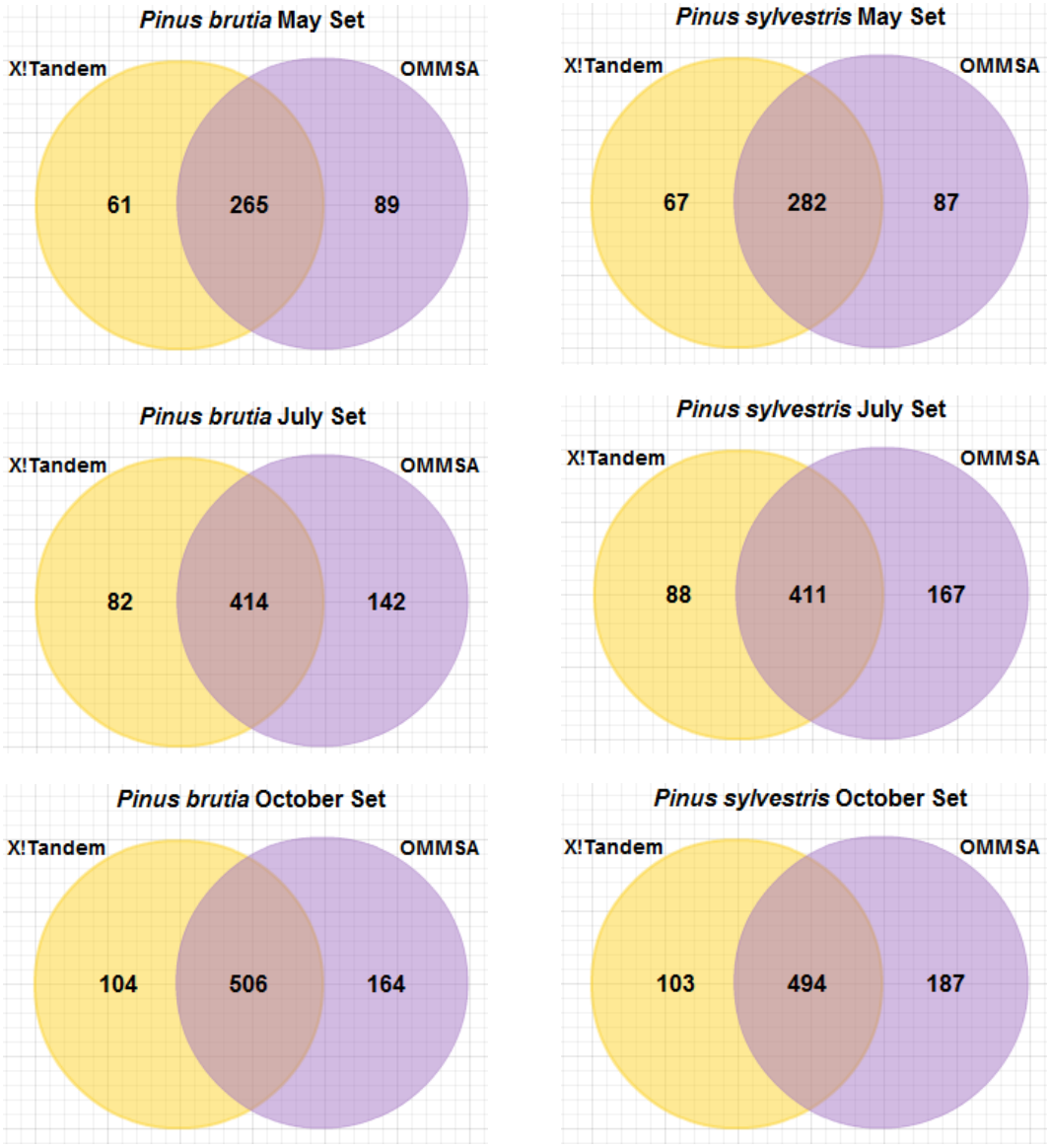

Figure L.1: BioVenn diagrams of OMSSA vs X!Tandem comparison for all three MS applications of both species

APPENDIX M

The Phosphorespiratory Glycolate Pathway

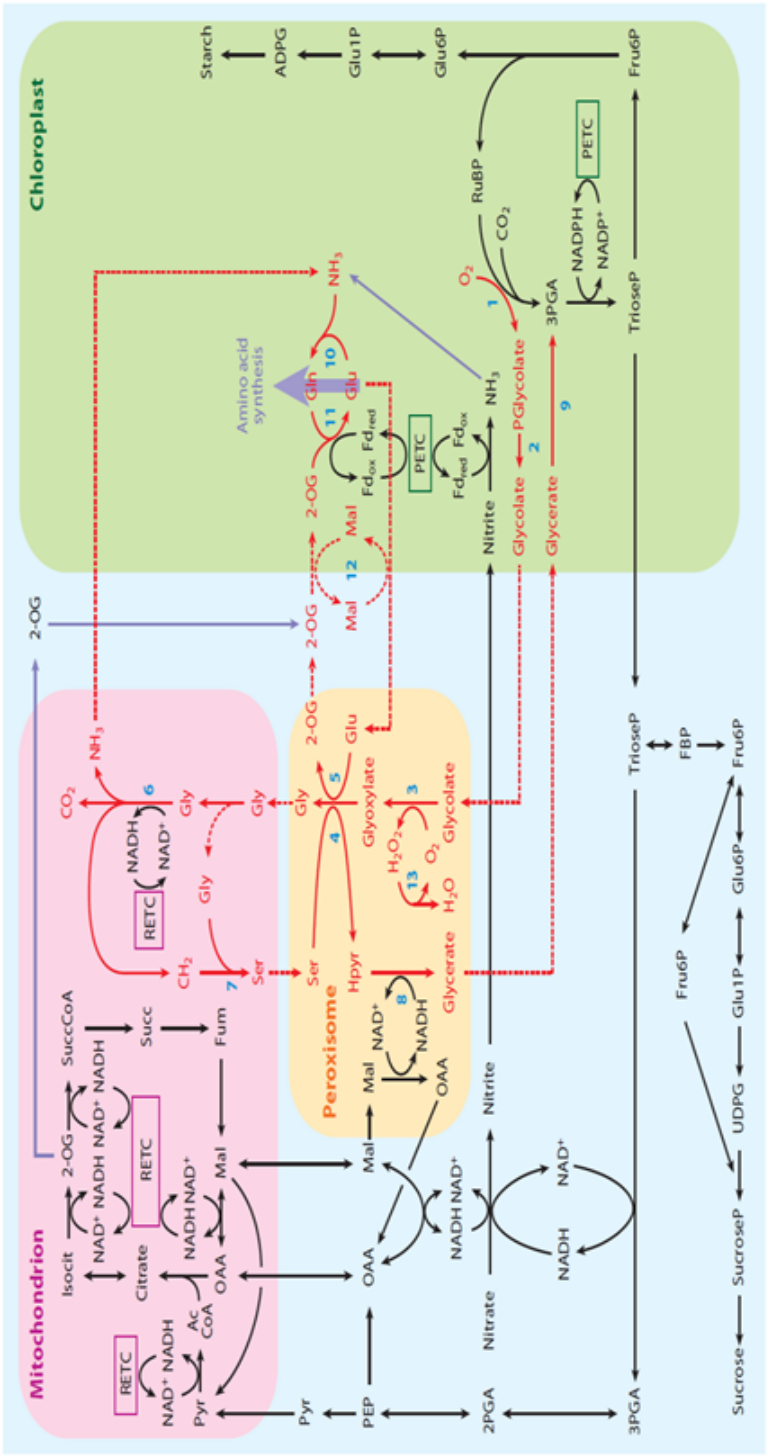

Figure M1: The photorespiratory glycolate pathway. Numbered reactions are catalyzed by the following enzymes (Christine H. Foyer, Arnold J. Bloom, Guillaume Queval, and Graham Noctor, 2009, Photorespiratory Metabolism: Genes, Mutants, Energetics, and Redox Signaling, Annual Review of Plant Biology, 60, 455-484):

1, Rubisco
2, Phosphoglycolate phosphatise
3, Glycolate oxidase
4, Serine:glyoxylate aminotransferase
5, Glutamate:glyoxylate aminotransferase
6, Glycine decarboxylase
7, Serine hydroxymethyltransferase
8, Hydroxypyruvate reductase
9, Glycerate kinase
10, Glutamine synthetase
11, Glutamate synthase (GOGAT)
12, Dicarboxylate exchangers
13, Catalase

APPENDIX N

Daily Temperature Changes

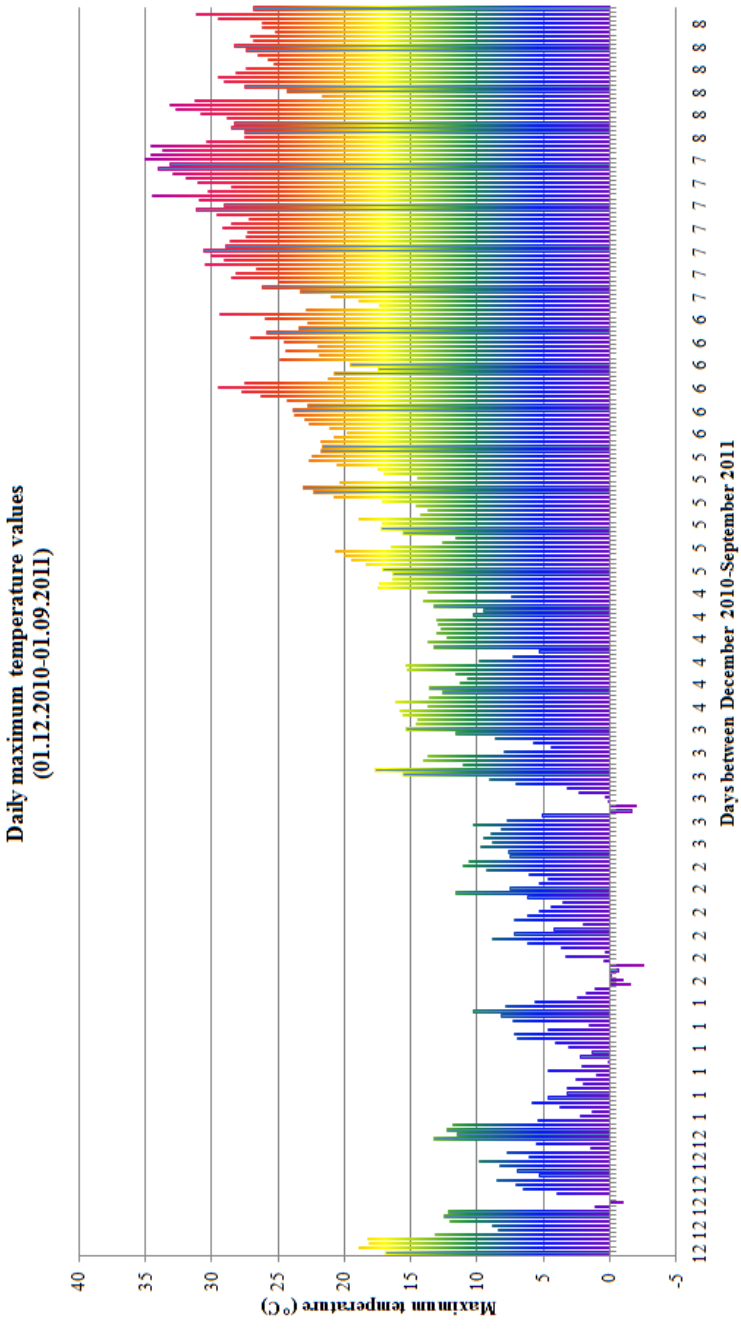

Figure N.1: Daily maximum temperature values between 01.12.2010-01.09.2011. Data were provided by Turkish State Meteorological Service (station number 17134)

APPENDIX O

Daily Minimum Temperature Values

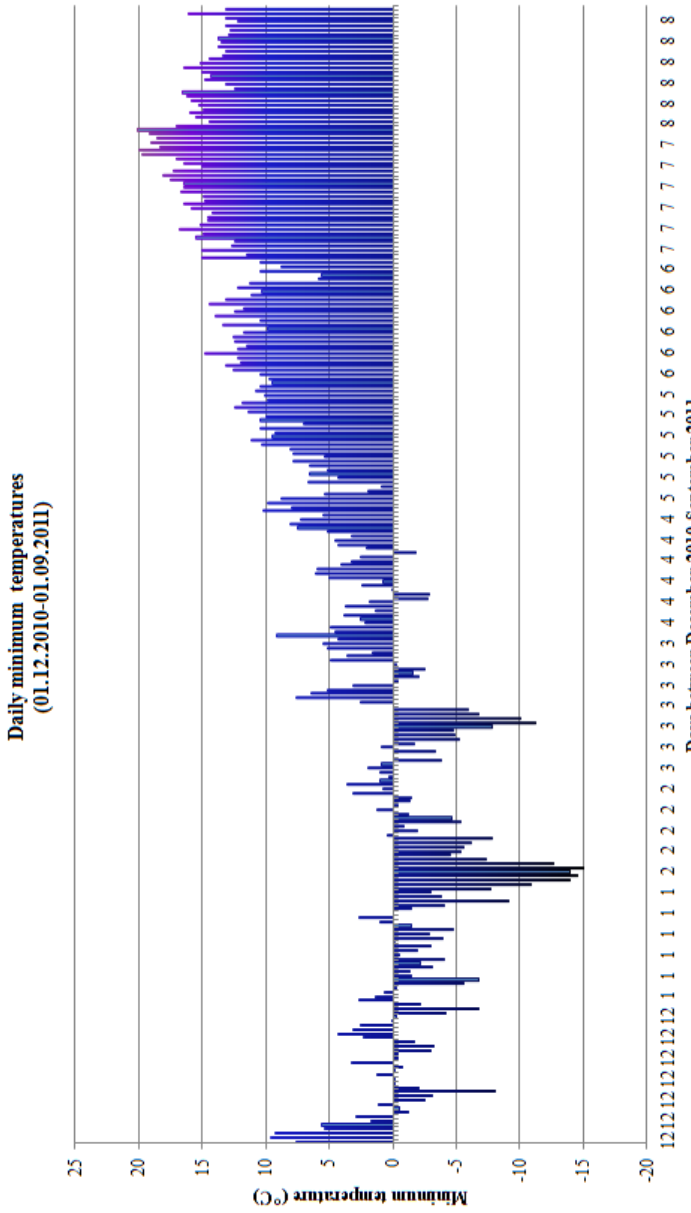

Figure O.1: Daily minimum temperature values between 01.12.2010-01.09.2011. Data were provided by Turkish State Meteorological Service (station number 17134).

APPENDIX P

The Number and Dispersion of Freeze Incidents

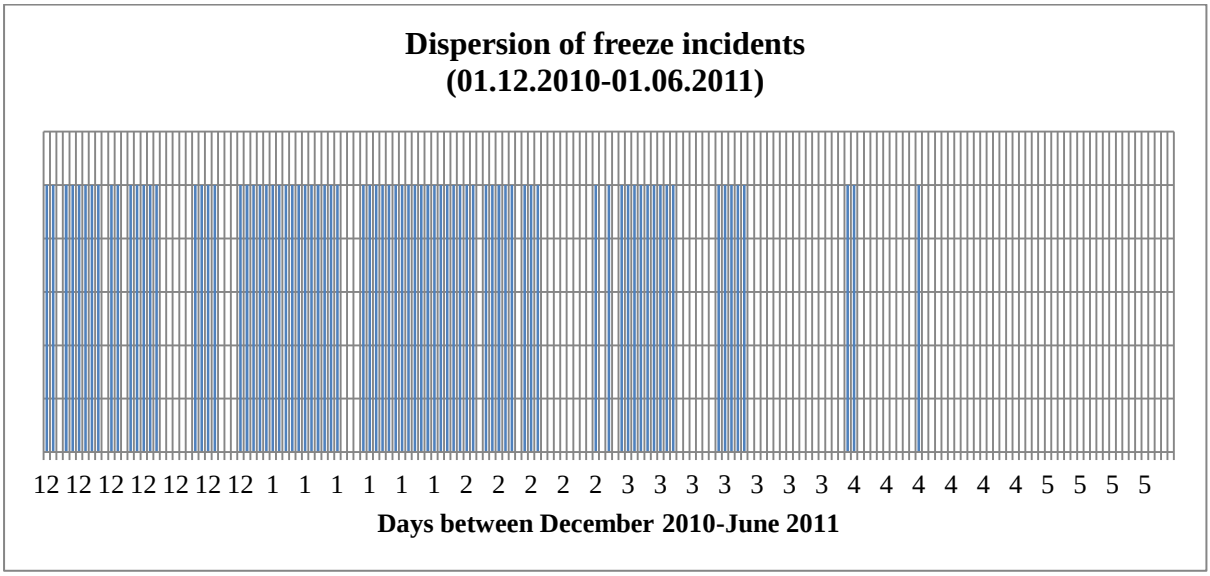

Months	Number of frost incidents
December 2010	16
January 2011	25
February 2011	20
March 2011	16
April 2011	3
May 2011	0

Figure P.1: The number and dispersion of freeze incidents between 01.12.2010-01.06.2011. Data were provided by Turkish State Meteorological Service (station number 17134).

APPENDIX Q

Average Daily Air Humidity Values

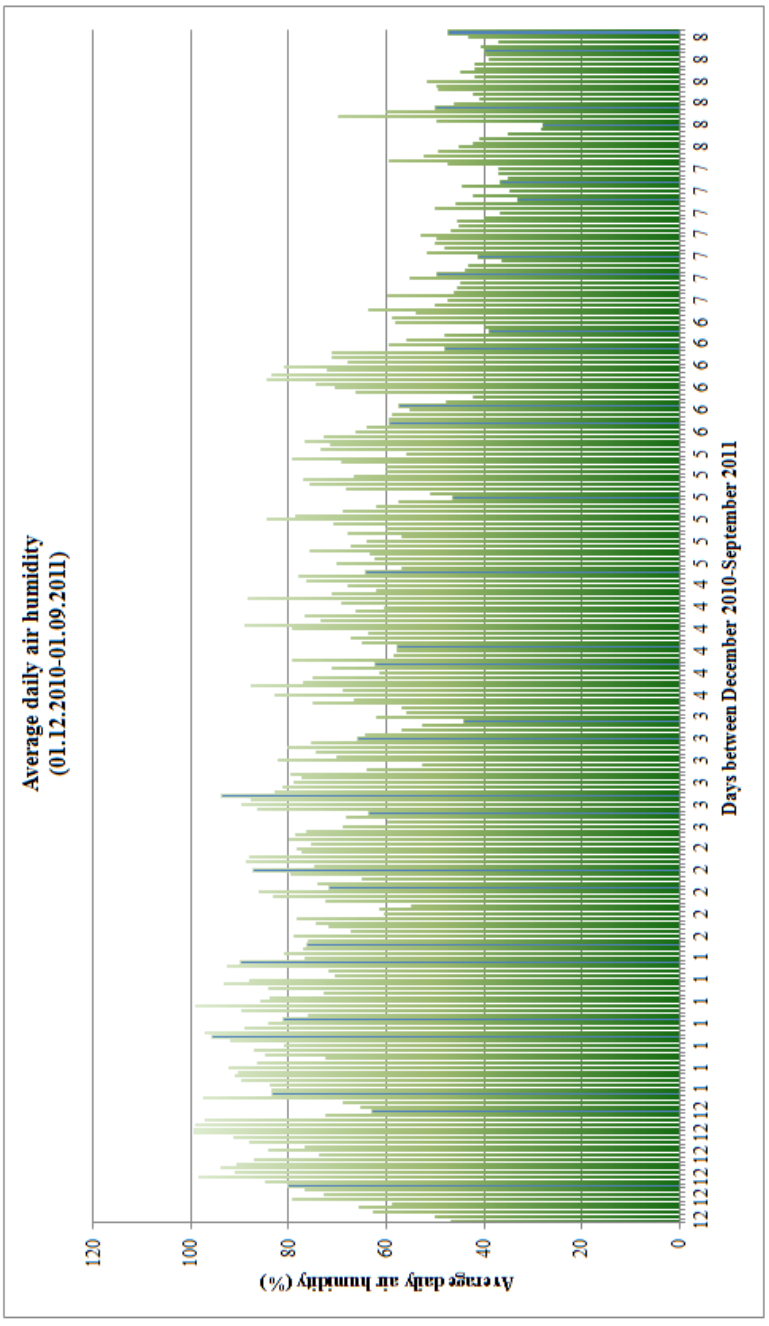

Figure Q.1: Average daily air humidity values between 01.12.2010-01.09.2011. Data were provided by Turkish State Meteorological Service (station number 17134).

APPENDIX R

Average Daily Total Precipitation Values

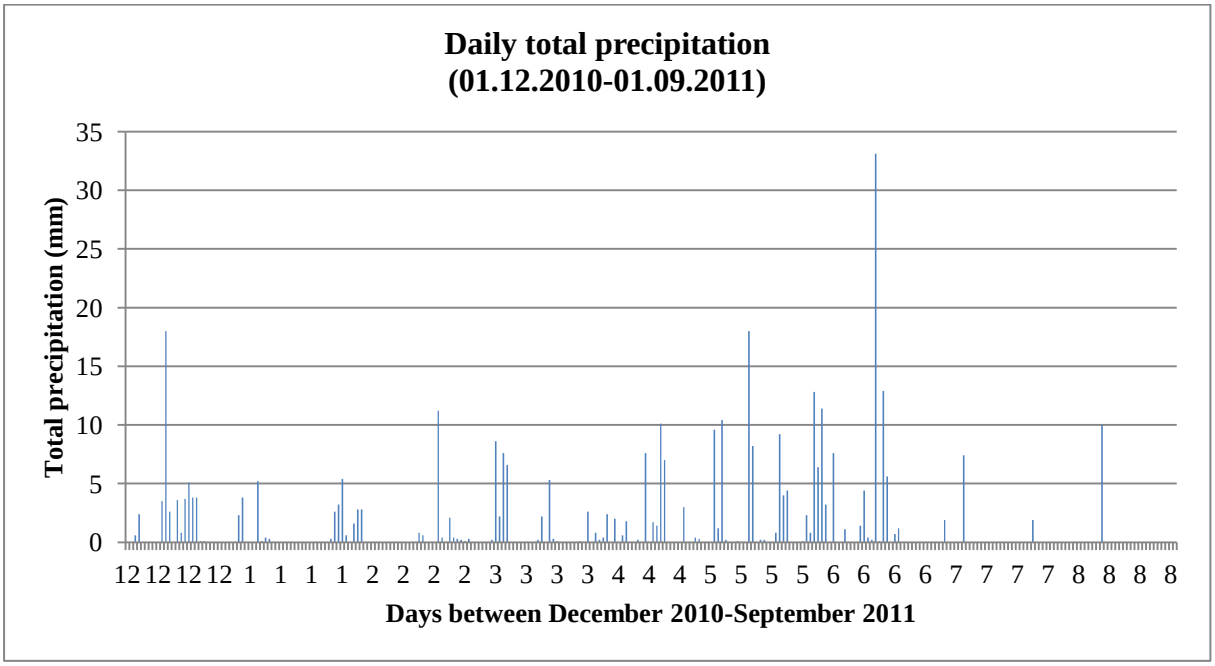

Season	Amount of total precipitation (mm)	Number of days with precipitation
Winter	95.9	37
Spring	176.1	46
Summer	93.1 Almost half of (46 mm) this amount was fallen in just 3 days!	17

Figure R.1: Average daily total precipitation values between 01.12.2010-01.09.2011. Data were provided by Turkish State Meteorological Service (station number 17134).

CURRICULUM VITAE

Personel Information

Name, Surname:	Can YILMAZ
Date of Birth:	15.12.1980
Place of Birth:	Divriği/SİVAS
Current Affiliation:	Middle East Technical University, Dpt. of Biological Sciences
Phone:	+90 312 210 6461
e-mail:	cnylmz@metu.edu.tr scientistcan@gmail.com

Education

2006-2013	PhD	METU, Ins. of Nat. and App. Sci., Biochemistry, Ankara, TURKEY
2003-2006	MSc	METU, Ins. of Nat. and App. Sci., Biochemistry, Ankara, TURKEY
1998-2003	BSc	METU, Ins. of Nat. and App. Sci., Dpt. of Bio., Ankara, TURKEY

Employment Record

2006-	Reseach Assistant at Dpt. of Biol. Sciences, METU, Ankara, TURKEY
Dec 2011-Dec 2012	Visiting researcher in AG Hippler, at Institute of Plant Biochemistry and Biotechnology, WWU University of Muenster, Muenster, GERMANY

Teaching Experience

2005-2010	Bioanalytical Chemistry Laboratory	METU, Dpt. of Biol. Sciences
2005-2013	Biochemistry Laboratory	METU, Dpt. of Biol. Sciences

Academic Publications

Oral Presentations:

YILMAZ, Can, BALD, Till, HAWAT, Susan, İŞCAN, Mesude, HIPPLER, Michael, 2013, Soğuk ve kuraklık baskısı altındaki *Pinus brutia* ve *Pinus sylvestris* proteomlarının karşılaştırılması, Türk Biyokimya Kongresi, İzmir, TÜRKİYE

Conference Papers:

YILMAZ, Can, İŞCAN, Mesude, 2013, 2D-PAGE Gel-based Comparison of Proteomes of two Pine Species under Environmental Stress Conditions, FEBS Congress, Saint Petersburg, RUSSIA

YILMAZ, Can, SAATÇİ, Ebru, İŞCAN, Mesude, 2009, Hg^{+2} ve Zn^{+2}'nun *Pinus brutia* Glutatyon S-transferazları Üzerindeki Bütünleşik Etkisi, Türk Biyokimya Kongresi, İstanbul, TÜRKİYE

YILMAZ, Can, SAATÇİ, Ebru, İŞCAN, Mesude, 2009, Inhibition Mechanisms of Heavy Metals on *Pinus brutia* Glutathione S-transferases, FEBS Congress, Prague, CZECH REPUBLIC

YILMAZ, Can, İŞCAN Mesude, 2006, Glutathione S-transferases Against Drought Stress in Plants, FEBS Congress, İstanbul, TÜRKİYE

Book Chapters:

Moleküler Biyoloji, NOBEL Akademik Yayıncılık, 2012; Bölüm 13- Genetik Kod ve Protein Sentezi

Projects

2006-2013 OYP project, (METU-BAP-08-11-DPT2002-K120510); A Proteomic Approach to the Comparison of two Pine Species: Proteomes of *Pinus brutia* and *Pinus sylvestris* under Environmental Stress

2003-2006 BAP project, (BAP-2005-07-02-00-03); Glutathione s-Transferase Activity and Glutathione Levels in Drought Stressed *Pinus brutia* Ten. Trees Growing in Ankara

Fellowships/Awards

2008-2010 TUBITAK Yurt içi Doktora Burs Programı

Languages

English (Fluent)

German (Beginner)

French (Beginner)